



NAVFAC
Naval Facilities Engineering Command

ENGINEERING SERVICE CENTER
Port Hueneme, California 93043-4370

CONTRACT REPORT
CR -NAVFAC EXWC-EV-1302

**Title: Verification of Methods for Assessing
the Sustainability of Monitored Natural
Attenuation**

By
Carmen A. Lebrón, NAVFAC EXWC
Francis H. Chapelle, U.S. Geological Survey
Mark A. Widdowson and John T. Novak, Virginia Tech
Jack C. Parker, University of Tennessee
Michael A. Singletary, NAVFAC Southeast

January 2013



Verification of Methods for Assessing the Sustainability of Monitored Natural Attenuation (MNA)

**Final Report
ESTCP Project Number ER-0824**

January 2013

Carmen A. Lebrón, NAVFAC EXWC
Francis H. Chapelle, U.S. Geological Survey
Mark A. Widdowson and John T. Novak, Virginia Tech
Jack C. Parker, University of Tennessee
Michael A. Singletary, NAVFAC Southeast

REPORT DOCUMENTATION PAGE

*Form Approved
OMB No. 0704-0188*

The public reporting burden for this collection of information is estimated to average 1 hour per response, including the time for reviewing instructions, searching existing data sources, gathering and maintaining the data needed, and completing and reviewing the collection of information. Send comments regarding this burden estimate or any other aspect of this collection of information, including suggestions for reducing the burden, to the Department of Defense, Executive Services and Communications Directorate (0704-0188). Respondents should be aware that notwithstanding any other provision of law, no person shall be subject to any penalty for failing to comply with a collection of information if it does not display a currently valid OMB control number.

PLEASE DO NOT RETURN YOUR FORM TO THE ABOVE ORGANIZATION.

1. REPORT DATE (DD-MM-YYYY)		2. REPORT TYPE		3. DATES COVERED (From - To)	
4. TITLE AND SUBTITLE				5a. CONTRACT NUMBER	
				5b. GRANT NUMBER	
				5c. PROGRAM ELEMENT NUMBER	
6. AUTHOR(S)				5d. PROJECT NUMBER	
				5e. TASK NUMBER	
				5f. WORK UNIT NUMBER	
7. PERFORMING ORGANIZATION NAME(S) AND ADDRESS(ES)				8. PERFORMING ORGANIZATION REPORT NUMBER	
9. SPONSORING/MONITORING AGENCY NAME(S) AND ADDRESS(ES)				10. SPONSOR/MONITOR'S ACRONYM(S)	
				11. SPONSOR/MONITOR'S REPORT NUMBER(S)	
12. DISTRIBUTION/AVAILABILITY STATEMENT					
13. SUPPLEMENTARY NOTES					
14. ABSTRACT					
15. SUBJECT TERMS					
16. SECURITY CLASSIFICATION OF:			17. LIMITATION OF ABSTRACT	18. NUMBER OF PAGES	19a. NAME OF RESPONSIBLE PERSON
a. REPORT	b. ABSTRACT	c. THIS PAGE			19b. TELEPHONE NUMBER (Include area code)

TABLE OF CONTENTS

Tables	v
Figures	v
Appendices	vi
Acronyms	vii
Acknowledgements	ix
Executive Summary	ix
1.0 Introduction	1
1.1 Background	1
1.1.1 <i>Environmental Problem Addressed</i>	<i>1</i>
1.1.2 <i>Technology Overview</i>	<i>1</i>
1.1.3 <i>Potential Benefit Compared to Conventional Practices</i>	<i>2</i>
1.2 Objective of the Demonstration	2
1.3 Regulatory Drivers	3
2.0 Technology	4
2.1 Technology Description	4
2.1.1 <i>MNA Sustainability Assessment</i>	<i>4</i>
2.1.2 <i>Potential Bioavailable Organic Carbon (PBOC)</i>	<i>5</i>
2.1.3 <i>Source Zone Depletion (SZD)</i>	<i>6</i>
2.1.4 <i>SEAM3D and Long-Term Sustainability (LTS)</i>	<i>6</i>
2.2 Technology Development	7
2.3 Advantages and Limitations of the Technology	7
3.0 Performance Objectives	9
3.1 Performance Objective: Validation of the PBOC Method	12
3.1.1 <i>Explanation of Objective</i>	<i>12</i>
3.1.2 <i>Data Requirements</i>	<i>12</i>
3.1.3 <i>Success Criteria</i>	<i>12</i>
3.1.4 <i>Evaluation of Success</i>	<i>12</i>
3.2 Performance Objective: Time Estimates of SZD	13
3.2.1 <i>Explanation of Objective</i>	<i>13</i>
3.2.2 <i>Data Requirements</i>	<i>13</i>
3.2.3 <i>Success Criteria</i>	<i>13</i>
3.2.4 <i>Evaluation of Success</i>	<i>14</i>
3.3 Performance Objective: MNA Sustainability Assessment	14
3.3.1 <i>Explanation of Objective</i>	<i>14</i>
3.3.2 <i>Data Requirements</i>	<i>14</i>
3.3.3 <i>Success Criteria</i>	<i>14</i>
3.3.4 <i>Evaluation of Success</i>	<i>15</i>
3.4 Performance Objective: Ease of Implementation	15
3.4.1 <i>Explanation of Objective</i>	<i>15</i>
3.4.2 <i>Data Requirements</i>	<i>15</i>
3.4.3 <i>Success Criteria</i>	<i>15</i>
3.4.4 <i>Evaluation of Success</i>	<i>15</i>

4.0	Site Description	16
4.1	Site Location and History	17
4.1.1	<i>East Gate Disposal Yard, Joint Base Lewis-McChord, WA.....</i>	17
4.1.2	<i>Areas I&J, NAES Lakehurst, NJ.....</i>	18
4.1.3	<i>Site 45, MCRD Parris Island, SC.....</i>	19
4.2	Site Geology/Hydrogeology.....	20
4.2.1	<i>East Gate Disposal Yard, Joint Base Lewis-McChord, WA.....</i>	20
4.2.2	<i>Areas I&J, NAES Lakehurst, NJ.....</i>	20
4.2.3	<i>Site 45, MCRD Parris Island, SC.....</i>	21
4.3	Contaminant Distribution	22
4.3.1	<i>East Gate Disposal Yard, Joint Base Lewis-McChord, WA.....</i>	22
4.3.2	<i>Areas I&J, NAES Lakehurst, NJ.....</i>	23
4.3.3	<i>Site 45, MCRD Parris Island, SC.....</i>	23
5.0	Test Design.....	25
5.1	Conceptual Experimental Design	25
5.2	Baseline Characterization	25
5.3	Treatability or Laboratory Study Results.....	25
5.4	Design and Layout of Technology Components	25
5.5	Field Testing.....	25
5.6	Sampling Methods.....	25
5.7	Sampling Results	27
5.7.1	<i>Overall PBOC Results.....</i>	27
5.7.2	<i>Spatial Variability of PBOC.....</i>	28
6.0	Performance Assessment.....	32
6.1	Performance Objective: Validation of PBOC Method.....	32
6.1.1	<i>Metric 1: Correlation with Site Monitoring Data</i>	32
6.1.2	<i>Metric 2: Correlation with TOC and HAA Concentrations</i>	35
6.1.3	<i>Metric 3: Correlation with Laboratory Measures of Reductive Dechlorination</i>	38
6.2	Performance Objective: Time Estimates of SZD	39
6.2.1	<i>Site 1: East Gate Disposal Yard, Joint Base Lewis-McChord, WA</i>	40
6.2.2	<i>Site 2: Areas I&J, NAES Lakehurst, NJ</i>	42
6.2.3	<i>Site 3: Site 45, MCRD Parris Island, SC.....</i>	43
6.2.4	<i>Summary of SZD Model Verification.....</i>	44
6.3	Performance Objective: MNA Sustainability Assessment.....	44
6.3.1	<i>Summary of STS Assessment.....</i>	44
6.3.2	<i>Summary of LTS Assessment</i>	46
6.4	Performance Objective: Ease of Implementation	48
7.0	Cost Assessment	49
7.1	Cost Model	49
7.1.1	<i>Cost Element: Characterization of PBOC.....</i>	50
7.1.2	<i>Cost Element: Application of Site Models.....</i>	50
7.2	Cost Drivers.....	51
8.0	Implementation Issues.....	52
8.1	Implementation of PBOC Test.....	52
8.2	Implementation of SZD Analysis.....	52
8.3	Implementation of MNA Sustainability Assessment.....	53

8.4	Implementation of the Technology at Other Sites	53
9.0	References.....	55
APPENDIX A: POINTS OF CONTACT		1
APPENDIX B: Standard Procedures: Potentially Bioavailable Organic Carbon (PBOC)		
Total Organic Carbon (TOC) Hydrolyzable Amino Acid (HAA).....		1
B.1	Potentially Bioavailable Organic Carbon (PBOC).....	1
B.1.1	<i>Purpose.....</i>	<i>1</i>
B.1.2	<i>General Procedure</i>	<i>1</i>
B.1.3	<i>Required Supplies and Equipment.....</i>	<i>1</i>
B.1.4	<i>Procedure for PBOC Extraction Method</i>	<i>2</i>
B.2	Total Organic Carbon (TOC)	2
B.3	Hydrolyzable Amino Acid (HAA).....	3
APPENDIX C: Description of Sequential Electron Acceptor Model, 3D (SEAM3D)		1
APPENDIX D: Remediation Activities at East Gate Yard, Fort Lewis, WA		1
APPENDIX E: Description of Sampling Methods.....		1
APPENDIX F: Site Monitoring Data for Performance Objective 1		1
APPENDIX G: Model description for Source zone depletion analysis (Performance objective 2).....		1
G.1	DNAPL Source Depletion Model	1
G.2	Groundwater Flow Field Mapping.....	2
G.3	Dissolved Plume Transport Model.....	3
G.4	East Gate Disposal Yard, Joint Base Lewis-McChord, WA.....	5
G.4.1	<i>Model Calibration</i>	<i>5</i>
G.4.2	<i>Model Verification.....</i>	<i>11</i>
G.5	Areas I&J, NAES Lakehurst, NJ.....	15
G.5.1	<i>Model Calibration</i>	<i>15</i>
G.5.2	<i>Model Verification.....</i>	<i>17</i>
G.6	Site 45, MCRD Parris Island, SC.....	18
G.6.1	<i>Model Calibration</i>	<i>18</i>
G.6.2	<i>Model Verification.....</i>	<i>19</i>
APPENDIX H: Model description for SUSTAINABILITY ASSESSMENT (Performance objective 3).....		1
H.1	Modeling Objective and Approach	1
H.2	Model Domain and Grid Discretization.....	1
H.3	Boundary Conditions.....	1
H.3	Material Properties	4
H.3	Calibration to Observed Conditions.....	4

TABLES

Table 1-1. Federal Maximum Contaminant Levels (MCLs) for Selected DNAPL Constituents...	3
Table 3-1. Performance Objectives.....	10
Table 4-1. Summary of Sites for PBOC Validation	16
Table 5-1. Total Number and Types of Samples Collected.....	26
Table 5-2. Analytical Methods for Sample Analysis.....	27
Table 7-1. Cost Model for MNA Sustainability Assessment.	49
Table 7-2. Cost Model for Application of Site Models.	51

FIGURES

Figure 2-1. Flow Chart Diagramming the Evaluation of Reductive Dechlorination Sustainability (Chapelle et al. 2007).....	5
Figure 4-1. Location of Joint Base Lewis-McChord, WA and East Gate Disposal Yard (USGS 2005).	18
Figure 4-2. Areas I & J of the Lakehurst site, NJ including groundwater plumes of cis-1,2 DCE in August 1998 (modified from Dames and Moore, 1999).	19
Figure 4-3. Site 45, MCRD Parris Island, SC (modified from USGS 2009).....	20
Figure 4-4. Hydrogeologic section of Joint Base Lewis-McChord EGDY Site (USGS 2005)....	21
Figure 4-5. Contaminant distribution at EGDY, Joint Base Lewis-McChord, WA (USGS 2005).	22
Figure 4-6. Cross section of chloroethene plume along north plume centerline at Areas I&J, NAES Lakehurst (Dames and Moore, 1999).....	23
Figure 4-7. Generalized distribution of tetrachloroethene in groundwater at Site 45, MCRD, Parris Island, SC in 2006-2008 (USGS 2009).	24
Figure 5-1. Range of mean potentially bioavailable organic carbon (PBOC) values for aquifer (blue) and non-aquifer (gray) samples.....	28
Figure 5-2. Sampling locations at NAB Little Creek Site 12.	29
Figure 5-3. Comparison of mean potentially bioavailable organic carbon (PBOC) in shallow (upper 8 ft of saturated zone) and deep (lower 6 ft) at NAB Little Creek Site 12.....	29
Figure 5-4. Frequency distribution of potentially bioavailable organic carbon (PBOC) results at Site 45, MCRD Parris Island, SC.....	30
Figure 5-5. Frequency distribution of potentially bioavailable organic carbon (PBOC) results at Site 45, MCRD Parris Island, SC.....	31
Figure 6-1. Mean dissolved oxygen (DO) in groundwater versus concentrations of potentially bioavailable organic carbon (PBOC) measured in aquifer sediments at 11 study sites. Standard deviations for DO concentrations are shown with error bars.	33
Figure 6-2. Mean potentially bioavailable organic carbon (PBOC) for two terminal electron acceptor processes (TEAPs). Error bars indicate standard deviations of PBOC.....	34
Figure 6-3. Mean hydrogen (H ₂) concentration in groundwater versus concentrations of potentially bioavailable organic carbon (PBOC) measured in aquifer sediments at 5 sites. Standard deviations for H ₂ concentrations are shown with error bars.....	35

Figure 6-4. Natural attenuation capacity (NAC) of chloroethenes plumes versus concentrations of potentially bioavailable organic carbon (PBOC) measured in aquifer sediments at 10 study sites.	35
Figure 6-5. Mean site values for potentially bioavailable organic carbon (PBOC) and total organic carbon (TOC) measured in aquifer sediments at 15 study sites. Two values for NABLC are represented as means for the upper and lower surficial aquifer. Mean PBOC-TOC values at NWIRP and Hill AFB was omitted from the regression.	36
Figure 6-6. Concentrations of total hydrolysable amino acids (THAA) plotted versus potentially bioavailable organic carbon (PBOC).	37
Figure 6-7. Mean site values for total hydrolysable amino acids (THAA) and potentially bioavailable organic carbon (PBOC) measured in aquifer sediments at 9 study sites.	38
Figure 6-8. Rate of CO ₂ production in incubation tests versus potentially bioavailable organic carbon (PBOC) and total hydrolysable amino acids (THAA).	39
Figure 6-9. Simulated total source mass discharge rate for EGDY from 2000 to 2100 based on pre-TSR (top) and post-TSR calibration (bottom). Dashed lines represent predicted best estimates and shades areas are their confidence limits. Red lines denote the range of field-measured discharge before and after TSR and red circles represent median values.	41
Figure 6-10. Simulated total source mass discharge for Areas I and J from 2000-2100.	42
Figure 6-11. Simulated total source mass discharge at MCRD Site 45 from 2000-2100.	43
Figure 6-12. Comparison between observed and simulated groundwater elevations in the surficial aquifer at Site 45.	45
Figure 6-13. LTS assessment results (Scenario 1) showing long-term projections of dissolved oxygen (DO) concentrations for two monitoring locations (source zone and background) in the surficial aquifer at Site 45.	47
Figure 6-14. Additional long-term projections of dissolved oxygen (DO) concentrations downgradient of the source zone in the surficial aquifer at Site 45 under changes in the background DO flux resulting from changes in land use (Scenario 2).	48

APPENDICES

Appendix A	Points of Contact
Appendix B	Standard Procedures: Potentially Bioavailable Organic Carbon (PBOC) and Total Organic Carbon (TOC)
Appendix C	Description of Sequential Electron Acceptor Model, 3D (SEAM3D)
Appendix D	Remediation Activities at Study Sites used for Performance Objectives 2 and 3
Appendix E	Description of Sampling Method
Appendix F	Site Monitoring Data for Performance Objective 1
Appendix G	Model Description for Source Zone Depletion Analysis (Performance Objective 2)
Appendix H	Model Description for Sustainability Assessment (Performance Objective 3)

ACRONYMS

ACS	American Chemical Society
AFB	Air Force Base
bgs	below ground surface
CVOC	chlorinated volatile organic compound
DCE	cis-1,2-Dichloroethylene
DNAPL	dense non-aqueous phase liquid
DO	dissolved oxygen
DOC	dissolved organic carbon
DoD	Department of Defense
EGDY	East Gate Disposal Yard
ESTCP	Environmental Security Technology Certification Program
GMS	Groundwater Modeling Systems
LTS	long-term sustainability
MCL	maximum contaminant level
MCRD	Marine Corps Recruit Depot
MNA	monitored natural attenuation
NAC	natural attenuation capacity
NAES	Naval Air Engineering Station
NAPL	non-aqueous phase liquid
NAS	Natural Attenuation Software
NAS	Naval Air Station
NAWC	Naval Air Warfare Center
NIROP	Naval Industrial Reserve Ordnance Plant
NSB	Naval Submarine Base
NTC	Naval Training Center
NUWC	Naval Undersea Warfare Center
NWIRP	Naval Weapons Industrial Reserve Plant
PBOC	potentially bioavailable organic carbon
PCE	tetrachloroethene
PFM	passive flux meter
RAO	remedial action objective

RCRA	Resource Conservation Recovery Act
RPM	remedial project manager
SEAM3D	Sequential Electron Acceptor Model, 3D
SERDP	Strategic Environmental Research and Development Program
SOM	sedimentary organic carbon
SSM	Site Selection Memo
STS	short-term sustainability
SZD	source zone depletion
TCE	trichloroethene
TDP	Technical Demonstration Plan
TEAP	terminal electron acceptor process
THAA	total hydrolyzable amino acids
THNS	total hydrolyzable neutral sugars
TOC	total organic carbon
TOR	time of remediation
TSR	thermal source removal
USGS	United States Geological Survey
VC	vinyl chloride
VOC	volatile organic compound
WWTP	waste water treatment plant

ACKNOWLEDGEMENTS

This work was funded by the Environmental Security Technology Certification Program (ESTCP). Additional support was provided by the Charles E. Via, Jr. Fellowship program at Virginia Tech.

This project was assisted by the efforts of many people from the following organizations:

- Virginia Tech: Dr. Lashun King-Thomas, Dr. Michael Mobile, Jody Smiley, Janelle Boncal, Reed Barton
- United States Geological Survey: Dr. Paul Bradley
- GSI Environmental, Inc.: Dr. Tom McHugh

Several remedial models are discussed in this technical report. NAVFAC EXWC does not endorse the use of any specific software, technology or vendor. The information pertaining to the modeling attributes and limitations is included solely for comparison purposes and the source of the information that is included is available to the general public. Citations are provided so as to provide additional reading opportunities. NAVFAC EXWC does not endorse the use of any modeling or simulations software programs used in this exercise, nor does it endorse the use of any particular model.

EXECUTIVE SUMMARY

Sustainability of any technology requires that the energy and material inputs required for efficient and consistent operation are available for the life-cycle of a project. In the case of Monitored Natural Attenuation (MNA) as a remediation technology, this requirement is no different. For the specific problem of chlorinated solvents where microbially-mediated reductive dechlorination is the primary attenuation mechanism, the three required conditions for sustainable operations are:

- 1) A consist and active population of halorespiring bacteria,
- 2) Groundwater at levels of dissolved oxygen (DO) below threshold levels necessary for efficient reductive dechlorination, and
- 3) An energy source in the form of dissolved hydrogen and carbon for microbial respiration.

The microbial community is responsible for the conversion of parent compounds such as tetrachloroethene (PCE) to innocuous compounds and the latter two components provide the material and energy (along with the chlorinated compounds themselves, but to a lesser degree) for the technology to operate in a sustainable fashion over the project life-cycle.

The technology demonstrated and validated thru this project is an approach to assessing MNA sustainability as applied to chlorinated solvents in groundwater. One specific application for this assessment technology is the case where microbially-mediated reductive dechlorination is the primary remediation strategy for plume management at a site contaminated with chlorinated ethenes and residual mass may or may not be present in a source zone. An alternative application would be the case where an aggressive strategy to reduce source mass is recommended (i.e., outcome of a site feasibility study), and MNA is the projected follow-up remediation strategy. At a given site, the assumed starting point is that site characterization efforts and data analysis has proven that the proper environmental conditions for microbially-mediated reductive dechlorination exist in the groundwater and that ample evidence exists to confirm that the microbial community is reducing chlorinated compounds.

The MNA sustainability assessment validated consists of three components designed to answer specific questions pertaining to the three conditions necessary for sustainable of naturally-occurring microbially-mediated reductive dechlorination. These components, and the questions addressed (*italics*) are:

- 1) Determine if the amount of potentially bioavailable organic carbon (PBOC) is present in the aquifer sediment and overlying soils. *Is there an adequate source of fuel for reductive dechlorination in the long term?*
- 2) Quantify the range in estimates for the contaminant source zone to deplete over time to acceptable levels. *What is the required life-cycle for MNA at a given site and how long must MNA be effective and self-sustaining?*

- 3) Estimate the long-term trend of DO in groundwater using a site model calibrated to current site conditions. *Will DO levels trend upward to the point in which microbially-mediated reductive dechlorination will not be sustained?*

The associated quantitative performance objectives of this project were to either validate or demonstrate the three components of the MNA sustainability assessment:

- 1) Validate a methodology for quantifying PBOC by establishing correlations with field-measured DO concentrations, concentrations of chlorinate volatile organic compounds (CVOCs), concentrations of natural organic carbon compounds present in aquifer sediment, and rate and extent of reductive dechlorination;
- 2) Verify the upscaled source zone depletion (SZD) function using site CVOC concentration data for a range of source zone geometries; and
- 3) Validate current site conditions (i.e., short-term sustainability or STS) using PBOC and DO concentration data and demonstrate long-term MNA sustainability (i.e., LTS) using the SEAM3D model at a site where TOR is estimated using the SZD function.

For the first performance objective, PBOC was quantified at 17 chlorinated solvent sites representing a range of conditions, including sites where microbially-mediated reductive dechlorination was not active. PBOC data was compared to redox indicator data, CVOC concentration data in groundwater derived from monitoring reports for study sites, and the results of sophisticated laboratory tests. The success criteria were achieved for the primary metric using DO data at 12 sites and through comparison of PBOC levels with the natural attenuation capacity calculated at 10 sites. Positive correlations were observed between PBOC and three additional parameters: 1) concentration of dissolved hydrogen in groundwater, 2) concentration of amino acids present in aquifer sediment, and 3) CO₂ production in laboratory incubations but in each case, stated correlation coefficient targets ($R^2 < 0.75$) were not achieved.

The second quantitative objective was assessed by comparing the results of the SZD function to historical CVOC concentration data in groundwater at three validation sites. The sites ranged from a complex multi-aquifer system with multiple DNAPL sources within a waste burial yard with extensive site characterization and monitoring data (Site 1), to a site of moderate complexity and data availability (Site 2), and a site with a single source and limited characterization and monitoring data over time (Site 3). The success criteria were achieved but quantifying confidence limits on predictions of the SZD model coupled transport and reaction models proved difficult as the level of site complexity increased (i.e., Site 1). Model verification criteria could not be achieved at Site 2 due to noise in the historical data and at Site 3 due to limited data availability.

For the last quantitative objective, a site model for groundwater flow and solute transport was developed at Site 3 using MODFLOW and SEAM3D, respectively. Simulation results were compared to observed hydraulic head data to calibrate the model to current site conditions for flow. The transport model was calibrated to observed DO concentration data to validate STS and then implemented to demonstrate LTS. The success criteria were achieved with the largest error in DO concentration of 0.1 mg/L between observed and simulated. The LTS results indicated no

significant change in DO levels over time but some increase could be expected over the 100-year timeframe in which no changes to the incoming oxygen flux were expected. For a scenario in which the background flux of oxygen increased by an order of magnitude due to a hypothetical change in land use, DO levels within the CVOC plume increase to levels that would prevent efficient reductive dechlorination.

The final component of the MNA sustainability assessment (i.e., LTS assessment) that answers the relevant question (*will microbially-mediated reductive dechlorination be sustained over the project life-cycle?*) was demonstrated and successfully implemented. An associated qualitative performance objective was to evaluate the ease of implementing the MNA sustainability assessment. The associated success criteria were achieved with only limited success. The Natural Attenuation Software (NAS) was modified to incorporate the SZD function for long-term NAPL dissolution simulations. However, based on input from stakeholders and evaluation of the procedure, it was determined that an alternative modeling platform (GMS, Groundwater Modeling System) would provide a superior approach. The sustainability assessment was easily implemented using GMS. By no means, utilization of the GMS software constitutes an endorsement by the Navy, the Department of Defense, nor ESTCP.

Costs for implementing the MNA sustainability assessment were estimated for each component. Sample collection for PBOC analysis is accomplished using conventional methods. These costs were not evaluated in the Cost Estimate but could be easily determined based on the sampling strategy. Because no specialized equipment or procedure is required to collect samples for PBOC analysis, the sampling effort could utilize existing programs. The estimated cost for running a single PBOC test is \$75 per sample. This did not include the cost of reporting and assumes that the environmental laboratory would have the required infrastructure and equipment for sample analysis. The estimate cost for the combined effort to produce a report that includes the range of SZD estimates and sustainability assessment is approximately \$50k. Hourly rates may vary as will the estimate per sample costs depending on geographic location and other economic factors. The one-time cost of a site license for GMS (version 8.3) is presently under \$10k but is free of charge Department of Defense (DoD) personnel and DoD on-site contractors.

The quality and quantity of available data is an important consideration when implementing this technology at other sites. One rate-limiting step when implementing this technology at any site comes in estimating the depletion of the source zone mass flux (i.e., component 2). Verification of the SZD function showed that the nature and extent of long-term historic CVOC data will determine if the probability distributions of predicted outcomes can be quantified. In the event that the SZD analysis is problematic or produces an unacceptable level of uncertainty, the last component of this technology may be implemented using a reasonable life-cycle time estimate. For example, a 100-year analysis could be an acceptable starting point for conducting the MNA sustainability assessment. As with any modeling investigation, post-auditing of modeling results is recommended as new data is collected and evaluated at future points in time.

1.0 INTRODUCTION

1.1 Background

1.1.1 Environmental Problem Addressed

Monitored Natural Attenuation (MNA) is a component of corrective action plans at many Department of Defense (DoD) facilities nationwide. For most sites, the effectiveness of MNA, and specifically reductive chlorination, is assessed over short time periods, often only a few months or years. However, when MNA becomes part of a long-term remediation strategy, it is assumed that natural attenuation processes documented during site assessment will continue over the system's operational lifetime. This operational lifetime depends on the length of time that contaminants will continue to be released from source zones (NRC 2000), which may span decades or even centuries. This raises an important question. Will the natural attenuation processes observed during site assessment continue with the same efficiency in the future? In other words, will MNA be sustainable throughout the required operational life of the remediation system?

The sustainability of MNA over time depends upon (1) the presence of chemical/biochemical processes that transform wastes to innocuous byproducts, and (2) the availability of energy to drive these processes to completion Chapelle et al. (2007). The presence or absence of contaminant-transforming chemical/biochemical processes can be determined by observing contaminant mass loss over time and space (mass balance). The energy available to drive these processes to completion can be assessed by measuring the pool of metabolizable organic carbon available in a system, and by tracing the flow of this energy to available electron acceptors (energy balance). For the special case of chlorinated ethenes in ground-water systems, for which a variety of contaminant-transforming biochemical processes exist, natural attenuation is sustainable when the pool of bioavailable organic carbon is large relative to the carbon flux needed to drive biodegradation to completion Chapelle et al. (2007).

1.1.2 Technology Overview

Chapelle et al. (2007) developed a methodology for assessing MNA sustainability at chlorinated solvent sites. In addition to considering all relevant physical attenuation processes, sustainability of reductive dechlorination is evaluated as documented by Chapelle et al. (2007) which suggests that sustainability of reductive dechlorination requires a flux of potentially bioavailable organic carbon (PBOC) over time sufficient to consume dissolved oxygen (DO) and to maintain reductive dechlorination conditions over the project life cycle. Short-term sustainability (STS) is determined by comparing current fluxes of carbon and oxygen. Long-term sustainability (LTS) is determined by evaluating electron donor and acceptor balances over the duration of the source using version 2.1 of the solute transport code SEAM3D, Sequential Electron Acceptor Model 3D developed by Waddill (Navy) and Widdowson (Virginia Tech) in 2000.

Chapelle et al. (2007) demonstrated this approach at a chlorinated ethene-contaminated site located on a DoD facility (NSB Kings Bay, Georgia). This preliminary demonstration illustrated that the short- and long-term sustainability of MNA can be assessed by:

1. Estimating the time required for contaminants to dissolve/disperse/degrade under ambient hydrologic conditions (time of remediation, TOR);
2. Quantifying the organic carbon flux to the system needed to consume competing electron acceptors (in particular, DO) and direct electron flow toward chloroethene degradation under current site conditions (i.e., STS); and
3. Comparing the required flux of organic carbon to the pool of renewable and non-renewable organic carbon to maintain environmental conditions needed to support microbially-mediated reductive dechlorination over the estimated time of remediation (i.e., LTS).

1.1.3 Potential Benefit Compared to Conventional Practices

A methodology for evaluating MNA sustainability was identified as a high priority Science Needs in the October 2011 Strategic Environmental Research and Development Program/Environmental Security Technology Certification Program (SERDP/ESTCP) Workshop Report. This project addresses this need and aims to demonstrate and validate a framework and methods to assess the long-term sustainability of MNA-based remediation strategies. DoD remedial project managers (RPMs) currently lack a conventional practice for assessing MNA sustainability at sites. The benefit of this work is a methodology that has been validated at sites that exhibit a range in the level of reductive dechlorination and a demonstration of the MNA sustainability framework to make reliable, defensible estimates.

This approach is designed to be both useful and expedient for RPMs. Using the MNA sustainability framework, the use of MNA can be improved, resulting in direct savings in capital and O&M costs. DoD faces remediation of 1400 (RMIS AF's database, April 2003) to 3,000 (EPA 1997) chlorinated plume sites. AFCEE's Natural Attenuation protocol estimated that 20% of all sites would be amenable to MNA. Assuming that 20% of DoD sites are amenable to natural attenuation, implementation of MNA could potentially save DoD an estimated \$11.6 to \$25B over chemical oxidation and/or thermal treatment over the next 30 years.

1.2 Objective of the Demonstration

The purpose of this project was to demonstrate and validate an integrated methodology (Chapelle et al. 2007) for assessing the long-term sustainability of MNA that was developed through SERDP project ER-1349 (Integrated Protocol for the Assessment of the Long-Term Sustainability of MNA of Chlorinated Solvent Plumes). The method, which captures the full range of NA processes (diminishing source mass flux, dilution and dispersion, biological and abiotic transformations, volatilization and plant uptake) was developed as an enhancement to SEAM3D, also a product of a SERDP-funded project (CU-1062). The specific objectives of this project were to:

1. Validate a methodology for calculating PBOC by establishing correlations with field-measured DO and chloroethene concentrations, concentrations of natural organic carbon compounds present in aquifer sediment, and rate and extent of reductive dechlorination;

2. Verify the upscaled source zone depletion (SZD) function using site contaminant concentration data for a range of source zone geometries; and
3. Validate STS using PBOC and DO concentration data and demonstrate long-term MNA sustainability (i.e., LTS) using SEAM3D at a site where TOR is estimated using the SZD function.

This project was designed to validate the PBOC method by demonstrating correlations with the rate and extent of reductive dechlorination for sites representing a wide range of conditions. The SZD function and the overall MNA sustainability framework will be demonstrated and validated using data from a subset of this group of sites. The goal was to validate both the PBOC methodology using data from sites representing a wide range of environmental conditions and the SZD function at a subset of sites. The final objective was to demonstrate the MNA sustainability framework at a test site where both the PBOC methodology and SZD function were employed.

1.3 Regulatory Drivers

Aqueous solubilities of common chemicals of concern associated with chlorinated solvents found at DoD facilities greatly exceed drinking water standards including Federal maximum contaminant limits (MCLs). Table 1-1 lists Federal MCLs for selected chlorinated ethenes derived from the discharge of solvents, often in the form of dense non-aqueous phase liquids (DNAPLs) and daughter products of reductive dechlorination.

Table 1-1. Federal Maximum Contaminant Levels (MCLs) for Selected DNAPL Constituents.

Constituent	Federal MCL (µg/L)
Tetrachloroethylene (PCE)	5
Trichloroethylene (TCE)	5
cis-1,2-Dichloroethylene (DCE)	70
Vinyl chloride (VC)	2

Source for MCLs: <http://water.epa.gov/drink/contaminants/index.cfm>

2.0 TECHNOLOGY

According to EPA (1999), the naturally-occurring processes that contribute to attenuation include “a variety of physical, chemical, or biological processes that under favorable conditions, act without human intervention to reduce mass, toxicity, mobility, volume, or concentration of contaminants in soil or groundwater.”

MNA is often proposed as a post-source zone treatment “polishing” step, or as a stand-alone technology. Regulators, however, are reluctant to approve such MNA-based remediation strategies in the absence of direct evidence that MNA will be sustained over the life-cycle of the site. Currently, the effectiveness of MNA, and specifically reductive chlorination, is typically assessed over short time periods, often only a few months or years. However, when MNA becomes part of a long-term remediation strategy, it is assumed that natural attenuation processes documented during site assessment will continue over the system’s operational lifetime. This operational lifetime depends on the length of time that contaminants will continue to be released from source zones (NRC 2000), which may span decades or even centuries. This question can be addressed using the framework and computational tool to make reliable, defensible estimates of MNA sustainability that will be validated through this project.

2.1 Technology Description

2.1.1 MNA Sustainability Assessment

The MNA sustainability assessment framework developed in Chapelle et al. (2007) considers all relevant microbially-mediated and physical attenuation processes and addresses this fundamental issue: Will the natural attenuation processes observed during site assessment continue with the same efficiency in the future? In other words, will MNA be sustainable throughout the required operational life of the remediation system? This requires a site-specific evaluation of a) dominant NA mechanisms controlling plume attenuation, b) operational lifetime to reach a remedial action objective (RAO), and c) an assessment of MNA sustainability.

The methodology developed in Chapelle et al. (2007) involves quantification of a flux balance of electron donors (bioavailable carbon) and electron acceptors (particularly DO) at a site over time. Because reductive dechlorination is often the critical NA mechanism at chlorinated solvent sites, Chapelle et al. (2007) modeled MNA sustainability with a focus on reductive dechlorination. In this case, sustainable reductive dechlorination requires a flux of PBOC over time sufficient to consume DO and to maintain reductive dechlorination conditions for the period that the source zone chlorinated ethene flux exceeds risk levels.

Figure 2-1 depicts the methodology for assessing MNA sustainability at chlorinated solvent sites (Chapelle et al. 2007). Short-term sustainability is determined by comparing current fluxes of bioavailable organic carbon and oxygen and LTS is determined by evaluating electron donor and receptor balances over the duration of the source using SEAM3D. The MNA sustainability protocol can be summarized in the following primary steps:

1. **Estimate STS of MNA:** The short-term requirement for sustainability of reductive dechlorination is that the current source zone PBOC flux exceeds the flux of DO, after

stoichiometric adjustment to H₂-equivalent fluxes, indicating that anoxic conditions exist that will enable biodegradation of chlorinated ethenes.

2. **Estimate LTS of MNA:** The ability of the groundwater system to sustain long-term reductive dechlorination is determined by running a site solute transport model developed using SEAM3D with the calibrated source zone depletion model along with field-estimates of oxygen and PBOC fluxes until a time that the source contaminant concentration decreases below a level of regulatory significance (i.e., TOR). If PBOC fluxes remain sufficient to yield anoxic conditions in the plume downgradient of the source zone, then long-term MNA sustainability is indicated.

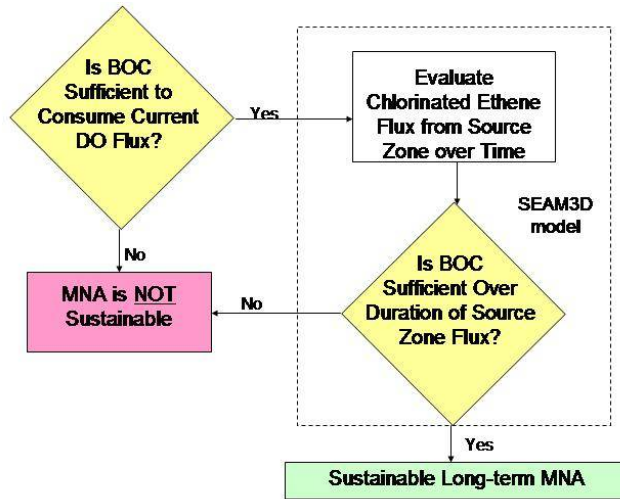


Figure 2-1. Flow Chart Diagramming the Evaluation of Reductive Dechlorination Sustainability (Chapelle et al. 2007).

2.1.2 Potential Bioavailable Organic Carbon (PBOC)

Quantifying effective carbon fluxes within the groundwater system requires a methodology for measuring bioavailable carbon concentrations in aquifer sediment. Sources of organic carbon to drive reductive dechlorination include fluxes in groundwater recharge, advective transport of organic carbon from groundwater upgradient of the source, transport by traverse dispersion from groundwater adjacent to the plume, mobilization of organic carbon from solid phase organic carbon in the aquifer, and dissolution of anthropogenic organics other than chlorinated ethenes that may occur within the source zone. Rectanus et al. (2007) developed the PBOC method and described the laboratory validation experiments. A detailed description of the laboratory methods are provided in Appendix B.

2.1.3 Source Zone Depletion (SZD)

SERDP project ER-1349 led to the development of a practical field-scale model for estimating chlorinated ethane fluxes versus time from source zones considering effects of mass depletion that was shown to be applicable to DNAPL pool sources, residual DNAPL sources, as well as intermediate and combined source types (Parker and Park 2004; Park and Parker 2005; Parker et al. 2008). The SZD function may be written in the form

$$\dot{M}_i = \kappa \left(\frac{M}{M_o} \right)^\beta Q (C_{eq,i} - C_i) \quad (2.1)$$

where \dot{M}_i is mass discharge of species i leaving the source zone, κ is a dimensionless mass transfer coefficient, $C_{eq,i}$ is the effective solubility of species i , C_i is the average dissolved phase concentration exiting the source, Q is the volumetric flow rate through the source, M is the current total source mass, M_o is the mass at a specified time, and β is a depletion exponent. For a pure solvent source, $C_{eq,i}$ is a constant, while for a multicomponent NAPL source, it is equal to the product of the pure solubility of each species and its respective mole fraction in the NAPL mixture (i.e., via Raoult's Law).

Version 2.1 of SEAM3D includes an update to the NAPL Dissolution Package (implemented in ER-1349) that calculates grid-block dissolution rates for each NAPL component based on Equation 2.1:

$$J_i^N = k_i^N \left(\frac{M}{M_o} \right)^\beta (C_{eq,i} - C_i) \quad (2.)$$

where J_i^N is the rate of interphase mass transfer mass of species i and k_i^N is the initial lumped mass transfer coefficient. By design, the function does not involve any parameters that would require small-scale characterization of the distribution or geometry of DNAPL, groundwater velocities, etc., which are generally impractical to obtain in the real world.

The SZD function was developed by upscaling high resolution simulations that considered detailed representations of aquifer heterogeneity, DNAPL distributions, and interfacial surface area. Thus, the upscaled SZD function considers the effects of decreases in interfacial surface area with time as NAPL mass depletes, but not in an explicit manner. Likewise, the upscaled model is able to describe mass depletion and flux reductions vs. time for different source zone "architectures" (via the source depletion exponent in the upscaled model), but explicit parameterization of source geometry, "ganglia/pool ratios" or other small-scale variables is not required to use the model.

2.1.4 SEAM3D and Long-Term Sustainability (LTS)

SEAM3D is an advective-dispersive solute transport model that simulates the full range of natural attenuation processes (biodegradation, sorption, dilution and dispersion, volatilization, and diminishing source mass flux) in groundwater systems (Waddill and Widdowson, 1998;

2000). A complete description of the mathematical model utilized in SEAM3D is provided in Appendix C.

The SEAM3D Biodegradation Package simulates mass loss of electron donors (e.g., hydrocarbon compounds derived from light NAPL sources) that serve as growth substrates for heterotrophic bacteria in the subsurface, and the consumption of electron acceptors (EAs) associated with aerobic and anaerobic respiration. Mass loss terms due to biodegradation are functions of the specific process (e.g., sulfate reduction) and electron donor/acceptor concentrations. SEAM3D is innovative in that it allows for the evolution of redox conditions within a plume with time and space as solid-phase electron acceptors are depleted. SEAM3D also accounts for the contribution of aerobic biodegradation around the edges of a plume due to the mixing of DO.

The SEAM3D NAPL Package calculates the mass balance of each NAPL component using a field-scale mass transfer function that models mass flux at the grid-block size. SEAM3D solves the equation of mass balance for multiple species and categories of solutes including chlorinated volatile organic compounds (CVOCs) in the mobile aqueous phase. The SEAM3D Reductive Dechlorination Package ties the rate and extent of bioattenuation of chloroethenes (i.e., reductive dechlorination and aerobic and anaerobic direct oxidation) to the concentrations of electron acceptors (Widdowson 2004).

2.2 Technology Development

Elements of the technology were developed during previous SERDP and ESTCP projects. Results of these projects are documented in the corresponding SERDP and ESTCP reports. The overall MNA assessment method was developed as research supported by SERDP (ER-1349). In addition, the PBOC method and the SZD function were also developed as research under SERDP project ER-1349. The first version of the SEAM3D NAPL Package was developed through SERDP project CU-1062. The code has been enhanced over time, including improvements to the NAPL Package and the inclusion of physically-based attenuation mechanisms under SERDP project ER-1349.

2.3 Advantages and Limitations of the Technology

The PBOC method is relatively straight-forward and offers many advantages relative to more gross measures of organic carbon (e.g., total organic carbon, TOC) and more aggressive methods (e.g., total hydrolyzable amino acids, THAA, and total hydrolyzable neutral sugars, THNS). Chapelle et al. (2009) suggested THAA and THNS as measures of the bioavailability of organic carbon based on an analysis of two sites. However, both analyses are relatively much more expensive compared to analysis of PBOC.

Application of the MNA sustainability assessment technology involves all components including the application of SEAM3D to develop a site model. SEAM3D is currently the most comprehensive model available to simulate the fate and transport of chlorinated ethenes in groundwater. The code incorporates state-of-the-science formulations for source zone depletion and microbially-mediated reaction kinetics. The code considers electron acceptor and electron donor controls of redox conditions and fluxes of biologically-available dissolved organic carbon (DOC) from groundwater recharge, advective transport of organic carbon in groundwater

upgradient of the source, transport by traverse dispersion, dissolution of organic carbon from solid phase organic carbon in the aquifer, as well as dissolution of anthropogenic carbon within the source zone. No other models are available that are capable of considering long-term sustainability of organic carbon to maintain aquifer conditions conducive to reductive dechlorination.

The program BIOBALANCE (GSI 2006) was recently developed to assess MNA sustainability using a simple electron donor and electron acceptor stoichiometric balance. Limitations of BIOBALANCE arise due to its omission of carbon fluxes due to dissolution of natural solid phase organic carbon, recharge fluxes and transverse dispersion. These omissions can significantly affect inferred sustainability. Furthermore, BIOBALANCE uses a DNAPL source model that represents a special case of Equation 2.1 with a source depletion exponent (β) or 1. Since β may deviate significantly from 1, inaccurate estimates of contaminant fluxes versus time and TOR will result.

BIOCHLOR (Aziz et al. 2000) and REMChlor (Falta et al. 2007) are analytical models for chlorinated solvent transport in steady state velocity fields. BIOCHLOR uses the same simplified DNAPL source model as BIOBALANCE, while REMChlor employs a variable depletion exponent as given by Equation 2.1. Both models consider spatially variable first-order decay of solvent species. REMChlor also considers time-dependent decay, but no means is available for computing if or how decay coefficients might change over time due to organic carbon fluxes. In addition, first-order decay models do not take into account the reservoir of BOC in sustainability. By contrast, in the SEAM3D Biodegradation Package, time-dependent equations of mass balance for the utilization of BOC, DO, and other electron acceptors are quantified. The redox state in each model cell is determined by the presence or absence of electron acceptors, and this is used to determine the rate and extent of mass loss for each chloroethene compound in the Reductive Dechlorination Package.

The major disadvantage of using SEAM3D is the requirements for input parameters and data for calibration associated with any comprehensive 3D solute transport model. In theory, these limitations are moderated by implementing SEAM3D using analytical models such as the Natural Attenuation Software (NAS) software package. However, as described in the next section (Performance Objectives) and Section 6 (Performance Assessment), it was determined that implementing the STS and LTS assessments were best performed using a platform designed for existing site models utilizing MODFLOW and SEAM3D.

Mention of software attributes and limitations is done for comparison purposes only and does not constitute an endorsement or lack thereof by the Navy, the Department of Defense, nor ESTCP of a specific methodology.

3.0 PERFORMANCE OBJECTIVES

Specific quantitative performance objectives for MNA sustainability assessment were paired with the three component of the methodology:

1. Measurement of PBOC levels
2. TOR estimation using the SZD function
3. LTS assessment using SEAM3D as a site model.

The first quantitative objective was validated by analyzing aquifer sediment samples from 17 chlorinated solvent sites and comparing results to redox indicator concentration data and CVOC concentration data in groundwater derived from monitoring reports for study sites. The study sites represented a wide range of hydrogeological conditions and levels of microbially-mediated reductive dechlorination.

The second quantitative objective was assessed by comparing the results of the SZD function to historical CVOC concentration data in groundwater at three study sites. The sites ranged from a complex multi-aquifer system with multiple DNAPL sources within a waste burial yard with extensive site characterization and monitoring data (Site 1), to a site of moderate complexity and data availability (Site 2), and a site with a single source and limited characterization and monitoring data over time (Site 3).

For the last quantitative objective, a site model developed using SEAM3D was compared to observed hydraulic head data and observed DO concentration data to validate STS and then implemented to demonstrate LTS. One qualitative performance objective was designed to evaluate the ease of implementing the MNA sustainability assessment.

The quantitative performance objectives and the qualitative performance objective described above are summarized in Table 3-1. A synopsis of their evaluation is provided in this section, and further details are provided in Section 6.0.

Table 3-1. Performance Objectives

Performance Objective	Data Requirements	Success Criteria	Results
Quantitative Performance Objectives			
Validate PBOC Method	VOC and redox indicator concentrations in groundwater. Amino acid concentrations in aquifer sediment samples. Extent of dechlorination in radio-labeled laboratory tests.	Routine statistical measures to establish relationships between PBOC and each metric parameter. Correlation coefficient (R^2) will be 0.75 or greater.	The success criteria were achieved for the primary metric using DO and NAC. Positive correlations were found H_2 but the stated correlation coefficient was not achieved ($R^2 < 0.75$). For the remaining two metrics, again positive correlations were observed for THAA and CO_2 production, respectively, but the stated correlation coefficient was not achieved ($R^2 < 0.75$).
Estimating Source Zone Depletion Time	Monitoring well data near source and in dissolved plume. Aquifer characteristics and site history. Mass recovery estimates from partial source mass reduction.	Out-of-sample data set consistent with predicted 95% confidence limits based on calibrated model.	The success criteria were achieved but quantifying confidence limits on predictions of the SZD model coupled transport and reaction models proved difficult as the level of site complexity increased (i.e., Site 1). Model verification criteria could not be achieved at Site 2 due to noise in the historical data and at Site 3 due to limited data availability.
Demonstrate Sustainability Assessment Methodology	VOC and Redox Indicator Monitoring Well Data	<ul style="list-style-type: none"> ● Match SEAM3D output to observed site DO data along flow path <ul style="list-style-type: none"> ○ ± 0.5 mg/L DO at wells where $DO > 1.0$ mg/L ○ ± 0.25 mg/L DO at wells 	The success criteria were achieved with the largest error in DO concentration of 0.1 mg/L between observed and simulated. The groundwater system at Site 3 was strongly

		<p>where $DO < 1.0 \text{ mg/L}$)</p> <ul style="list-style-type: none"> • Simulate redox conditions along flow path 	<p>anaerobic, and the redox condition showed no variation along the flow path due to the truncated plume length. LTS assessment was successfully demonstrated.</p>
Qualitative Performance Objectives			
Ease of Implementation	Feedback from potential stakeholders on applicability, ease of use, and data requirements	User can successfully complete the assessment using NAS or other modeling platform	The success criteria were achieved with only limited success. NAS was modified to incorporate the SZD function for long-term NAPL dissolution simulations. However, based on input from stakeholders and evaluation of the procedure, it was determined that an alternative DoD-supported modeling platform (GMS, Groundwater Modeling System) would provide a superior approach. The sustainability assessment was easily implemented using GMS.

3.1 Performance Objective: Validation of the PBOC Method

3.1.1 Explanation of Objective

The first objective was to validate a method proposed in Rectanus et al. (2007) to quantify the concentration of an operationally-defined bioavailable organic carbon in sediment samples (aquifer and soil). Specifically, PBOC concentrations were determined using samples collected or provided from study sites representing a wide-range of conditions. Three independent metrics were identified for validating the PBOC method: one primary metric and two secondary metrics. The primary metric was correlation of PBOC concentrations with DO concentrations and other geochemical indicators of in-situ redox conditions and the presence/absence of reductive dechlorination daughter products. The two secondary metrics were correlation of PBOC concentrations with (1) concentrations of TOC and amino acids (AA) present in aquifer sediments known to be readily biodegradable; and (2) ability of sediment organic carbon to support active reductive dechlorination.

3.1.2 Data Requirements

Data requirements for the first metric were levels of DO and redox indicators such as dissolved hydrogen (H_2). They are clear and strong indicators of environmental conditions necessary for reductive dechlorination (Bradley, 2000). The first metric included chloroethene concentration data. From the latter, a specific quantitative metric related to the rate of reductive dechlorination (natural attenuation capacity or NAC) was compared to PBOC. For the second metric concentrations of THAA and THNS were analyzed as described by Kaiser and Benner (2005) using the sediment samples collected from a subset of the PBOC study sites. As an additional metric, laboratory incubation tests were performed using aquifer sediment samples at selected study sites spiked with TCE. Data included headspace concentrations of ethene, CH_4 and CO_2 .

3.1.3 Success Criteria

A primary criterion for success for this quantitative objective was that relatively high levels of PBOC matched site conditions indicative of high levels of reductive dechlorination (both rate and extent) and that low levels of PBOC matched sites where reductive dechlorination was negligible. Specifically, statistical correlations between PBOC and site monitoring parameters should have exhibited a correlation coefficient (R^2) of 0.75 or greater. A second independent measure was provided by the degree to which PBOC and TOC along with PBOC and THAA were positively correlated. Lastly, to evaluate the third metric, the production of CO_2 , formed by the oxidation of reductive dechlorination daughter products, were expected to correlate with PBOC concentration. Thus, test results from sites with low PBOC were expected to exhibit limited production of CO_2 .

3.1.4 Evaluation of Success

For the primary metric, the success criterion was achieved for both DO and the NAC based on data from 11 and 9 sites, respectively. A hyperbolic correlation for DO was apparent with $R^2 = 0.96$. Simple linear regression between PBOC and NAC showed a positive correlation with $R^2 = 0.75$. For the other site variable associated with the primary metric (H_2), a positive correlation were apparent ($R^2 = 0.62$) but with $R^2 < 0.75$. However, a distinct difference between PBOC at

sites where sulfate-reducing conditions was observed and methanogenic sites was noted. For the secondary metric, the success criterion was nearly achieved with a positive log-log correlation between PBOC and TOC ($R^2 = 0.72$). Similarly, THAA showed positive log-log correlation with PBOC; however, the success criterion was only achieved but removing outliers (2 sites) where low levels of THAA were measured. The amount of CO_2 produced at the end of the incubation tests showed a positive correlation with both PBOC and THAA.

3.2 Performance Objective: Time Estimates of SZD

3.2.1 Explanation of Objective

The goal of this performance objective was to evaluate the ability of the proposed source zone depletion (SZD) model to estimate source longevity under natural or engineered conditions and the magnitude of source mass reduction prior to MNA needed to meet cleanup goals with definable uncertainty. The specific performance criteria involved comparing field-measured source discharge rates with confidence limits for simulated discharge rates using a model calibrated to field data (with no discharge measurements included in the calibration data set). If measured source discharge rates (median values for multiple values) lie within 95% confidence limits for the model predictions, the SZD model is considered to be valid.

Complete details of the methods and results associated with Performance Objective 2 are provided in Appendix G. Descriptions of the DNAPL source depletion and dissolved phase transport models used to construct site models and methods used for model calibration and prediction uncertainty analysis are described in Section G.1. Results for model applications to three field sites are given in Sections G.2 through G.4.

3.2.2 Data Requirements

Data requirements for this objective include dissolved phase concentrations of chlorinated hydrocarbons in monitoring wells within source zones and downgradient dissolved plumes over time, estimates of contaminant flux from sources based on passive flux meters (PFMs) or other methods, estimates of the contaminant mass in sources at a given time (e.g., based on soil borings or operational data), estimates of mass recovery from prior source reduction efforts, information on source zone location and areal and vertical extent, DNAPL release timing, estimates of groundwater flow paths and velocity, aquifer thickness, porosity, and organic carbon content, and remediation history. Best estimates of all model parameters prior to calibration are quantified based on available site and literature data. For parameters whose uncertainty is considered to be unacceptably high (i.e., if the level of uncertainty strongly affects remediation decisions), a prior estimate of the uncertainty in the prior best estimate must also be quantified (i.e., standard deviation if a normal distribution is assumed or log standard deviation if log-normal) based on available site data, literature or professional judgment. These parameter estimates and their uncertainty are refined through the calibration process.

3.2.3 Success Criteria

Success criteria for analysis of the SZD function was based on the ability of the model to match a subset of the available data time-series, referred to as the “out-of-sample” data set. This subset was omitted from the data used for calibration of the transport model and used only for model

verification. Once calibrated to the earlier data (full concentration data less the out-of-sample data), the model was used to simulate the out-of-sample observations and error propagation methods was used to determine prediction confidence limits. If the out-of-sample observations were consistent with 95 percent prediction confidence intervals, results will be considered validated.

3.2.4 *Evaluation of Success*

Results of the verification step demonstrate that the SZD model is suitable for predicting source zone depletion and mass discharge rate versus time. Nevertheless, it is critical to quantify confidence limits on predictions of the SZD model as well as transport and reaction models to which it may be coupled. The results documented in this SZD verification study show that prediction uncertainty generally increases with greater site complexity and decreases as the amount and quantity and quality of data available for model calibration increases. This is seen in generally increasing width of confidence bands from Site 1 to Site 3 as well as within Site 1 for a model calibrated to a pre-TSR data set or one that also uses post-TSR data. Within the context of these observations, our conclusion, that the proposed SZD model is a valid and useful tool for evaluating the feasibility of MNA, is given conditionally on our suggestion that probability distributions of predicted outcomes be quantified. Such information will enable site managers to assess the consequences and likelihood of various outcomes to realistically evaluate tradeoffs among various remediation and monitoring strategies.

3.3 **Performance Objective: MNA Sustainability Assessment**

3.3.1 **Explanation of Objective**

The goal of this performance objective was to demonstrate the MNA sustainability assessment at Site 45, MCRD, Parris Island, SC. Results of the SZD served as an estimate for the operational life of the site model, and thus, the modeling timeframe. The approach involved calibrating a site model using MODFLOW2000 to water levels in the hydrostratigraphic unit(s) representative of current site conditions. Using the dissolved PBOC flux and PBOC levels in aquifer sediment as input, the site solute transport model using SEAM3D was calibrated to simulate current site (redox) conditions. The last stage involved simulation DNAPL depletion and plume attenuation over the operational life of the site. Complete details of the methods and results associated with Performance Objective 2 are provided in Appendix H.

3.3.2 *Data Requirements*

The additional data required for this phase of the sustainability assessment was primarily site-specific PBOC results derived from site sediment analysis and DO data derived from site monitoring wells. The latter would be likely derived from existing environmental consulting reports, similar to the data sources described in this report. The PBOC data is the subject of Performance Objective 1, and costs are described in Section 7.

3.3.3 *Success Criteria*

A primary criterion of success for this objective was matching site redox conditions for the STS assessment. Specific calibration targets were simulation of DO concentrations within ± 0.5 mg/L at each monitoring well within the contaminant plume at wells where $DO > 1.0$ mg/L and within \pm

0.25 mg/L DO at wells where DO < 1.0 mg/L. The LTS assessment component was evaluated based on the ability of SEAM3D to operate without significant computational problems over the total simulation time (no more than 2 hours of run time).

3.3.4 *Evaluation of Success*

Results of the STS assessment were successful in that the site model results reasonably matched the observed DO data at Site 45. Observed DO levels were < 0.5 mg/L at the monitoring wells associated with the CVOC plume, and the success criteria were achieved with the largest error in DO concentration of 0.1 mg/L between observed and simulated DO levels. Using the calibrated model as a starting point, the LTS assessment was successfully demonstrated. Using a 100-year analysis timeframe, the run times ranged from 40 to 45 minutes on a desktop computer.

3.4 **Performance Objective: Ease of Implementation**

3.4.1 **Explanation of Objective**

The Technical Demonstration Plan (TDP) called for STS and LTS assessments to be conducted using the NAS platform. NAS is a screening tool for TOR calculations that is designed to run SEAM3D with proven reliability. However, based on input from RPMs and after evaluating the procedures and concerns about run time limitations, it was determined that other platforms were better suited for STS and LTS assessments. Specifically, software platforms for running comprehensive models were determined to be superior and advantageous to software for analytical models.

3.4.2 *Data Requirements*

Data requirements included the complexity of the procedure, the ability to directly query model results over time and within the domain, and computer run time for performing the LTS assessment.

3.4.3 *Success Criteria*

In the TDP, it was proposed that the objective will be considered to be met if a test user could successfully complete a MNA assessment using the proposed platform (i.e., NAS). With the revised approach, an existing platform (GMS, Groundwater Modeling System) was utilized. GMS has many advantages over simpler modeling platforms, particularly for model calibration. Implementing STS and LTS assessments within GMS is extremely straight-forward and requires minimal additional cost in time and resources.

3.4.4 *Evaluation of Success*

Although the success criteria for this qualitative objective described in the TDP was not applicable, NAS was modified to incorporate the SZD function for long-term NAPL dissolution simulations. Ease of implementation of STS and LTS assessments was demonstrated using the MODFLOW and SEAM3D modeling suite within GMS. Calibrating to the redox conditions (i.e., STS) was relatively simple and not time-consuming. Run times for the LTS were based on the SZD results but did not involve significant effort.

4.0 SITE DESCRIPTION

Chlorinated solvent sites used for the performance objectives are listed in Table 4-1. The study sites represent a range of TOC content, geochemical conditions and degree of daughter product formation (based on peak DCE and VC concentrations). Where possible, the specific anaerobic terminal electron accepting processes (TEAP) are identified.

Table 4-1. Summary of Sites for PBOC Validation

Site	Daughter product formation		Geochemistry (TEAP)	Organic carbon (sediment TOC)
	DCE	VC		
OU2 – NAS Jacksonville, FL	≤ 1,600 µg/L	< 710 µg/L	Anaerobic	Moderate
OU2 – NTC Orlando, FL	≤ 230 µg/L	≤ 100 µg/L	Anaerobic ^{1,2}	Low- Moderate
SWMU 118 NWIRP Dallas, TX	≤ 810 µg/L	< 360 µg/L	Aerobic with isolated anaerobic areas	Moderate
Honeywell Site Kansas City, MO	~1,000 µg/L	~ 200 µg/L	Anaerobic ^{2,3}	High (river sediment)
Site 12 NSB Kings Bay, GA	~1,000 µg/L	~ 800 µg/L	Anaerobic ^{1,2,3}	High
NAWC Site Trenton, NJ	≤ 10,000 µg/L	≤ 1,000 µg/L	Anaerobic ^{1,2,3}	High (overburden soils)
WWTP NAS Pensacola, FL	≤ 470 µg/L	≤ 628 µg/L	Anaerobic ^{1,3,4}	High
Site 10 Beale AFB, CA	< 100 µg/L	ND	Aerobic	Low
Areas I&J NAES Lakehurst, NJ	≤ 514 µg/L	< 10 µg/L	Anaerobic ¹ with isolated aerobic areas	Low
East Gate Yard Lewis-McCord, WA	≤ 20,000µg/L	< 4,000 µg/L	Aerobic (upper aquifer); Anaerobic (lower zone)	Low- Moderate
OU 24 NAS North Island, CA	≤ 160,000 µg/L	≤ 450 µg/L	Anaerobic ^{1,2,3}	Moderate
OU4 NTC Orlando, FL	≤ 1,400 µg/L	≤ 28 µg/L	Anaerobic ¹	Low-Moderate
OU2 Hill AFB, UT	≤ 209 µg/L	ND	Aerobic	Low
Site 45 – MCRD Parris Island, SC	≤ 110,000 µg/L	< 3,400 µg/L	Anaerobic ^{1,2,3}	Moderate
OU1 NIROP, MN	Unknown	Unknown	Unknown	Low-Moderate
Site 12 NABLC, VA	≤ 10,000 µg/L	< 400 µg/L	Anaerobic ^{1,2,3}	Moderate
OU1 NUWC Keyport, WA	≤ 61,000 µg/L	≤ 5,100 µg/L	Anaerobic ^{1,2,3}	High
Notes:				
TEAP – terminal electron accepting processes: ¹ Fe(III)-reducing ² Sulfate-reducing ³ Methanogenic ⁴ Mn(IV)-reducing		TOC – Total organic carbon; DCE – cis-1,2-dichloroethene; VC – vinyl chloride.		

Sites where MNA has been or can be evaluated as a remedial strategy were selected but were not limited to locations in which reductive dechlorination was a dominant mechanism for attenuation of a chlorinated solvent plume. Sites where physical mechanisms (e.g., dilution) are a major component to plume attenuation were considered.

Multiple samples were obtained at most of the 17 sites listed in Table 4-1, and all samples were measured for PBOC (Performance Objective 1). For Performance Objective 2, three sites were selected for validation of the SZD function based on data quality and diversity of site conditions. These sites were:

- East Gate Disposal Yard (EGDY), Joint Base Lewis-McChord, WA
- Areas I&J, Naval Air Engineering Station (NAES) Lakehurst, NJ
- Site 45, Marine Corps Recruit Depot (MCRD) Parris Island, SC

Details on the site history, hydrogeology and contaminant distribution are summarized below. Site 45 at MCRD Parris Island, SC was selected for demonstration of the MNA sustainability assessment. After evaluating the quality and quantity of available data, it was determined that Site 45 represented the most well-characterized site where reductive dechlorination was active.

4.1 Site Location and History

4.1.1 East Gate Disposal Yard, Joint Base Lewis-McChord, WA

The Fort Lewis Logistics Center is a 650-acre facility near the northeast corner of the 86,000-acre Joint Base Lewis-McChord complex about 10 miles south of the city of Tacoma in the Puget Sound lowlands of western Washington (Figure 4-1). The Logistics Center, a National Priority List Site, has been an Army facility since 1917, performing aircraft and vehicle maintenance, repairing and refurbishing weapons, and neutralizing caustic paint stripping waste and battery acids. Between 1946 and 1960, the East Gate Disposal Yard (EGDY), also known as Landfill 2, was used for disposing waste from equipment cleaning and degreasing. Material was transported to the disposal yard in barrels and vats from various areas. About seven barrels of liquid waste per month were disposed during peak operation. A TCE plume in the shallow aquifer evolved from the disposal site with concentrations in the range of hundreds $\mu\text{g/L}$ in the source area and concentrations exceeding 5 $\mu\text{g/L}$ over 4 km downgradient (USGS 2005; USACE 2008).

Groundwater contamination was discovered in 1985, a remedial investigation was performed in 1988, and a feasibility study in 1990. Active remediation began in 1995 with installation of two pump and treat systems. Additional extraction wells were added in 2005 and 2006. Disposal trenches were excavated in 2000 to remove contaminated waste buried above the water table. About 1260 drums of contaminant were removed. To reduce DNAPL mass below the water table, thermal source removal (TSR) was implemented for three source zones between late 2003 and early 2007. Tables D-1 and D-2 in Appendix D summarize the activities.

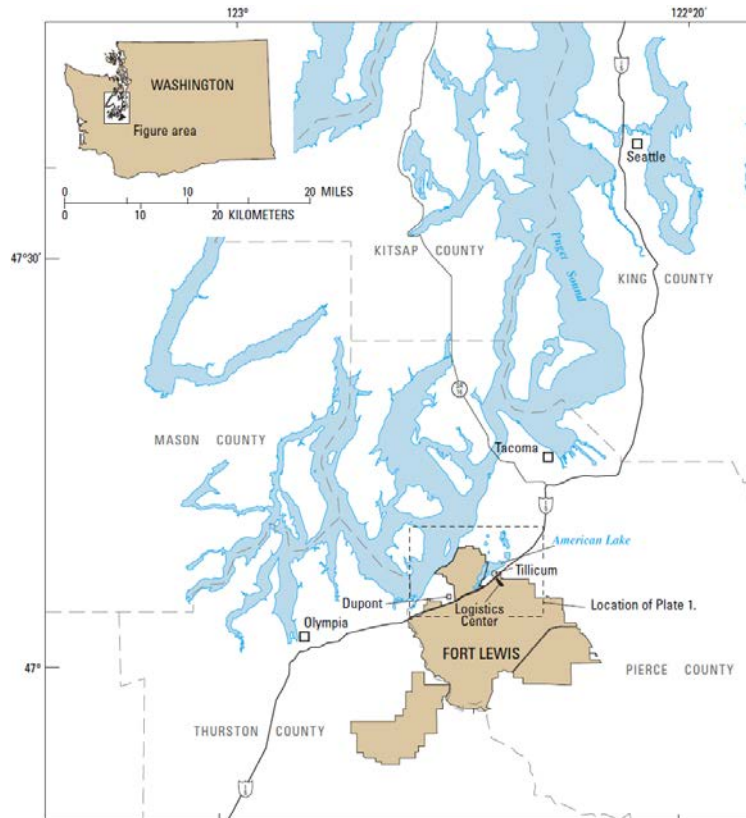


Figure 4-1. Location of Joint Base Lewis-McChord, WA and East Gate Disposal Yard (USGS 2005).

4.1.2 Areas I&J, NAES Lakehurst, NJ

The Naval Air Engineering Station (NAES) Lakehurst station is located within the Pinelands National Reserve in central New Jersey. Lakehurst began as a remote ammunition proving ground in 1915. Currently, Lakehurst operates as the Aircraft Platform Interface Group for technical mission support. Area I, which consists of five contaminants sites, is located in the south central portion of the facility and catapult test facility built in 1958. Area J, which consists of four contaminants sites, is located in the central-western portion of the facility to the west of Area I. In 1960s and subsequent years, disposal of industrial waste water into holding ponds and swales were typical on-site operations at Areas I and J. Figure 4-2 depicts the site map and the cis-1,2-dichloroethene (DCE) plume in groundwater (Dames and Moore 1999).

The first remedial alternative proposed to clean the aquifer at Areas I&J was a ground-water recovery, treatment, and recharge system. Later, a study conducted in late 1993 and early 1994 revealed that this system was not going to be effective in removing the contaminant. Furthermore, it will cause the loss of several acres of wetland. Instead, an MNA-based approach was proposed as a new remedial alternative to restore the aquifer. The MNA remedial alternative started in 1996 and it has proved to be efficient in degrading the CVOC plume in Areas I and J.

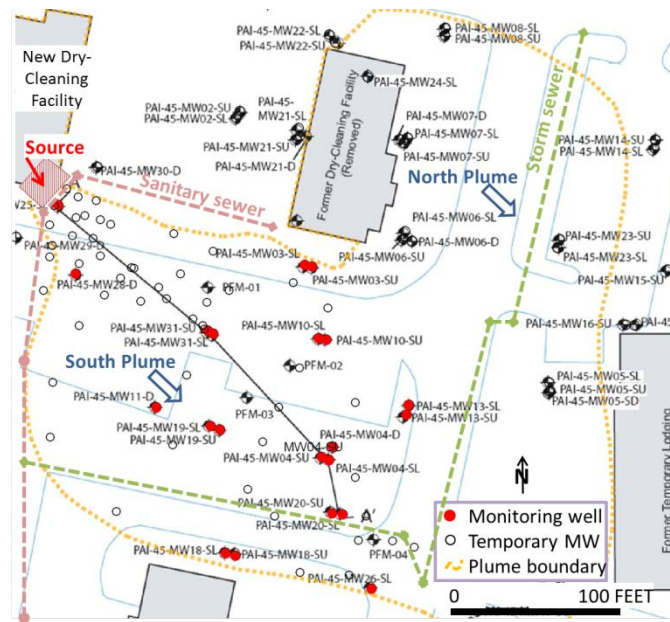


Figure 4-3. Site 45, MCRD Parris Island, SC (modified from USGS 2009).

4.2 Site Geology/Hydrogeology

4.2.1 East Gate Disposal Yard, Joint Base Lewis-McChord, WA

Joint Base Lewis-McChord sits atop a gently rolling upland plain about 200 to 300 feet above sea level. The climate of Fort Lewis is characterized by warm dry summers and cool wet winters with a mean annual temperature of about 13 degrees Celsius and mean annual precipitation of about 1000 mm. Fort Lewis is underlain by a complex and heterogeneous sequence of glacial and non-glacial deposits including a shallow aquifer (Vashon) and a deep aquifer (Sea Level Aquifer, SLA). The Vashon aquifer is unconfined and continuous throughout the area. It ranges in thickness between about 30 to 60 meters. The Vashon and SLA aquifers are separated by a mostly continuous low permeability aquiclude. However, a “window” occurs about 2 km downgradient of the disposal area that allows water and contaminants from the shallow Vashon aquifer to migrate to the deep SLA aquifer. Groundwater generally flows to northwest in the Vashon aquifer and west-southwest in the SLA aquifer. A simplified geologic cross section of the site is shown in Figure 4-4. More details on the site geology are found in USGS (2005), Truex et al. (2006), and USACE (2008).

4.2.2 Areas I&J, NAES Lakehurst, NJ

NAES Lakehurst is located in the Atlantic Coastal Plain. The uppermost aquifer is the Cohansey Sand Formation which is exposed throughout most of the county surface. This formation is permeable and constitutes one of the principal aquifers in the Ocean County. In the vicinity of the NAES, this formation has reported as being a characteristically yellowish-brown, unfossiliferous, cross-stratified, pebbly, ilmenitic fine to very coarse-grained quartz sand that is

locally cemented with iron oxide. Based on excavations conducted within the NAES borders, the upper 20 to 100 feet of strata underlying the center is primarily a fine to coarse grained quartz sand. Fine gravel and silt is commonly present intermixed with the sand. The depth of bedrock in the surrounding area of the NAES Site is approximately 1,800 feet. Pumping tests conducted in the main aquifer of Area I yielded values for the horizontal hydraulic conductivity between 63 and 99 ft/day. The water table is typically shallow with regional values fluctuating between 6 and 40 feet below the surface. The regional horizontal flow rate has been reported to be between 0.15 and 4 ft/day (Dames and Moore 1999).

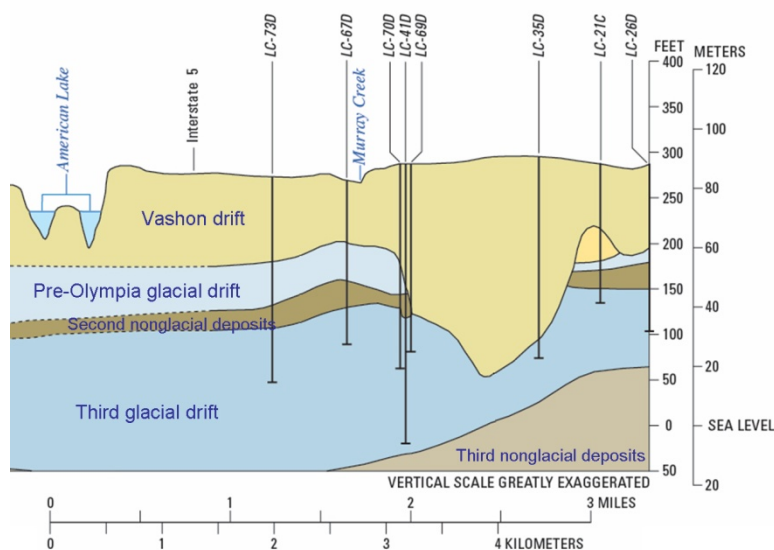


Figure 4-4. Hydrogeologic section of Joint Base Lewis-McChord EGDY Site (USGS 2005).

4.2.3 Site 45, MCRD Parris Island, SC

Site 45 is underlain by a surficial aquifer and the Floridan Aquifer which are separated by confining units comprised of the Hawthorn Formation and Cooper Marl (Tetra Tech NUS, Inc. 2004). The surficial aquifer consists of fine sand interspersed with discontinuous beds of clay, silty clay, silty clayey sand, and clayey silt and extends to a depth of about 18 ft below ground surface (bgs) (Tetra Tech NUS, Inc. 2004). A thin (less than 1 to 3 feet) layer of a complex mixture of sand, silt, clay and a substantial amount of black to brown organic material was encountered below the shallow sandy sediments at depths ranging from 17 to 21 feet bgs (Vroblesky et al. 2009). This complex organic layer is directly underlain by a 3 to 6 foot-thick clay unit, encountered at depths ranging from approximately 18 to 27 feet bgs (Tetra Tech NUS, Inc. 2004). The complex organic layer and clay layer function as a local confining bed at Site 45. The part of the aquifer below this clay is considered to be the “D” horizon (USGS 2009). The surficial aquifer at Site 45 is unconfined and the depth to water is approximately 2 to 6 ft bgs (USGS 2009). Groundwater levels in both the SU and SL wells showed a general movement from the northwest to the southeast with hydraulic influence from the storm sewers (USGS 2009). Primarily for characterizing the chloroethene plume, the surficial aquifer was subdivided into two zones designated as either SU (surficial upper) or SL (surficial lower) for wells deeper than about 10 ft bgs (USGS 2009).

4.3 Contaminant Distribution

4.3.1 East Gate Disposal Yard, Joint Base Lewis-McChord, WA

TCE disposed in trenches produced a dissolved groundwater plume that extends over 15,000 feet downgradient of the source. The contaminant plume migrates in a northwesterly direction in the upper aquifer from the source area towards American Lake (Figure 4-5). South of the lake a large fraction of the plume migrates through a gap in the confining unit to the Sea Level Aquifer where it forms a westerly trending plume.

The upper aquifer is aerobic. Dissolved organic content is low, although high organic content layers occur interbedded with finer grained sediments. The lower aquifer is generally anaerobic, except in areas that receive high recharge from the upper aquifer, which unfortunately includes the plume downgradient of the confining unit window through which the plume migrates.

Near the source area, TCE concentrations generally range from 500 to >50,000 $\mu\text{g/L}$ with DCE concentrations from 100 to >500 $\mu\text{g/L}$. In the body of the plume, TCE concentrations range from 100 to 200 $\mu\text{g/L}$ with c-DCE from 10 to 50 $\mu\text{g/L}$. VC concentrations in the unconfined aquifer have been below detection in all but two source area well. The USGS (2005) performed detailed studies of groundwater geochemistry at the site including an analysis of common ions, redox conditions and isotopic tracers.

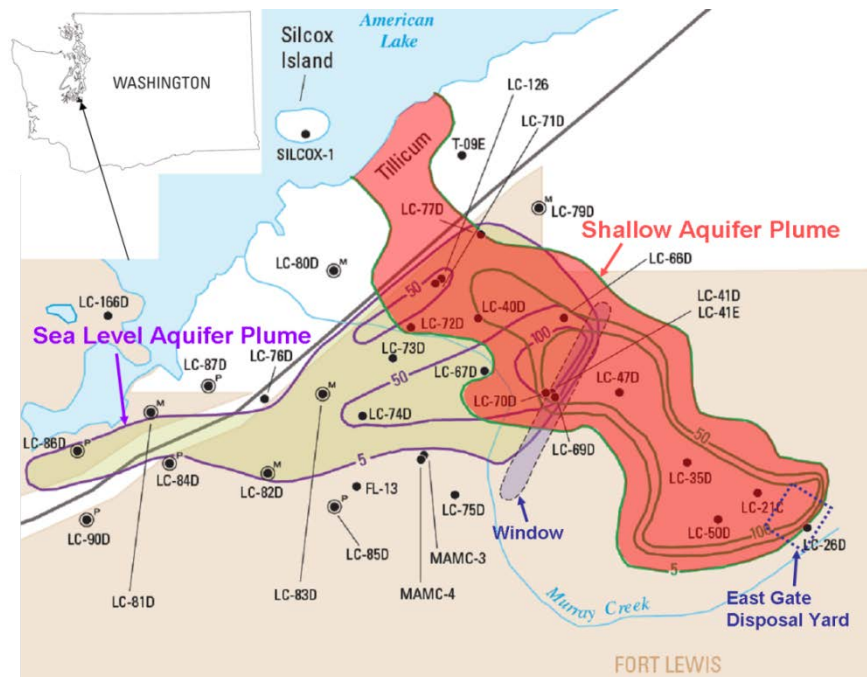


Figure 4-5. Contaminant distribution at EGDY, Joint Base Lewis-McChord, WA (USGS 2005).

4.3.2 Areas I&J, NAES Lakehurst, NJ

Contaminant plumes located in Areas I & J (one North plume and two South plumes; see Figure 4-2 above) are primarily due to the discharge of water containing TCE, hydraulic fluid and ethylene glycol, along with the steam-cleaning operation of equipment. The North plume starts in a region close to Site 25, and then, contaminants are transported by the ground-water system in the east direction approximately 5,000 feet (see Figure 4-2). This plume is widely spread due to changes observed in the flow direction. The South plume nearest North plume derives from an area covered by Sites 6, 7, and 24 and spans 4,000 feet in the east direction. The second South plume extends to the southeast from Site 3 over a distance of 3,000 feet.

The highest levels of contaminants are registered in deep wells (between 50 and 70 feet depth) in all three plumes (Figure 4-6). The predominant constituent in these three plumes is DCE. The concentration data suggest that the plumes are in steady state due to natural attenuation (Dames and Moore 1999). The aquifer is primarily anaerobic in nature, but approximately 2400 ft downgradient of the source zone of the north plume, the redox condition of the aquifer is aerobic. Contaminant data in the source well clearly supports that the redox conditions existing in the aquifer promote the reductive dechlorination as the preferential biodegradation process.

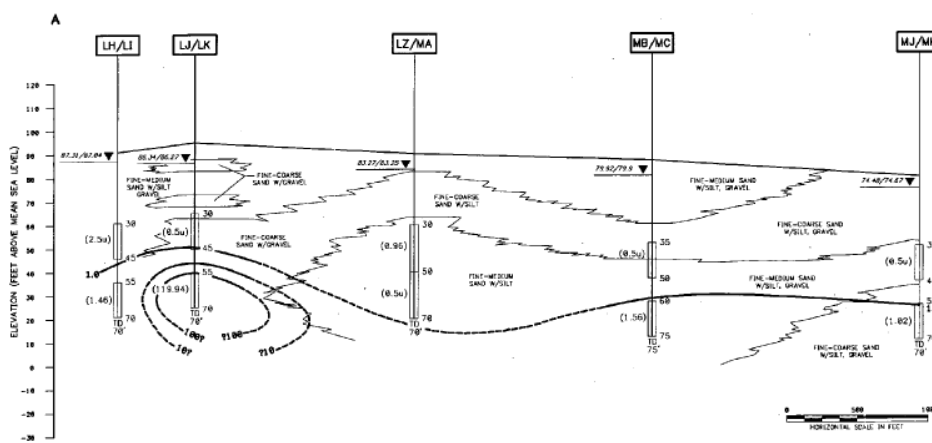


Figure 4-6. Cross section of chlorothene plume along north plume centerline at Areas I&J, NAES Lakehurst (Dames and Moore, 1999).

4.3.3 Site 45, MCRD Parris Island, SC

The two PCE plumes at Site 45, identified as the northern plume and the southern plume, are illustrated in Figure 4-7. The focus of this project is the southern plume which primarily is located in the lower depths of the surficial aquifer (i.e., SL wells). Source area concentrations of PCE (62,400 $\mu\text{g/L}$) indicate the presence of a DNAPL (USGS 2009). High concentrations of TCE, DCE and VC throughout the plume combined with oxygen-depleted groundwater indicate conditions promoting reductive dechlorination. Peak concentrations of TCE, DCE and VC were located along the centerline of the plume (7,590, 2,180 and 377 $\mu\text{g/L}$, respectively).

5.0 TEST DESIGN

5.1 Conceptual Experimental Design

Evaluation of the quantitative performance objectives was achieved using historical monitoring well data and measures of PBOC. Evaluation of the SZD function required data indicating historical trends in contaminant source depletion while explicitly addressing uncertainty of predictions. In the evaluation of STS and LTS at Site 45 (MCRD, Parris Island, SC), readily-biodegradable carbon must be quantified and incorporated into the model as input. The MNA sustainability assessment requires a site model constructed using SEAM3D to simulate current site conditions (i.e., STS) and estimate the potential for sustaining conditions favorable for reductive dechlorination over the project life cycle (i.e., LTS).

5.2 Baseline Characterization

No baseline characterization activities were required for this project other than screening sites for required data from reports such as RI/FS or annual monitoring assessments. Based on this information, sites were characterized as either exhibiting high, moderate or low levels of reductive dechlorination as a means of obtaining a wide range of conditions for validation of the PBOC method. PBOC analysis was performed following site selection, and results were not utilized for baseline characterization. No additional measurements were required.

5.3 Treatability or Laboratory Study Results

Because MNA is based on natural processes only, no treatability studies were performed during this project.

5.4 Design and Layout of Technology Components

No design and layout of technology components were proposed; therefore, this section is not applicable.

5.5 Field Testing

No field testing of technology components was conducted during execution of this project; therefore, this section is not applicable.

5.6 Sampling Methods

Table 5-1 provides a summary of the number of samples collected at each of the 17 study sites. Note that an unequal number of samples were collected at each site. The aim was to obtain at least one representative sample at each site in a hydrostratigraphic unit where contaminant migration was known to occur. At several sites, resources were available to collect more samples, and in a few cases, a significant number of samples (> 20) were obtained. In particular,

significant sampling efforts were performed at Site 12, NAB Little Creek, VA and Site 45, MCRD Parris Island, SC.

Table 5-1. Total Number and Types of Samples Collected.

Component	Matrix	Number of Samples	Analyte	Location
Technology performance sampling	Aquifer sediment/Soil	1	PBOC, TOC	OU2 – NAS Jacksonville, FL
	Aquifer sediment/Soil	2	PBOC, TOC	OU2 – NTC Orlando, FL
	Aquifer sediment/Soil	3	PBOC, TOC	SWMU 118 NWIRP Dallas, TX
	Aquifer sediment/Soil	1	PBOC, TOC	Honeywell Site Kansas City, MO
	Aquifer sediment/Soil	8	PBOC, TOC	Site 12 NSB Kings Bay, GA
	Aquifer sediment/Soil	3	PBOC, TOC	NAWC Site Trenton, NJ
	Aquifer sediment/Soil	2	PBOC, TOC	WWTP NAS Pensacola, FL
	Aquifer sediment/Soil	11	PBOC, TOC	Site 10 Beale AFB, CA
	Aquifer sediment/Soil	1	PBOC, TOC	Areas I&J NAES Lakehurst, NJ
	Aquifer sediment/Soil	8	PBOC, TOC	East Gate Yard Fort Lewis, WA
	Aquifer sediment/Soil	3	PBOC, TOC	OU 24 NAS North Island, CA
	Aquifer sediment/Soil	2	PBOC, TOC	OU4 NTC Orlando, FL
	Aquifer sediment/Soil	4	PBOC, TOC	OU2 Hill AFB, UT
	Aquifer sediment/Soil	96	PBOC, TOC	Site 45, MCRD Parris Island, SC
	Aquifer sediment/Soil	2	PBOC, TOC	OU1 – NIROP, MN
	Aquifer sediment/Soil	21	PBOC, TOC	Site 12 – NABLC, VA
	Aquifer sediment/Soil	1	PBOC, TOC	OU1 NUWC Keyport, WA

Sample collection and laboratory analysis followed methods provided in the TDP. Not all samples were collected by project team. Instead, at a subset of sites, samples were collected during the course of routine field activities in cooperation with site RPMs. At these sites, the local facility plan for collection of samples was followed. However, no deviation from the method of preservation or storage of the samples occurred. Table 5-2 lists the analytical methods performed. Detailed descriptions of sampling methods are provided in Appendix E.

Table 5-2. Analytical Methods for Sample Analysis.

Matrix	Analyte	Method	Container	Preservative	Holding Time
Soil	PBOC	Appendix B	8-oz glass jar	Cooled – 4°C	60 days
	TOC	Appendix B	8-oz glass jar	Cooled – 4°C	60 days
	THAA	Appendix B	8-oz glass jar	Cooled – 4°C	60 days

5.7 Sampling Results

This section summarizes the primary sampling results from the PBOC analysis of site samples. Detailed sampling results for the sites where spatial distribution was evaluated (i.e., Site 12, NAB Little Creek, VA and Site 45, MCRD Parris Island, SC) are also included. Results and discussion including comparison to other site data (i.e., Metrics 1-3) in conjunction with Performance Objective 1 are presented in Section 6.

5.7.1 Overall PBOC Results

The total number of samples collected was 168 with 69% of the samples collected at two of the fifteen sites: Site 12, NAB Little Creek, VA and Site 45, MCRD Parris Island, SC, where spatial variability was investigated. The detailed sampling plan at these 2 sites was the result of an Action Item resulting from the February 2010 In Progress Review. The Action Item stated: “In the case of a site at which natural attenuation has been underway for several years, would one expect to see a difference in BOC close to the source zone relative to further away? Is it possible to investigate such a case in the field?”

The vast majority of the samples (~82%) were characterized as aquifer sediment with the remaining samples derived from over-burden soils or confining units that have some influence on concentrations of DOC in site groundwater. Figure 5-1 depicts the range in the mean PBOC concentrations for the 15 study sites. The graph shows that mean values of PBOC in aquifer sediment varied by two orders of magnitude. Mean site values for PBOC in aquifer sediment

ranged from 12.5 to 998 mg/kg. For the remaining samples, PBOC ranged from 549 mg/kg (soil) to 14,200 mg/kg (confining unit).

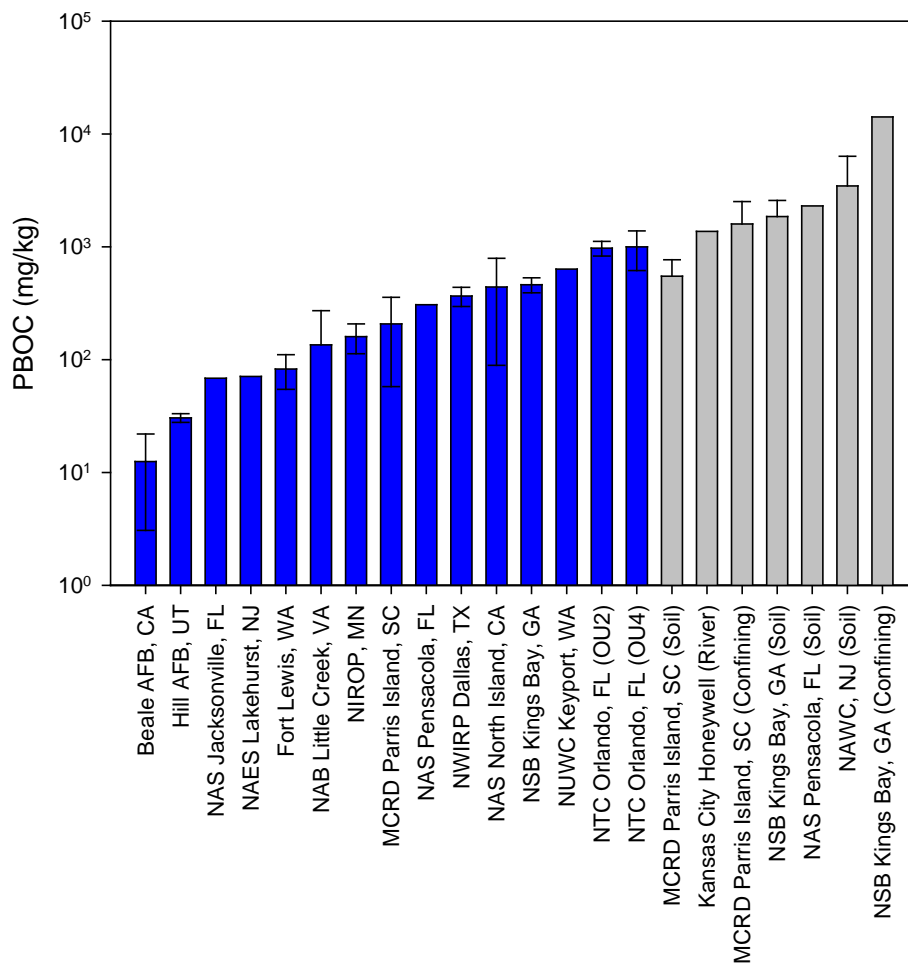


Figure 5-1. Range of mean potentially bioavailable organic carbon (PBOC) values for aquifer (blue) and non-aquifer (gray) samples.

5.7.2 Spatial Variability of PBOC

5.7.2.1 Site 12, NAB Little Creek, VA

Chloroethene contamination at NABLC Site 12 is limited to the Columbia Aquifer, the uppermost hydrostratigraphic unit (CH2M Hill 2000). The unconfined aquifer is approximately 20-25 feet thick and is comprised of Pleistocene deposits that are characterized by well-sorted, coarse sand with dispersed lenses of clay, silt, and gravel. Sampling locations within the Columbia unit are shown in Figure 5-2. MLS10 was located from outside and upgradient of the plume. Three locations within the plume were sampled: MLS12, MLS20, and MLS22. Shallow depth samples contained brown coarse sand. PBOC and TOC ranged from 6.4-180 mg/kg and 18-460 mg/kg, respectively. Deep samples were characterized as well sorted sand with grey silt and clay

dispersed throughout the sample. PBOC and TOC ranged from 36-440 mg/kg and 97-1200 mg/kg mg/kg, respectively. A spatial comparison of PBOC results are shown in Figure 5-3.

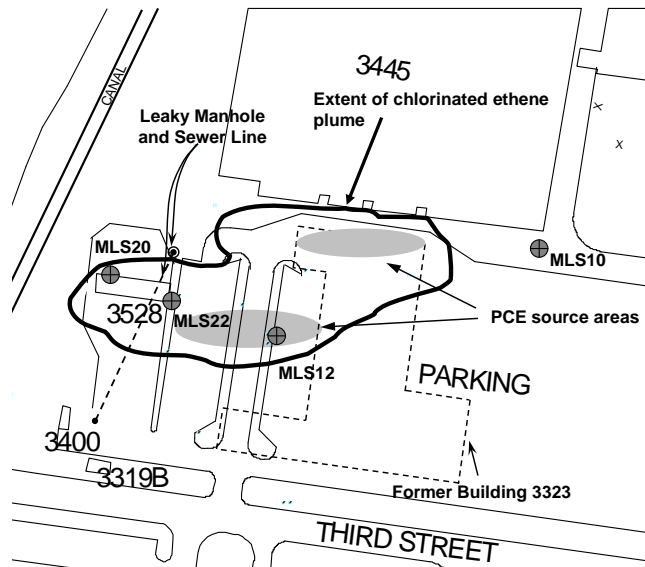


Figure 5-2. Sampling locations at NAB Little Creek Site 12.

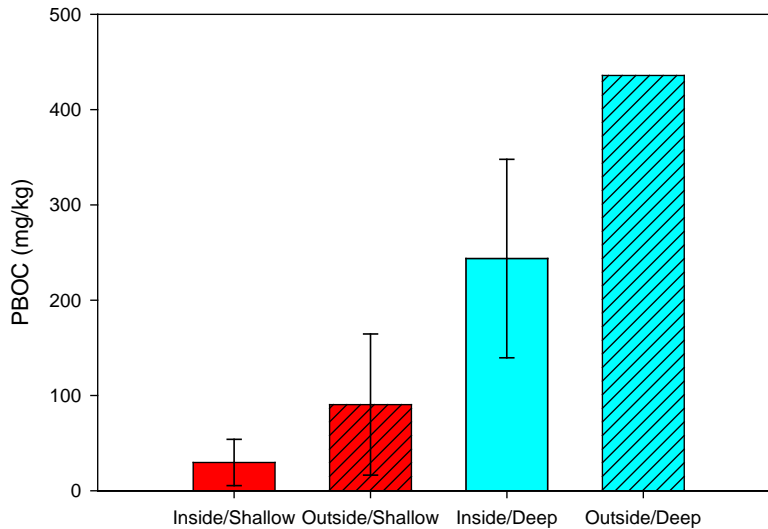


Figure 5-3. Comparison of mean potentially bioavailable organic carbon (PBOC) in shallow (upper 8 ft of saturated zone) and deep (lower 6 ft) at NAB Little Creek Site 12.

These results demonstrate how PBOC level are influenced by lithologic differences in a contaminated hydrostratigraphic unit. Shallow samples collected in the upper 8 ft of the saturated zone displayed lower PBOC levels compared to the deeper samples (lower 6 ft). Total

chloroethene concentrations inside the plume ranged from 13 to 5,650 $\mu\text{g/L}$ and 1,660 to 13,410 $\mu\text{g/L}$ at the shallow and deep sampling locations, respectively. A comparison of PBOC levels with background samples not impacted by chlorinated solvents show the mean values in both horizons of the aquifer were considerably lower inside the plume (Figure 5-3).

5.7.2.2 Site 45, MCRD Parris Island, SC

Figure 5-4 shows the distribution (N=96) of natural logarithm values of PBOC in sediments collected at MCRD Site 45. The plot suggests a log-normal distribution to the PBOC values. The average concentration for PBOC in aquifer sediments was 207 mg/kg with a standard deviation of 149 mg/kg. Relative to the aquifer sediment, samples collected in overburden soils showed higher levels of PBOC (mean = 549 mg/kg, N = 12). The highest levels of PBOC at Site 45 were found in the organic-rich confining layer, ranging from 593 to 3,320 mg/kg (mean = 1,590 mg/kg, N = 12).

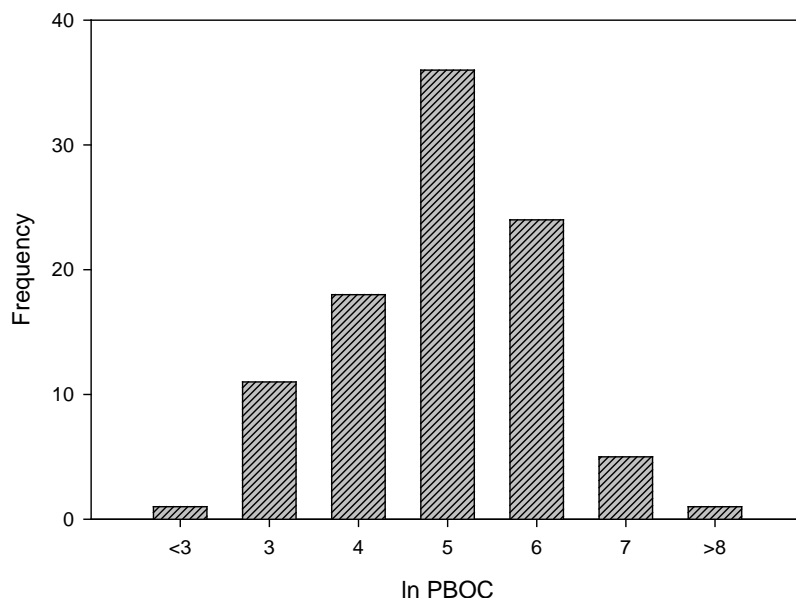


Figure 5-4. Frequency distribution of potentially bioavailable organic carbon (PBOC) results at Site 45, MCRD Parris Island, SC.

As shown in Figure 5-5, the quantity of PBOC in aquifer sediments outside the chloroethene plume was greater than inside of the plume by a factor of 2.0 and 1.4, respectively, for surficial upper and lower samples. PBOC was statistically significantly greater ($p < 0.05$) for sediment samples collected outside the chloroethene plume in the Surficial Upper (SU) samples, when compared to sediments collected inside the plume. For the Surficial Lower (SL) samples, there was not a statistically significant difference ($p > 0.05$) in PBOC levels for sediment samples collected inside and outside of the chloroethene plume.

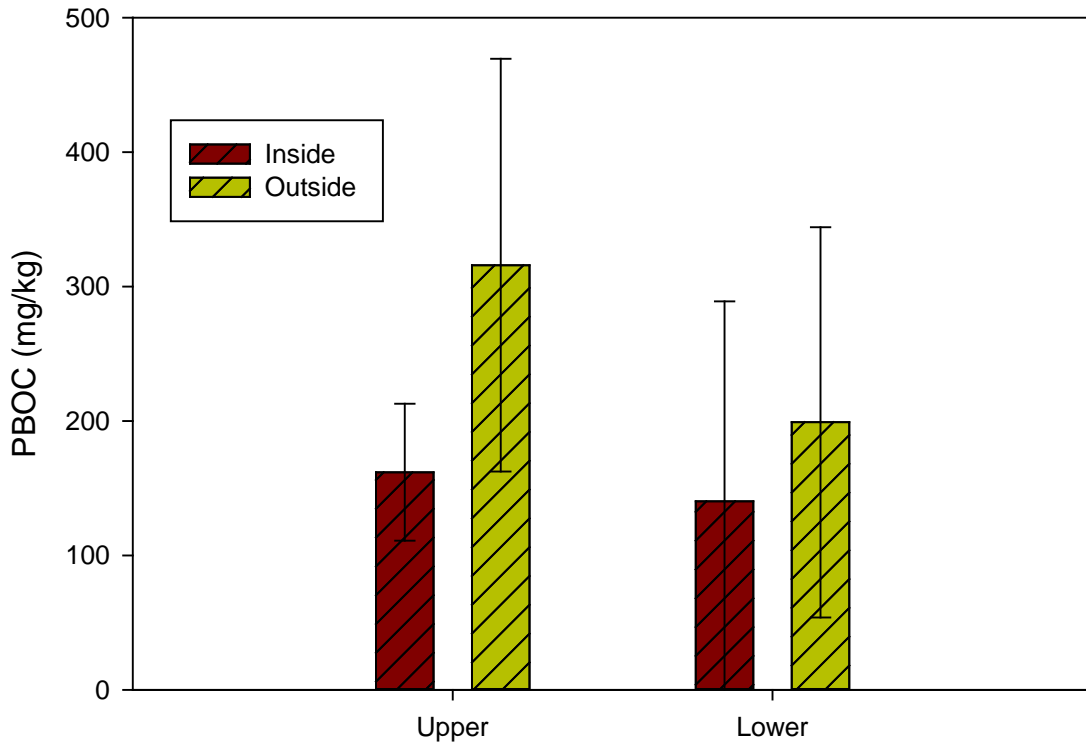


Figure 5-5. Frequency distribution of potentially bioavailable organic carbon (PBOC) results at Site 45, MCRD Parris Island, SC.

Although not statistically conclusive, the overall results from the intensive site studies indicate differences in extractable organic carbon from aquifer sediments with minimal chloroethene exposure relative to samples collected in the highly-contaminated areas of each site. Results show that chloroethene concentrations in the groundwater system inversely correlate with levels of PBOC in aquifer sediments and suggest that the long-term chloroethene exposure can contribute to the depletion of PBOC.

6.0 PERFORMANCE ASSESSMENT

6.1 Performance Objective: Validation of PBOC Method

One primary and two secondary metrics were identified for validating the PBOC method: The primary metric was correlation of PBOC levels with site monitoring data indicative of reductive dechlorination. Secondary metrics were correlation of PBOC levels with (1) TOC and AA concentrations in aquifer sediments and (2) laboratory measures of reductive dechlorination.

6.1.1 Metric 1: Correlation with Site Monitoring Data

DO concentrations were evaluated in groundwater samples using pre-remediation performance well data collected from 11 study sites. Appendix F provides tabulated information on the number of sampling events, DO concentrations, and corresponding standard deviation values for each study site. DO ranged from ND to 6.42 ± 0.83 mg/L. The lowest DO concentrations were observed at NSB Kings Bay, GA, which exhibited relatively efficient reductive dechlorination of chloroethenes (Chapelle et al. 2005). In contrast, the highest concentrations of DO were observed at Beale AFB, CA, which exhibited relatively inefficient reductive dechlorination (CH2M Hill).

Figure 4-1 shows the average concentrations of DO plotted versus PBOC for each site. At eight sites which exhibited moderate to high reductive dechlorination activity, the mean DO concentrations were ≤ 0.5 mg/L and PBOC concentrations were greater than 200 mg/kg. At sites where little or no reductive dechlorination activity was observed, mean concentrations of DO and PBOC were > 0.8 mg/L and < 75 mg/kg, respectively.

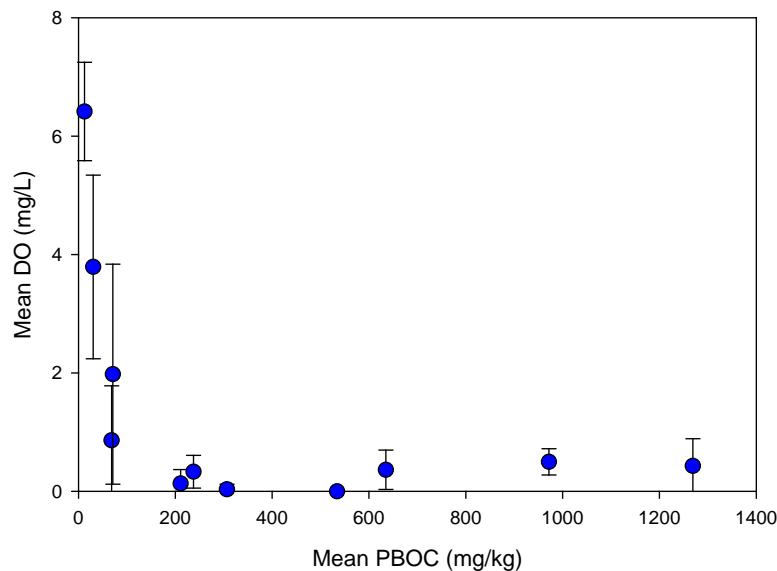
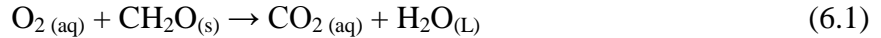


Figure 6-1. Mean dissolved oxygen (DO) in groundwater versus concentrations of potentially bioavailable organic carbon (PBOC) measured in aquifer sediments at 11 study sites. Standard deviations for DO concentrations are shown with error bars.

Regression results demonstrated statistically significant ($p < 0.0001$) inverse correlations for PBOC and DO concentrations following a hyperbolic regression equation. PBOC was a significant indicator of DO levels, accounting for 96% ($R^2 = 0.96$; $p < 0.0001$) of the variation in DO levels. These results can be explained by considering the reaction of DO and sedimentary organic carbon (SOM) in aquifer sediments which can be approximated by stoichiometry:



where $[CH_2O_{(s)}]$ represents the concentration of SOM with carbon of valence zero. In groundwater systems that are partially isolated from atmospheric oxygen and which lack photosynthesis, Equation 6.1 is irreversible and the reaction quotient (Q) can be written:

$$Q = \frac{[CO_2][H_2O]}{[CH_2O][O_2]} \quad (6.2)$$

The value of Q, which is not a constant, reflects the degree to which Equation 6.1 has proceeded from left to right. Assuming that reaction products do not affect reaction progress, unit concentrations can be assigned to $[CO_2]$ and $[H_2O]$ in Equation 6.2, and the expression becomes:

$$Q = \frac{1}{[CH_2O][O_2]} \quad (6.3)$$

Rearranging Equation 6.3 so that $[DO]$ is expressed as a function of $[CH_2O_{(s)}]$ gives:

$$[O_2] = \frac{1}{Q[CH_2O]} \quad (6.4)$$

Equation 6.4 is a decaying hyperbolic equation ($y = 1/x$), and this behavior stems directly from the stoichiometry of Equation 6.1. The inflection point between high DO-low SOM concentrations and low-DO-high SOM concentrations in Equation 6.4 is one measure of the amount of CH_2O needed to consume DO and initiate reductive dechlorination. Concentrations of CH_2O necessary to accomplish this cannot be determined *a priori*, but rather must be determined by field observations. Consistent with theory, the data show that there is a decaying hyperbolic relationship observed. *More importantly, the data suggests that DO concentrations approach zero at a PBOC concentration of approximately 200 mg/kg.* This, in turn, suggests that a PBOC concentration of approximately 200 mg/kg is necessary in order to establish anoxic conditions.

In addition to assessing DO concentrations, site monitoring data where H_2 concentrations in groundwater were collected was also evaluated. Hydrogen concentrations were derived from five study sites. Sampling locations included the following study sites: MCRD Parris Island, NAS Pensacola, NTC Orlando OU2, NUWC Keyport, NSB Kings Bay. Appendix G includes tabulated data on the number of sampling events, H_2 concentrations, and corresponding standard

deviation values for each selected site. Hydrogen levels for the selected sites ranged from 0.95 ± 1.64 to 5.67 ± 1.76 nM (NAS Pensacola and NTC Orlando OU2, respectively).

At four of the five sites which exhibited moderate to high reductive dechlorination activity (the exception being NTC Orlando OU2), the average H_2 concentrations were greater than or equal to 0.95 nM, with corresponding PBOC concentrations ranging from 211.0 to 635.0 mg/kg. For these sites, H_2 levels were characteristic of sulfate-reducing conditions. Greater levels of H_2 and PBOC were reported at NTC Orlando, FL (OU2), which exhibited methanogenic conditions. As shown in Figure 6-2, the data confirm the relationship between higher H_2 concentrations (i.e., strongly-reducing conditions), which is consistent with conditions favorable for reductive dechlorination, and higher concentrations of PBOC. However, results show only a moderate linear relationship existed between H_2 and PBOC concentrations ($R^2 = 0.62$; $p = 0.113$), and the slope of the correlation between PBOC and H_2 is not statistically significant ($p > 0.05$).

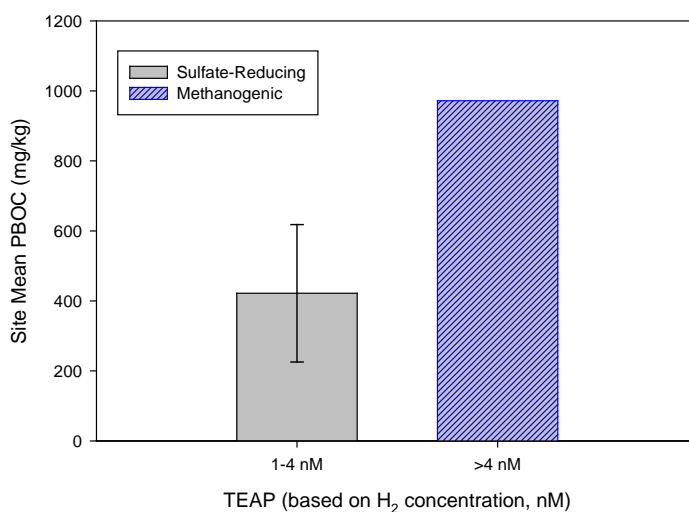


Figure 6-2. Mean potentially bioavailable organic carbon (PBOC) for two terminal electron acceptor processes (TEAPs). Error bars indicate standard deviations of PBOC.

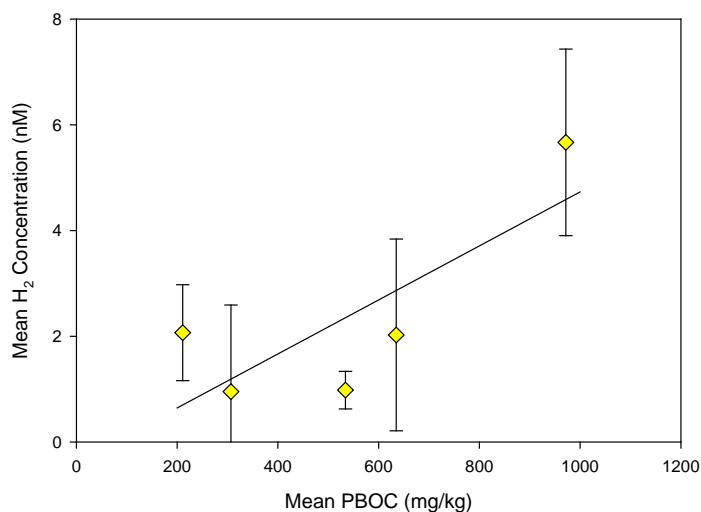


Figure 6-3. Mean hydrogen (H₂) concentration in groundwater versus concentrations of potentially bioavailable organic carbon (PBOC) measured in aquifer sediments at 5 sites. Standard deviations for H₂ concentrations are shown with error bars.

Concentrations of total chloroethenes were evaluated along the groundwater flowpath using pre-remediation performance well data collected from 10 study sites. Sampling locations included NAES Lakehurst, Hill AFB, Beale AFB, NAB Little Creek, MCRD Parris Island, NAS Pensacola, NTC Orlando OU4, NUWC Keyport, NAS North Island, and NSB Kings Bay. Figure 6-4 shows the NAC of each site plotted versus mean PBOC site values. At the latter seven sites, which exhibited moderate to high reductive dechlorination activity, NAC values were greater than or equal to 0.0060 ft⁻¹, and PBOC concentrations ranged from 211.0 to 1269.1 mg/kg. Lower NAC values and concentrations of PBOC were obtained for sites demonstrating minimal reductive dechlorination activity. Overall, results suggest a positive correlation. Linear regression exhibited a reasonable relationship between NAC and PBOC ($R^2 = 0.75$).

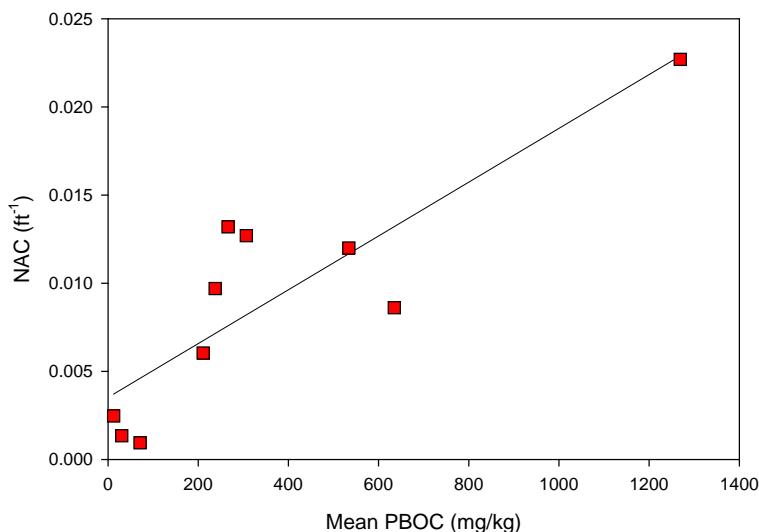


Figure 6-4. Natural attenuation capacity (NAC) of chloroethenes plumes versus concentrations of potentially bioavailable organic carbon (PBOC) measured in aquifer sediments at 10 study sites.

6.1.2 Metric 2: Correlation with TOC and HAA Concentrations

Concentrations of TOC plotted versus PBOC measured in aquifer sediments from the different study sites are shown in Figure 6-5. All results fell below the 1:1 line indicating that PBOC represents a fraction of the total carbon. A fairly consistent trend between TOC and PBOC is evident at all sites with the exception of Hill AFB and NWIRP. At each of the other sites, the ratio of TOC to PBOC was 10:1 or less. These sites represent outliers with ratios of 18:1 and 72:1, respectively. In particular, aquifer sediments collected at NWIRP demonstrated some of the highest levels of TOC while exhibiting a mean PBOC concentration just slightly greater than the average value of the site means. For the remaining data, regression results demonstrate a favorable relationship between PBOC and TOC, resulting in $R^2 = 0.79$.

The power relationship shown in Figure 6-5 where the exponent (b) $\neq 1$ indicates that TOC:PBOC is not a uniform ratio and that with $b < 1$, the amount of PBOC as a fraction of TOC declines with increasing total carbon. *This result strongly suggests that TOC, or some simple fraction thereof, is not an equivalent measure of PBOC.* Because TOC certainly overestimates the amount of bioavailable carbon, and because PBOC probably underestimates the amount of bioavailable carbon, it is likely that these two values effectively bracket the amount of bioavailable organic carbon in sediments.

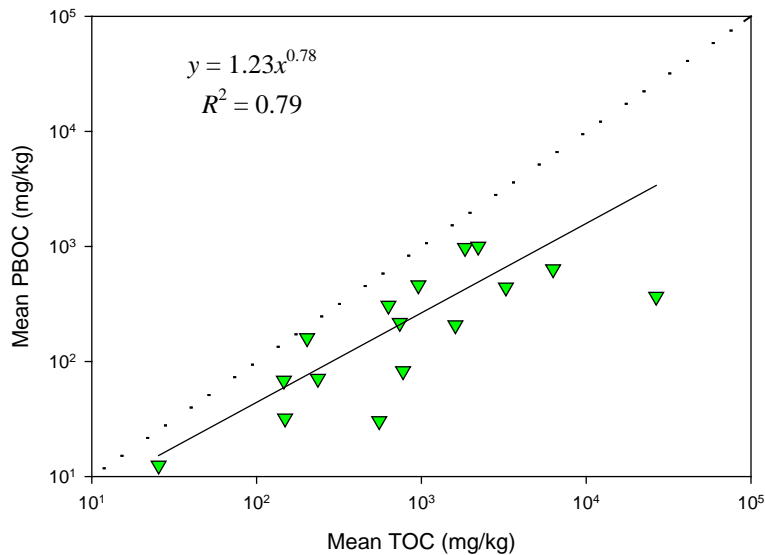


Figure 6-5. Mean site values for potentially bioavailable organic carbon (PBOC) and total organic carbon (TOC) measured in aquifer sediments at 15 study sites. Two values for NABLC are represented as means for the upper and lower surficial aquifer. Mean PBOC-TOC values at NWIRP and Hill AFB was omitted from the regression.

Sampling locations included the following study sites: NAB Little Creek, NSB Kings Bay, Beale AFB, NAS Pensacola, NAS North Island, NTC Orlando OU2, NTC Orlando OU4, MCRD Parris Island, Kansas City Site, and NAWC. In aquifer samples concentrations of THAA and PBOC ranged from 0.67 to 49.5 mg/kg and 4.21 to 1,270 mg/kg, respectively, with mean values of 9.9 and 391 mg/kg, respectively. Significantly larger THAA values (138 to 14,900 mg/kg) were observed in samples collected from surficial soils (NSB Kings Bay and NAWC), an aquitard (NSB Kings Bay) and riverbed sediment (Kansas City).

Results comparing THAA to PBOC concentrations suggest a moderate positive correlation (Figure 6-6). Concentrations of THAA and PBOC for the NTC Orlando sites do not follow similar regression trends as the remaining sites. NTC Orlando sites show relatively low levels of THAA (<2 mg/kg) along with relatively high levels of PBOC (>700 mg/kg). Generally, sites with the higher concentrations of THAA corresponded to sites with moderate to strong reductive dechlorination activity. The NTC Orlando sites exhibited THAA concentrations in the same range as Beale AFB, which exhibited minimal reductive dechlorination activity. Even by excluding the NTC Orlando sites from regression analysis, the scatter in the data for the aquifer samples yields a power equation with $R^2 = 0.58$.

In addition, it was observed that for concentrations of PBOC below approximately 200 mg/kg, concentrations of THAA were fairly constant at 3.6 ± 1.8 mg/kg. When PBOC concentrations were greater than 200 mg/kg, THAA concentrations increased steeply. Hydrolysable amino acids are an important component of microbial biomass. One interpretation of these data, therefore, is that the amount of viable microbial biomass increases linearly once PBOC concentrations rise above 200 mg/kg. In any case, there is evidence of an inflection point for THAA concentrations at a PBOC concentration of approximately 200 mg/kg which is consistent with the inflection point for DO (Figure 6-1).

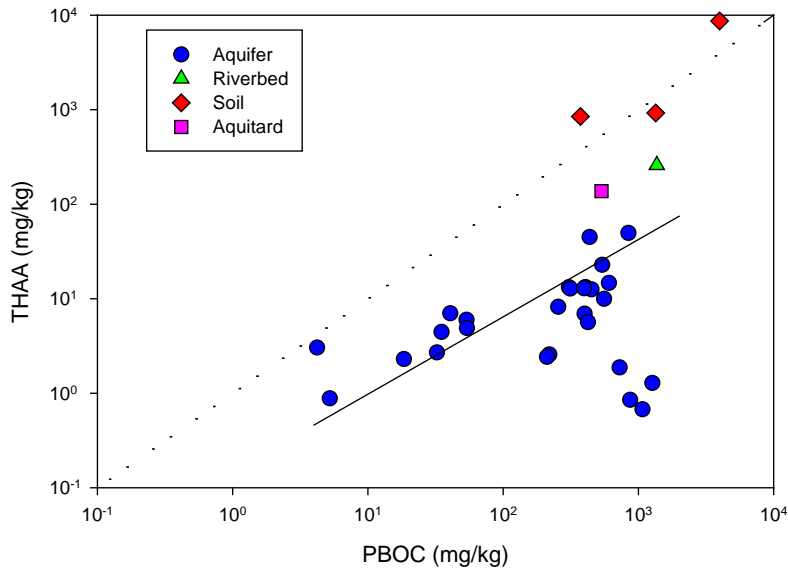


Figure 6-6. Concentrations of total hydrolysable amino acids (THAA) plotted versus potentially bioavailable organic carbon (PBOC).

Figure 6-7 shows mean THAA and mean PBOC values at the sites where aquifer sediment samples were analyzed. Mean values for NTC Orlando OU2 and OU4 were excluded from the plot and regression analysis. Regression analysis showed that THAA exhibited a positive log-log correlation with PBOC ($R^2 = 0.84$); however, the success criterion was only achieved but removing the outliers where low levels of THAA were measured.

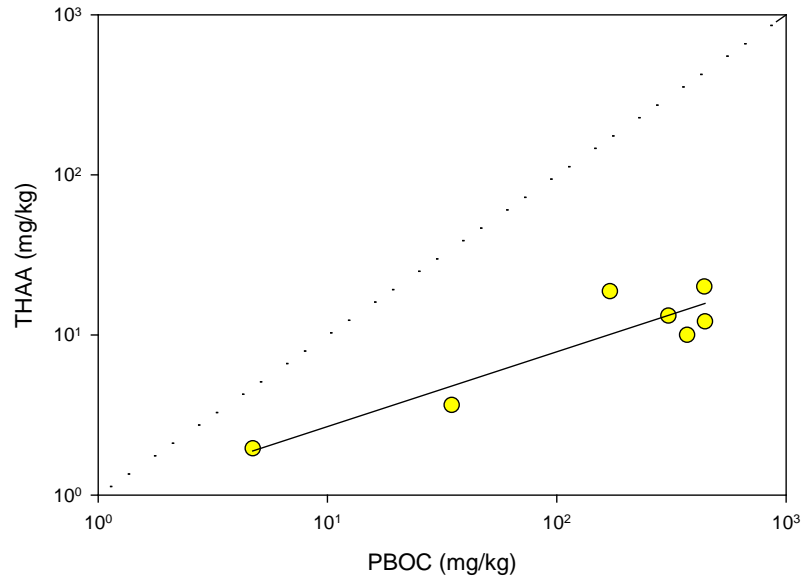


Figure 6-7. Mean site values for total hydrolysable amino acids (THAA) and potentially bioavailable organic carbon (PBOC) measured in aquifer sediments at 9 study sites.

6.1.3 Metric 3: Correlation with Laboratory Measures of Reductive Dechlorination

Laboratory incubation tests were performed using sediment samples from seven sites: NAES Lakehurst; NAS North Island; NAS Pensacola; NAS Jacksonville; MCRD Parris Island; NTC Orlando OU2 and OU4) and riverbed sediment at the Kansas City site. Production of CO₂ in microcosms resulting from oxidation of reductive dechlorination daughter products (VC and DCE) served as an indirect measure of reductive dechlorination activity. Figure 6-8 depicts the relationships between CO₂ production and levels of PBOC (upper plot) and THAA (lower plot). Positive correlations between the CO₂ production rate and concentrations of PBOC (linear, R²= 0.60) and THAA (power, R²= 0.72) were apparent.

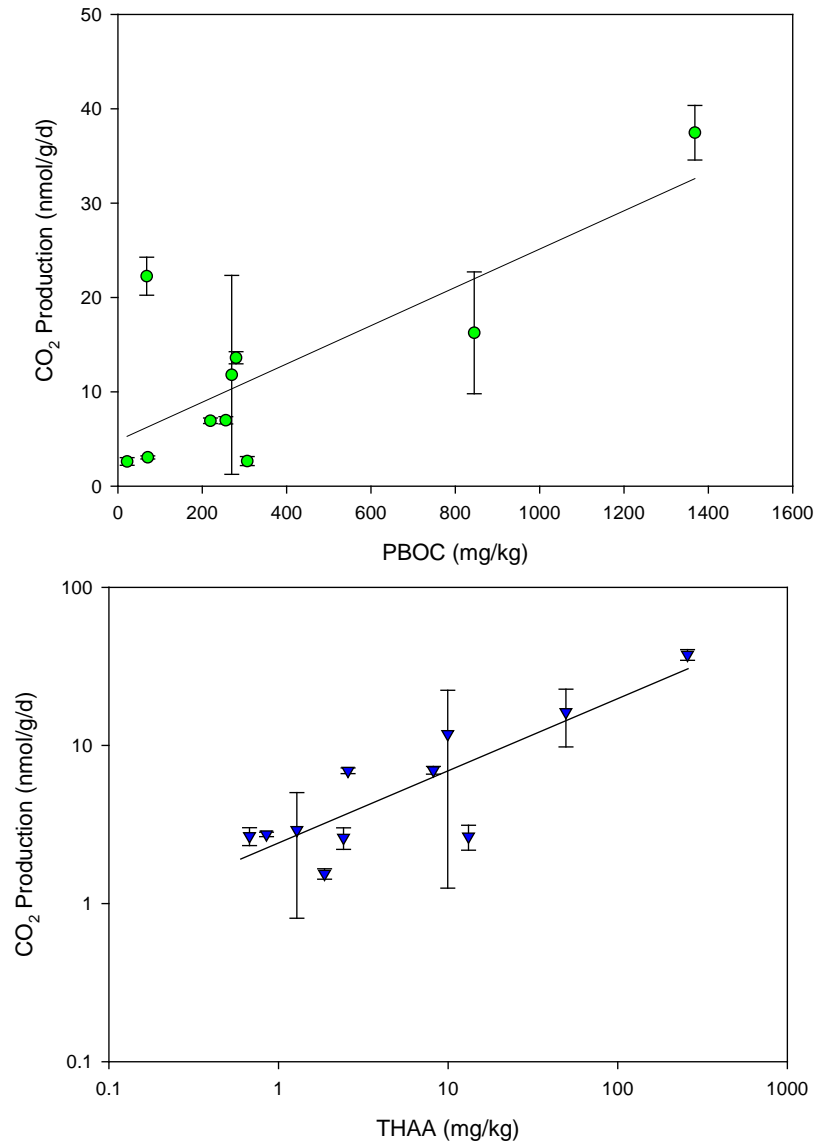


Figure 6-8. Rate of CO₂ production in incubation tests versus potentially bioavailable organic carbon (PBOC) and total hydrolysable amino acids (THAA).

6.2 Performance Objective: Time Estimates of SZD

Complete details of the modeling associated with Performance Objective 2 are provided in Appendix G. Descriptions of the DNAPL source depletion model and the solute transport model used to construct the site models are provided in Sections G.1 and G.3, respectively. The procedure of groundwater flow mapping is described in Appendix G.2.

6.2.1 Site 1: East Gate Disposal Yard, Joint Base Lewis-McChord, WA

A unique opportunity for verification of the SZD model was provided by extensive data available at Joint Base Lewis-McChord (JBLM), which included direct measurements of mass discharge from three delineated source zones before and after thermal source reduction (TSR) performed between 2004 and 2007. The three mostly TCE sources produce a single merged plume in the shallow unconfined aquifer. A secondary plume in a deeper semi-confined aquifer occurs due to vertical leakage through a "window" in the confining bed.

Measured dissolved concentrations of chlorinated solvent species were converted to "TCE-equivalent" concentrations such that their H-demand for complete reduction is equal to that of TCE. The sum of H-equivalent concentrations of all chlorinated ethenes was taken as the total TCE-equivalent solvent concentration. Model parameters were calibrated and their joint uncertainties determined for two different data sets:

- Pre-TSR calibration using total TCE-equivalent dissolved concentrations from 26 monitoring wells distributed over the entire plume from 1995 through 2001 prior to TSR.
- Post-TSR calibration using dissolved concentration data for 26 monitoring wells distributed over the plume and 14 newer wells near source areas (Figure H-6 inset) from 1995 through 2009 plus estimated mass removal during TSR.

Correlation coefficients between observed and predicted concentrations were 0.786 and 0.780 for pre- and post-TSR calibrations, respectively.

Multiple measurements of source mass discharge were performed for the three DNAPL source zones before and after TSR, which were not utilized for model calibration. Measurements were performed using downhole passive flux units and different pump test methods (USACE, 2008). Total source discharge was determined for each method by summing all sources and maximum, minimum and median total measured discharge was determined.

Results of Monte Carlo simulations of total source discharge versus time with 95 and 99 percent confidence bands are shown in Figure 6-9 for pre- and post-TSR calibrations. Maximum, minimum and median estimates of discharge rates from field measurements prior to and after TSR are also shown. Stepwise reductions in source discharge due to source mass reductions by TSR between 2004 and 2007 are evident. The 95% confidence bands are narrower for the post-TSR calibration, reflecting improved model precision associated with additional calibration data.

Model-simulated mass discharge agrees well with simulated values. Specifically, median measured values lie within 95% prediction confidence bands for both pre- and post-TSR calibration simulations. Thus, the criteria specified for model validity are explicitly met by the simulation results. Median measured values are closer to the center of the 95% confidence band, indicating that the additional calibration data not only improves model precision (narrower confidence bands) but improves accuracy (less deviation between median predictions and measurements).

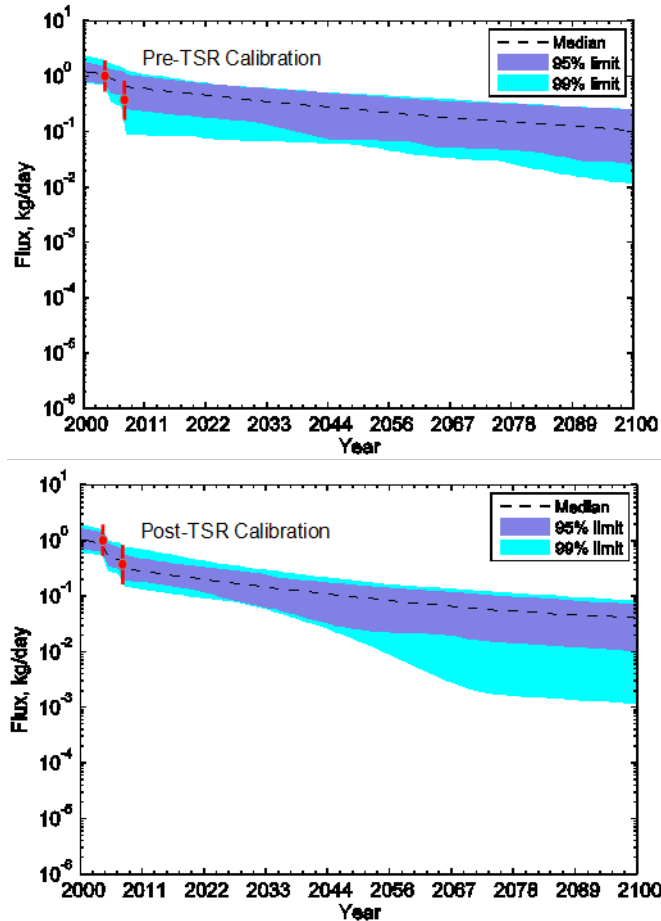


Figure 6-9. Simulated total source mass discharge rate for EGDY from 2000 to 2100 based on pre-TSR (top) and post-TSR calibration (bottom). Dashed lines represent predicted best estimates and shades areas are their confidence limits. Red lines denote the range of field-measured discharge before and after TSR and red circles represent median values.

The results indicate that source discharge measurements actually exhibit greater uncertainty than model simulations of discharge. This may reflect the fact that the calibration approach integrates data from numerous wells over the entire plume for a much longer time. Although it would be interesting and useful to compare model predictions of source discharge with future field data for longer term verification, the present analysis provides a sound basis for utilizing the proposed DNAPL source zone depletion model for long-term sustainability assessment.

Concentration at a downgradient compliance well following TSR (using field estimates of source mass removal) with no additional active remediation show a 50% probability of dropping below $5 \mu\text{g/L}$ after 2180 using the pre-TSR calibration. This date narrows to 2145 for the post-TSR calibration, which also exhibits a much narrower upper confidence band, emphasizing the strong influence of data available for calibration on prediction uncertainty.

6.2.2 Site 2: Areas I&J, NAES Lakehurst, NJ

Areas I and J include five identified source zones where TCE, hydraulic fluid and ethylene glycol had been disposed resulting in parallel partially-merged dissolved phase plumes. Calibration of source and dissolved plume transport parameters was performed using total 165 dissolved concentration measurement from 1996 through 2003. Stoichiometrically-weighted chlorinated solvent species concentrations for each well and sampling date were added to obtain TCE-equivalent total solvent concentrations for calibration. A correlation coefficient of 0.72 was obtained between observed and simulated concentrations for the calibration data.

Total source mass discharge summed over all five sources from 2000 to 2100 was computed along with 95 and 99% confidence bands based on the calibration results (Figure 6-10). Source mass reduction by contaminated sediment removal performed in 1993 from source zones S1 and S2 was not considered due to lack of information, resulting in a probable underestimation of mass of these sources in the calibration reference year of 1990.

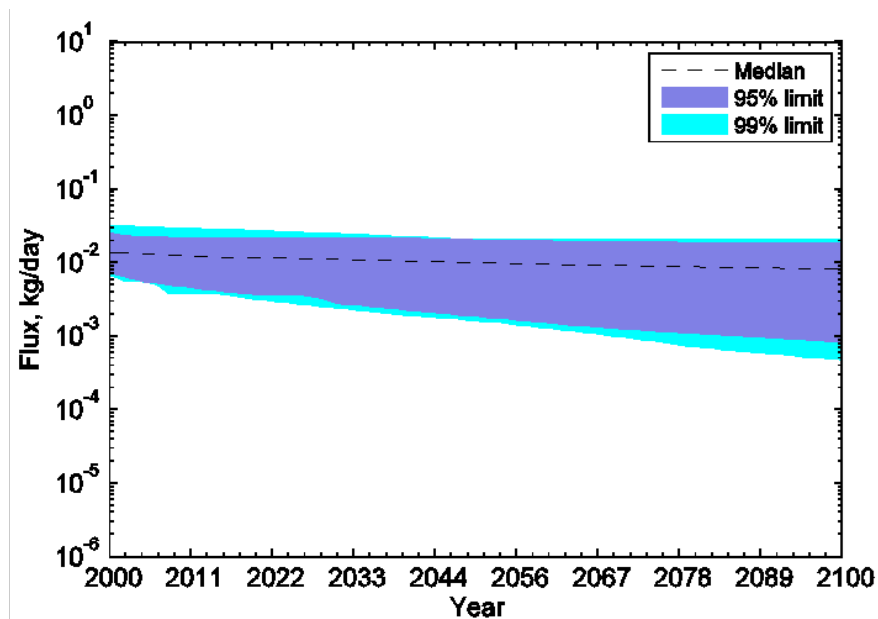


Figure 6-10. Simulated total source mass discharge for Areas I and J from 2000-2100.

Since no measurements of source mass discharge are available, model verification criteria cannot be directly evaluated for this site. Furthermore, since noise in concentration data is substantially greater than the uncertainty in predicted source discharge, it may take many years of monitoring before predictions can be verified or simulation performance substantially improved by recalibration.

Nevertheless, from a practical standpoint, the model indicates a very high probability that MNA will not be successful within a reasonable time frame without partial source mass reduction. Following source reduction measures, data on mass removed and dissolved concentration decreases in monitoring wells near source zones should enable model refinement by recalibration to better assess the prospects for successful MNA.

6.2.3 Site 3: Site 45, MCRD Parris Island, SC

Site 45 at the Marine Corps Recruit Depot (MCRD) in Parris Island SC consists of two plumes with PCE and its decay products. The source for the north plume is a former dry-cleaning facility. The south plume source has been identified as a sewer line that is thought to have acted as a conduit for contamination from the former dry-cleaning facility.

For the purpose of this demonstration, depth averages of total chlorinated hydrocarbon concentrations were stoichiometrically-weighted to obtain total PCE-equivalent concentrations for model calibration. A total of 74 concentration values measured from 2005 through 2008 were used for model calibration. A correlation coefficient of 0.78 was obtained between observed and simulated concentrations following calibration.

The calibrated model was used to simulate total source mass discharge and its confidence limits from 2000 through 2100 (Figure 6-11). Since no direct measurements of source mass discharge are available for this site, model verification criteria could not be evaluated. In any case, given the broad simulation confidence bands, statistical verification would not be very meaningful. The results indicate a 5% probability that the source may be essentially clean by around 2025, while a 50% probability exists that source discharge will take more than 100 years to decrease more than an order of magnitude. Provided there are no serious consequences of continuing to monitor the plume without further active remediation, periodic model recalibration should reduce prediction uncertainty and enable more accurate assessment of performance and of the advisability of further actions.

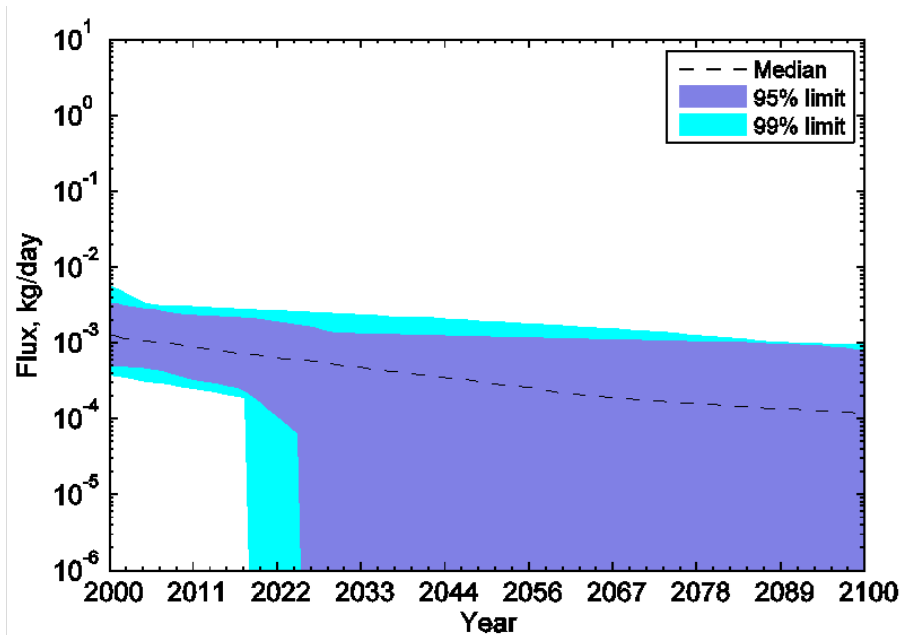


Figure 6-11. Simulated total source mass discharge at MCRD Site 45 from 2000-2100.

6.2.4 Summary of SZD Model Verification

The field applications of the SZD model coupled with a dissolved transport model, calibration methodology and stochastic forward simulation approach provide demonstrations for sites ranging from a complex multi-aquifer system with multiple DNAPL sources within a waste burial yard with extensive site characterization and monitoring data (Site 1), to a site of moderate complexity and data availability (Site 2), and a site with a single source and very limited characterization and monitoring data (Site 3). Explicit verification of source mass discharge predictions with field measurements was feasible only for Site 1, where measurements of source discharge before and after thermal source reduction (TSR) treatment were available.

Median measured values lay within 95% confidence bands for predictions based on models calibrated to pre-TSR monitoring data only as well as to a model that also included post-TSR data. This meets the criteria set forth for verification of the SZD model.

The demonstrations confirm that the SZD model is suitable for predicting source zone depletion and mass discharge rate versus time within reasonable limitations. This conclusion is conditional that probability distributions of predicted outcomes be quantified. Such information will enable site managers to assess the consequences and likelihood of various outcomes to realistically evaluate tradeoffs among various remediation and monitoring strategies.

6.3 Performance Objective: MNA Sustainability Assessment

The application of MODFLOW and SEAM3D to Site 45 was achieved without significant problems. Complete details of the modeling associated with this performance objective assessment are provided in Appendix H. Site 45 has been well-studied and properly documented over time, most recently by the U.S. Geological Survey (Vroblesky et al., 2009). This report serves as an excellent template for other sites in terms of leveraging data collected with other objectives in mind for an assessment of MNA sustainability. At present, feasibility studies for source mass reduction using conventional DNAPL remediation technologies has been ongoing at Site 45. It is expected that MNA will be a likely follow up to a successful reduction to the sources mass flux and a subsequent diminished CVOC plume.

6.3.1 Summary of STS Assessment

As described in Section 4, due to the relative shallow depth to water, groundwater flow and contaminant transport are influenced by underground utilities, primarily sewer lines. The site groundwater flow model was specifically constructed and calibrated to address this complexity. Figure 6-12 shows the results of the calibrated flow model plotted versus observed data. The minimal deviation from the 1:1 line demonstrates that an acceptable outcome was achieved using MODFLOW as a precursor to SEAM3D. The calibrated model produced an average head residual of 0.001 m and an average absolute head residual of 0.019 m.

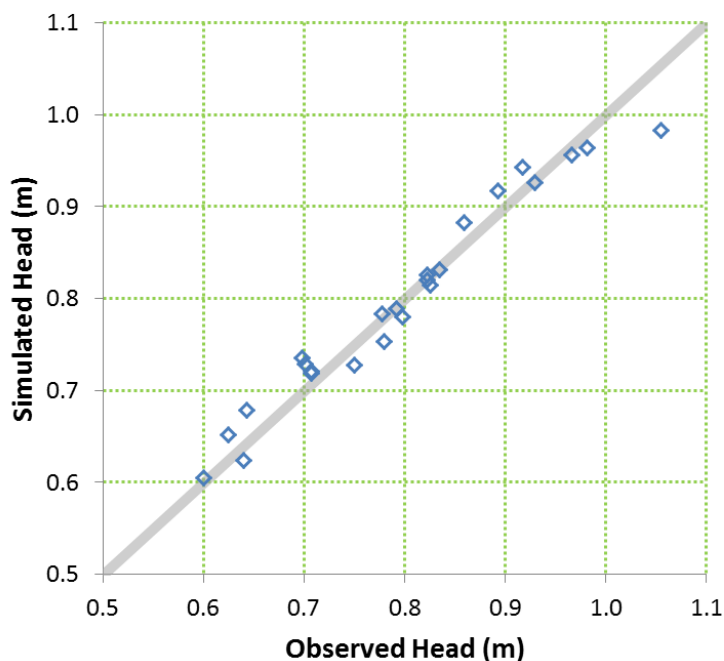


Figure 6-12. Comparison between observed and simulated groundwater elevations in the surficial aquifer at Site 45.

The primary objective of the STS assessment was matching the observed DO concentrations in the aquifer where CVOC contamination was present. CVOC concentrations were at a historic site-wide maximum at well MW25-SL and at a level to suggest the presence of DNAPL from the dry cleaning operation. PBOC levels at sampling location in the vicinity of well MW25-SL were some of the lowest levels observed site-wide (39.3 and 25.4 mg/kg at Borings 2 and 3, respectively) and were significantly below the mean PBOC concentration for aquifer sediment at Site 45 (207 mg/kg). Plausible explanations for these differences are discussed in Section 5.7.

The modeling objective was achieved using the pre-determined error criterion (± 0.25 mg/l) for DO concentrations applied to the STS assessment (see Appendix H). However, the degree of validation of the STS assessment at Site 45 was tempered by the limited range in DO concentrations within the plume. Vroblesky et al. (2009) reported DO levels ranging from 0.7 mg/L to below detection (< 0.025 mg/L). These DO concentrations in groundwater were obtained from monitoring wells with 5-ft well screens in the lower depth of the shallow aquifer. DO concentrations were reported as >1 mg/L at one well (MW20-SL) on two out of six sampling events but levels were typically closer to 0.2 mg/L at this location. It was interesting to note that DO levels at the source well (MW25-SL) were never below detection for the three sampling events reported at this location. Order-of-magnitude differences in the PBOC levels in the model did not impact calibration of the SEAM3D model to the DO data. However, application of this approach for the STS assessment at other sites that exhibit a greater range of DO, PBOC or both relative to Site 45 may require adjustment to the calibration procedure.

6.3.2 Summary of LTS Assessment

The primary objective of the LTS assessment was to utilize the calibrated site model to project forward in time and evaluate changes to the DO distribution primarily due to natural utilization but also to incorporate the impact of the DNAPL source and reductive dechlorination. Results of the SZD analysis at Site 45 (Section 6.2.3) and specifically the timeframe for change in contaminant mass flux from the source with reduced mass were inconclusive. This was attributed to increasing width of confidence bands due to the limited monitoring data at Site 45. Even though site investigations date back to the mid-1990s, the “southern plume” including the source zone was a fairly recent development (i.e., since 2007-09).

Given this result, the LTS assessment was performed using a 100-year timeframe. As discussed below in Section 8, the sustainability assessment can proceed if a SZD cannot be performed or if the uncertainty associated with the estimated range of time source flux reduction is unacceptable. However, the 100-year timeframe for the long-term simulation was selected because results of the SZD analysis were conducted over approximately the same period of time. This is a reasonable assumption at many sites where MNA is the primary remediation strategy.

For the LTS assessment, two scenarios were considered. In the first scenario, a key assumption is that land use and climate does not change over the 100-year period. Changes in land use could not only impact the rate of recharge but also the flux of oxygen entering the groundwater system. The most immediate effect of climate change would be the variability in recharge rates over time resulting from extreme events (e.g., hurricanes) but also the average annual precipitation. In the second scenario, the flux of background oxygen is increased by an order of magnitude to assess potential impacts of land use. This could be the consequence of any number of alterations in the existing local infrastructure, vegetation or some combination, and is not intended to simulate a specific change in land use.

The results of Scenario 1 are depicted in Figure 6-13 showing no appreciable change in the background level of DO in groundwater at Site 45. This suggests ample background levels of PBOC are present in the aquifer sediment and dissolved into the groundwater over the simulation period. The long-term simulation shows a minimal rise over time in DO concentration (0.04 mg/L) within the source zone. This rise is attributed to the diminished levels of PBOC observed in site sample and incorporated into the SEAM3D model. This upward trend is very slow to the point that it would be difficult to verify over time with field data given the continued likelihood of minor temporal variations in DO at Site 45. Furthermore, the ending DO value in the source zone is still well below threshold levels of DO commonly associated with microbially-mediated reductive dechlorination and even a slight increase of this nature would not be expected to influence the rate or extent of reductive dechlorination.

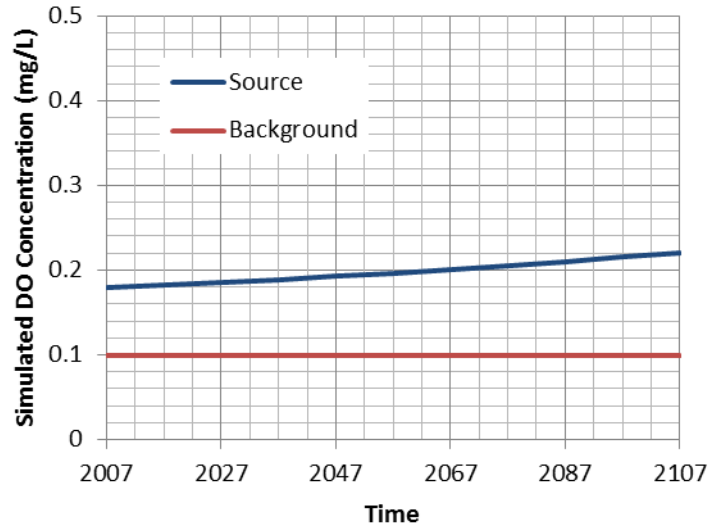


Figure 6-13. LTS assessment results (Scenario 1) showing long-term projections of dissolved oxygen (DO) concentrations for two monitoring locations (source zone and background) in the surficial aquifer at Site 45.

With changes in the background flux of oxygen (Scenario 2), presumably derived from recharge to the aquifer, a much different result is apparent compared to Scenario 1 results, even within a relatively short timeframe (in this case, 10 years). The order-of-magnitude increase in oxygen at the upgradient flow boundary results in a nearly-equivalent increase in DO in source zone groundwater (Figure 6-14). The increase in the DO level begins at year 2 and reaches a new apparent steady-state over a 4-year period as natural groundwater flow brings higher levels of DO into the CVOC plume. The impact on reductive dechlorination is apparent by the decreasing trend in DCE concentrations at the same location starting between years 5 and 6. The starting level of DCE is the result of reductive dechlorination in the plume and DCE derived from the DNAPL source zone. As the DO level increases, the concentration of DCE begins a downward trend as oxygen begins to inhibit reductive dechlorination of PCE and TCE and the generation of DCE. Although higher DO concentrations could conceivably have a beneficial effect due to the direct (aerobic) oxidation of DCE, the short-term effect indicate sustainable MNA based on reductive dechlorination is questionable under this scenario.

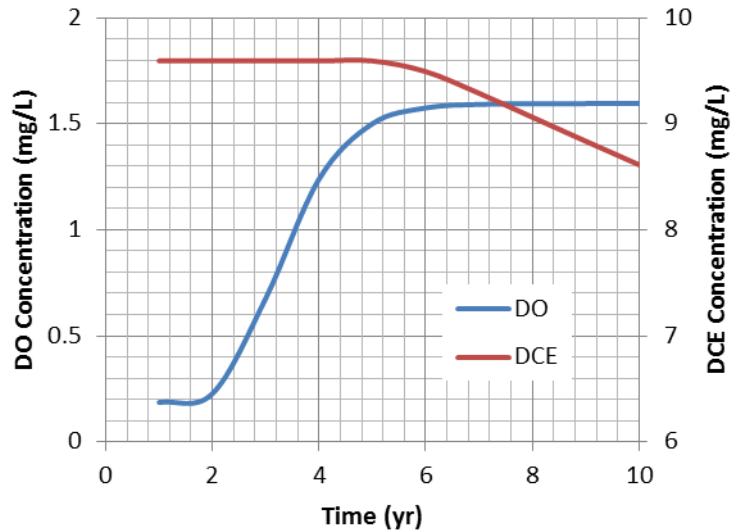


Figure 6-14. Additional long-term projections of dissolved oxygen (DO) concentrations downgradient of the source zone in the surficial aquifer at Site 45 under changes in the background DO flux resulting from changes in land use (Scenario 2).

6.4 Performance Objective: Ease of Implementation

NAS is a screening tool for TOR calculations that is designed to run SEAM3D with proven reliability. NAS was successfully modified to incorporate the SZD function for long-term NAPL dissolution simulations. This involved updating the NAS interface for several additional input parameters. Users have the option of using the older version of the NAPL dissolution model but can run the newer version with the exponent set to zero to achieve the same numerical results for concentration versus time.

Based on evaluation of implementation issues and procedure for conducting the SZD analysis and STS and LTS assessment, it was obvious that extended model runs using SEAM3D within the NAS platform did not conform to the input from RPMs and other stakeholders on run-time requirements. Instead, the DoD-supported GMS modeling platform was utilized for the STS and LTS assessments. GMS has many advantages over simpler modeling platforms, particularly for model calibration, making model calibration (i.e., STS assessment) straight-forward without the need for considerable cost in time and resources. Another factor is that software platforms for comprehensive site models are better suited to take advantage both a cost and efficiency perspective to utilize existing site models. Often site models have been developed over time through careful planning and considerable effort. Using existing site models for sustainability assessments allow leveraging of resources and may ensure a more accurate outcome. At site where modeling efforts have been limited to analytical models, these results would also serve a useful starting point for sustainability assessments.

7.0 COST ASSESSMENT

The objective of this project is to validate and demonstrate tools for assessing the sustainability of MNA at chlorinated solvent sites. To apply these tools in an effective manner, site characterization efforts should be in a relative mature state. MNA may be one component of a remedial action plan, the sole remediation strategy, or considered as part of a feasibility study. In general, the only additional data requirement is laboratory measurement of BOC. Therefore, the cost assessment for this technology demonstration will only address the incremental costs of performing the PBOC analysis and the application of computational tools for the assessment of STS and LTS.

7.1 Cost Model

The cost elements considered in the cost model for implementing the MNA sustainability assessment at a site are summarized in Table 7-1. The model considers the following four elements:

- Sample Collection
- Characterization of PBOC
- Estimation of Source Zone Depletion Timeframe
- Assessment of STS and LTS

Table 7-1. Cost Model for MNA Sustainability Assessment.

Cost Element	Data Tracked During the Demonstration	Costs	
Sample Collection for PBOC Analysis	<ul style="list-style-type: none"> • Personnel required and associated labor to design and perform sampling plan • Materials for sample collection • Mobilization and labor cost for sampling by direct-push or drill rig 	Standard practice	
Characterization of PBOC	<ul style="list-style-type: none"> • Analytical laboratory costs 	Per sample cost:	
		Unit: materials	\$20
		Unit: labor	\$55
Application of Site Models for Estimating SZD Timeframe	<ul style="list-style-type: none"> • See Table 7-2 		
Application of Site Models for Assessing STS and LTS	<ul style="list-style-type: none"> • See Table 7-2 		

Baseline hydrogeologic and contaminant characterizations were not included in assessing cost. It is assumed that baseline characterizations have been performed, that MNA is either an implemented remedial strategy or is under consideration as a remedy, and that a conceptual site model has been developed out of a RI/FS. For the latter, this may or may not include a working site model for solute transport and attenuation. As a result, the cost model for this technology demonstration only addresses the incremental costs of collecting sample and analysis of PBOC and computer modeling for estimating a timeframe for source zone depletion and assessing MNA sustainability.

Characterization of PBOC requires sample collection of soil and aquifer sediment using standard operating procedures and appropriate sampling equipment (e.g., direct push or drill rig), depending on site conditions. The sampling procedure for PBOC analysis is routine requiring no special method, supplies or equipment to obtain and collect each sample of material in 0.5-L jar. At some sites, samples preserved in cold storage may be adequate for laboratory analysis. Other costs for sampling include development of a sampling plan by personnel knowledgeable of the site hydrogeology and contaminant distribution.

7.1.1 Cost Element: Characterization of PBOC

Procedures followed in performing laboratory analysis for the concentration of PBOC are detailed in Appendix B. Unit costs provided in Table 7-1 reflect average values tracked during the demonstration. At sites where only a relative few samples are analyzed, higher unit costs may be possible. The cost of supplies includes the disposable items (e.g., centrifuge tubes) and chemicals for each extraction step (i.e., sodium pyrophosphate and sodium hydroxide). Laboratory start-up costs for equipment and associated overhead costs were not included in this cost element are not reflected in the unit costs of Table 7-1. As noted in Appendix B, the required equipment is not unique and may be operational in many environmental laboratories. These items include an analytical balance, rotary tumbler, centrifuge, and a TOC analyzer.

7.1.2 Cost Element: Application of Site Models

This cost element pertains to the application of site models for estimating the timeframe of source zone depletion and for assessing STS and LTS. The primary tasks associated with this cost element are site data analysis, computer modeling and reporting are listed in Table 7-2 along with the estimated labor effort required to complete them.

For this demonstration, MODFLOW and SEAM3D were utilized to complete the numerical modeling. SEAM3D is available at no cost to DoD employees and DoD's on-site contractors. The current cost to purchase SEAM3D via the GMS platform (version 8.3) is \$9,850 for a single license, which includes MODFLOW and other groundwater models.

Table 7-2. Cost Model for Application of Site Models.

Cost Element	Data Tracked During the Demonstration	Costs	
Data Review and Modeling Plan	<ul style="list-style-type: none"> Review of historical reports and site data Review of existing Conceptual Site Model (CSM) studies Development of modeling plan 	Project Engineer, 16 hr at \$150/hr	\$2,400
		Project Engineer, 8 hr	\$1,200
		Project Engineer, 12 hr	\$1,800
Source Zone Depletion Analysis	<ul style="list-style-type: none"> Site-specific groundwater flow field mapping Dissolved phase transport model calibration Uncertainty analysis 	Project Engineer, 12 hr	\$1,800
		Project Engineer, 18 hr	\$2,700
		Project Engineer, 20 hr	\$3,000
Source Zone Contaminant Parameters	<ul style="list-style-type: none"> Calibration of CSM including model construction and simulation of groundwater flow Short-Term Sustainability (STS) including calibration and sensitivity analysis Long-Term Sustainability (LTS) assessment and uncertainty analysis 	Project Engineer, 24 hr	\$3,600
		Project Engineer, 16 hr	\$2,400
		Project Engineer, 44 hr	\$6,600
Reporting	<ul style="list-style-type: none"> Summarize results Finalize report and develop appendices describing modeling steps 	Project Engineer, 42 hr Project Engineer, 120 hr	\$6,300 \$18,000

7.2 Cost Drivers

Section 7.1 includes information for developing a reasonable estimate cost for implementing a MNA sustainability assessment at other sites including each step of the procedures described in this report. One primary driver for the total cost to perform the assessment is the quality and quantity of long-term CVOC monitoring data. This is particularly the case for analysis of source zone depletion and estimation of the long-term reduction in contaminant source mass flux. Insufficient data can be remedied over time through additional routine monitoring data and employing new monitoring wells strategically positioned near the source. Additional high-intensity data collection, such as mass flux measurement, is also an option.

Other costs implementing a MNA sustainability assessment for data analyses will vary with the complexity of the site, the extent of data collection for PBOC tests, the level of previous mode investigations, and the level of experience that the modeler has with the site.

8.0 IMPLEMENTATION ISSUES

8.1 Implementation of PBOC Test

Implementation of the PBOC test is relatively straight-forward and simple compared to many other methods of analysis currently in use. It is more involved and labor intensive compared to TOC of the solid phase (soil or aquifer sediment) but is less costly compared to the bioavailable iron assay (ESTCP 2007). In fact, aquifer sediment samples previously collected and kept in cold storage are suitable. No specialized equipment or costly or labor-intensive handling of the samples is required.

The results presented in Section 5.6 for the two sites where multiple PBOC analyses were performed indicate that spatial variability of PBOC is to be expected. Spatial variability in PBOC will be likely to be more extreme between distinct geologic units but differences were clearly observed in similar materials. This demonstration, particularly at Site 45 MCRD, indicated that the impact of solvents at high concentrations will result in less PBOC, on average. Therefore, when designing an investigation to characterize PBOC, background samples are necessary for controls but one should account for differences in geologic material, particularly with depth, the vertical and horizontal distribution of dissolved-phase contamination, nature and age of the source, and the location of DNAPL or high-concentration source zones where diminished PBOC can be expected.

8.2 Implementation of SZD Analysis

Implementation issues for the SZD model center on availability of data. The SZD model, like any mathematical model, is merely an approximation of reality, which is subject to some degree of intrinsic uncertainty owing to inherent simplifications. Furthermore, these limitations are compounded by uncertainty in source model parameters, which must be inferred by fitting to characterization data and historical monitoring data, which are invariably limited in both quantity and quality. Therefore, it is critical to quantify confidence limits on predictions of the SZD model as well as transport and reaction models to which it may be coupled.

The results documented in this SZD verification study show that prediction uncertainty generally increases with greater site complexity and decreases as the amount and quantity and quality of data available for model calibration increases. This is seen in generally increasing width of confidence bands from Site 1 to Site 3 as well as within Site 1 for a model calibrated to a pre-TSR data set or one that also uses post-TSR data.

Therefore, our conclusion, that the proposed SZD model is a valid and useful tool for evaluating the long-term estimate of source mass flux within a MNA scenario, is given conditionally on the suggestion that probability distributions of predicted outcomes be quantified. Such information will enable site managers to assess the consequences and likelihood of various outcomes to realistically evaluate tradeoffs among various remediation and monitoring strategies.

8.3 Implementation of MNA Sustainability Assessment

Implementation issues of a MNA sustainability assessment are also tied to data availability at a given site along with resources to update conceptual site models. Sites where a mature site conceptual model has been developed and validated over time are ideal for sustainability assessment. As discussed in Section 3.4, previous modeling investigations including active site model should be leveraged whenever possible to minimize cost. Data to assess the nature and spatial distribution of redox in the relevant hydrostratigraphic unit of the groundwater system is particularly necessary.

The key data for understanding redox and conducting the sustainability assessment as it pertains to chlorinated solvents is DO. DOC in groundwater is also useful but not always necessary. At present, MNA parameters are collected at regular intervals but often not as frequently as routine monitoring of CVOCs. Site data should be evaluated for the most representative data set to be used for STS assessment, which is calibration of the solute transport model to DO. In addition, the quality of the DO data should be carefully evaluated. In some cases, DO collected with older model DO probes has led to excessively high readings (i.e., $DO > 1$ mg/L and above which is inconsistent with reductive dechlorination).

8.4 Implementation of the Technology at Other Sites

MNA sustainability assessment is not only applicable to sites where MNA is presently the primary remediation strategy but also at sites where the feasibility of MNA is under consideration. At this phase, the three-part process commences: 1) quantify PBOC, 2) conduct SZD estimates, and 3) assess sustainability. Based on the discussion above in Section 8.2, the rate-limiting step in this process is estimating the depletion of the source zone mass flux (i.e., part 2). Thus, at any site under consideration, the quality and the extent of long-term historic CVOC data will determine if the probability distributions of predicted outcomes can be quantified. In the event that the SZD analysis is problematic or produces an unacceptable level of uncertainty, the last component of this technology may be implemented using a reasonable life-cycle time estimate. For example, a 100-year analysis could be an acceptable starting point for conducting the MNA sustainability assessment. As with any modeling investigation, best practices call for post-auditing of estimates and projections and updates to the model and results as additional data becomes available. With this approach and with new data available, a more robust estimate could be achieved (i.e., complete part 2 and revisit the sustainability assessment).

Further, a question was posed as an Action Item after the February 2010 In Progress Review; “as part of the Final Report, plan to include an assessment of the types of sites at which this methodology will be most applicable and the types of sites at which this methodology may not be applicable.” In response, the technology demonstrated and verified in this report is an approach to assessing MNA sustainability as applied to chlorinated solvents in groundwater. One specific application for this assessment technology is the case where microbially-mediated reductive dechlorination is the primary remediation strategy for plume management at a site contaminated with chlorinated ethenes and residual mass may or may not be present in a source zone. An alternative application would be the case where an aggressive strategy to reduce source mass is recommended (i.e., outcome of a site feasibility study), and MNA is the projected follow-up remediation strategy. At a given site, the assumed starting point is that site characterization efforts and data analysis has proven that the proper environmental conditions for

microbially-mediated reductive dechlorination exist in the groundwater and that ample evidence exists to confirm that the microbial community is reducing chlorinated compounds.

The quality and quantity of available data is an important consideration when implementing this technology at other sites. One rate-limiting step when implementing this technology at any sites comes in estimating the depletion of the source zone mass flux (i.e., component 2). Verification of the SZD function showed that the nature and extent of long-term historic CVOC data will determine if the probability distributions of predicted outcomes can be quantified. In the event that the SZD analysis is problematic or produces an unacceptable level of uncertainty, the last component of this technology may be implemented using a reasonable life-cycle time estimate. For example, a 100-year analysis could be an acceptable starting point for conducting the MNA sustainability assessment. As with any modeling investigation, post-auditing of modeling results is recommended as new data is collected and evaluated at future points in time.

9.0 REFERENCES

- Aziz, C.E., C.J. Newell, J.R. Gonzales, P.E., Hass, T.P. Clement, and Y. Sun, BIOCHLOR natural attenuation decision support system. EPA/600/R-00/008: NRMRL, U.S. Environmental Protection Agency, Cincinnati, OH, p. 46.
- Barker, D.T., K.K. Schwall, and L.L. Pardy, (1994), Water Quality Control Plan for the San Diego Basin (9), California Regional Water Quality Control Board, San Diego Region.
- Bechtel National, Inc. (1996). Draft Remedial Investigation/RCRA Facility Investigation Report, Site 5 - Golf Course Disposal Area, Naval Air Station North Island, San Diego, CA.
- Bradley, P.M. (2000). Microbial degradation of chloroethenes in groundwater systems, *Hydrogeology Journal*, 8(1), 104-111.
- CH2MHill (2000). Supplemental remedial investigation for Site 12. Technical Report, CH2MHill
- Chapelle, F.H., and P.M. Bradley. (1998). Selecting remediation goals by assessing the natural attenuation capacity of groundwater systems. *Bioremediation Journal*, 2(3&4): 227-238.
- Chapelle, F.H., J.T. Novak, J.C. Parker, B.B. Campbell and M.A. Widdowson (2007). A framework for assessing the sustainability of monitored natural attenuation”, U.S. Geological Survey Circular Series, C-1303, 35 p.
- Chapelle, F.H.; P.H. Bradley, D.J. Goode, C. Tiedeman, P.J. Lacombe, K. Kaiser, and R. Benner (2009). Biochemical Indicators for the Bioavailability of Organic Carbon in Ground Water, *Ground Water*, 47(1), 108-121.
- Dames and Moore. (1999). Final Report – Groundwater Natural Restoration Study, Areas I and J. Contract Number N62472-90-D-1298.
- Dinicola, R.S. (2005). Hydrogeology and trichloroethene contamination in the sea-level aquifer beneath the Logistics Center, Fort Lewis, Washington: U.S. Geological Survey Scientific Investigations Report 2005-5035, 50 p.
- Doherty, J. (2005). PEST: Model-Independent Parameter Estimation.
- Ensaf/Allen and Hoshall. (1995). Final remedial investigation report, Naval Air Station Pensacola, Operable Unit 10 and site 13. Ensaf/Allen and Hoshall, Memphis, TN.
- ESTCP. (2007). *Bioavailable Ferric Iron (BAFeIII) Assay*, Cost and Performance Report, ER-0009, 29 pp.
- Falta, R. W., et al. (2007). REMChlor: Remediation evaluation model for chlorinated solvents, User’s Manual Version 1.0.
- GSI Environmental, Inc. (2007). BioBalance Toolkit User’s Manual.
- Harbaugh, A.W., Banta, E.R., Hill, M.C. and McDonald, M.G. (2000). MODFLOW-2000, the U.S. Geological Survey modular ground-water model -- User guide to modularization concepts and the Ground-Water Flow Process.
- Kaiser, K., and R. Benner. (2005). Hydrolysis-induced racemization of amino acids. *Limnol. Oceanogr. Methods*, 3: 318-325.

- Kitanidis, P. K. (1987). A first-order approximation to stochastic optimal control of reservoirs. *Stochastic Hydrology and Hydraulics* 1, 169-184.
- Naval Air Engineering Station. (2006). Five-Year Review Report, Lakehurst, New Jersey.
- National Research Council (2000). *Natural Attenuation for Groundwater Remediation*. National Academic Press, 274 p.
- Parker, J.C. and E. Park (2004). Modeling field-scale dense nonaqueous phase liquid dissolution kinetics in heterogeneous aquifers, *Water Resources Research*, 40(5), doi: 10.1029/2003WR002807.
- Park E. and J.C. Parker (2005). Evaluation of an up-scaled model for DNAPL dissolution kinetics in heterogeneous aquifers, *Advances in Water Resources*, 28, 1280-1291.
- Parker, J.C., E. Park and G. Tang (2008). Dissolved plume attenuation with DNAPL source remediation, aqueous decay and volatilization – Analytical solution, model calibration and prediction uncertainty, *J. Contam. Hydrol.*, DOI 10.1016/j.jconhyd.2008.03.009.
- Parker, J.C., U. Kim, P.K. Kitanidis, M. Cardiff, X. Liu, and G. Beyke (2011). Stochastic cost optimization of DNAPL site remediation: I. Method description and sensitivity studies. *J. Contam. Hydrol.*, in review.
- Rao, P. S. C., and J. W. Jawitz, (2003). Comment on “Steady-state mass transfer from single-component dense non-aqueous phase liquids in uniform flow fields” by T.C. Sale and D. B. McWhorter, *Water Resour. Res.*, 39, 1068, doi:10.1029/2001WR000599.
- Rectanus, H.V., M.A. Widdowson, J.T. Novak, and F.H. Chapelle (2005). “Method development for quantifying potential bioavailable organic carbon in sediments”, *Proceedings of the Third European Bioremediation Conference*, Chania, Crete, Greece.
- Rectanus, H.V. (2006). Sustainability of reductive dechlorination at chlorinated solvent contaminated sites: Methods to evaluate bioavailable natural organic carbon. PhD dissertation, Virginia Tech, 149 pp.
- Rectanus, H.V., M.A. Widdowson, J.T. Novak, and F.H. Chapelle (2007). Investigation of reductive dechlorination supported by natural organic carbon, *Ground Water Monitoring and Remediation*, 27(4), 53-62.
- Truex, M. J., C. D. Johnson, and C. R. Cole. (2006). Numerical Flow and Transport Model for the Fort Lewis Logistics Center, Fort Lewis, Washington, DSERTS NO. FTLE-33. Pacific Northwest National Laboratory, Richland, Washington. 121 p.
- US Army Corps of Engineers. (2008). East Gate Disposal Yard Thermal Remediation Performance Assessment After Action Report. 248 p.
- US Environmental Protection Agency. (1998). Technical protocol for evaluating natural attenuation of chlorinated solvents in ground water, EPA/600/R-98/128: Office of Research and Development, U.S. Environmental Protection Agency, Washington, D.C., p. 232.
- US Environmental Protection Agency. (1999). *Use of Monitored Natural Attenuation at Superfund, RCRA Corrective Action, and Underground Storage Tank Sites*. OSWER

- Directive 9200.4-17P. Office of Solid Waste and Emergency Response.
www.cluin.org/download/reg/d9200417.pdf
- U.S. Geological Survey. (1999). Natural Attenuation of Chlorinated Ethenes and Chlorinated Benzenes, Wastewater Treatment Plant, NAS Pensacola, U.S. Geological Survey, Columbia, South Carolina.
- Vroblesky, D.A., Petkewich, M.D., Landmeyer, J.E., and Lowery, M.A. (2009). Source, transport, and fate of groundwater contamination at Site 45, Marine Corps Recruit Depot, Parris Island, South Carolina: U.S. Geological Survey Scientific Investigations Report 2009-5161, 80 p.
- Waddill, D.W. and M.A. Widdowson (1998). Three-Dimensional Model for Subsurface Transport and Biodegradation. *ASCE J. of Environmental Engineering*. 124(4): 336-344.
- Waddill, D.W. and M.A. Widdowson (2000). *SEAM3D: A Numerical Model for Three-Dimensional Solute Transport and Sequential Electron Acceptor-Based Biodegradation in Groundwater*. U.S. Army Engineer Research and Development Center Technical Report ERDC/EL TR-00-18, Vicksburg, MS.
- Wiedemeier and Associates (2006). Evaluation Monitored Natural Attenuation, Installation Restoration Site 5, Unit 2, Naval Air Station North Island, San Diego, California.
- Widdowson, M.A. (2004). Modeling natural attenuation of chlorinated ethenes under spatially-varying redox conditions. *Biodegradation*, 15, 435-451.

APPENDIX A: POINTS OF CONTACT

POINT OF CONTACT Name	ORGANIZATION Name Address	Phone Fax E-mail	Role in Project
Carmen A. Lebrón	NAVFAC ESC EV31 1100 23 rd Ave. Port Hueneme, CA 93043	Tel: 805-982-1616 Fax: 805-982-4304 carmen.lebron@navy.mil	PI and Project Manager
Francis H. Chapelle	U.S. Geological Survey 720 Gracern Rd, Suite 129, Columbia, SC 29210	Tel: (803) 750-6116 chapelle@usgs.gov	PBOC validation; Application of framework
Mark A. Widdowson	Virginia Tech, The Via Dept. of Civil and Environmental Engineering, Blacksburg, VA 24061-0105	Tel: 540-231-7153 Fax: 540-231-7532 mwiddows@vt.edu	SEAM3D modeling and site data
John T. Novak	Virginia Tech, The Via Dept. of Civil and Environmental Engineering, Blacksburg, VA 24061-0105	Tel: 540-231-6132 Fax: 540-231-7532 mwiddows@vt.edu	PBOC validation
Jack C. Parker	University of Tennessee, Civil and Environmental Engineering Dept., Knoxville TN 37996-2669	Tel: 865 974-7718 Fax: 865 974-2669 parkerjc@utk.edu	SZD modeling
Michael A. Singletary	NAVFAC Southeast, POB 30 Bldg. 903, EV3 Naval Air Station Jacksonville, FL 32212-0030	Tel: 904.542.6303 Fax - 904.542.6345 michael.a.singletary@navy.mil	Identification of candidate study sites and locating field data

**APPENDIX B: STANDARD PROCEDURES:
POTENTIALLY BIOAVAILABLE ORGANIC CARBON (PBOC)
TOTAL ORGANIC CARBON (TOC)
HYDROLYZABLE AMINO ACID (HAA)**

B.1 Potentially Bioavailable Organic Carbon (PBOC)

B.1.1 Purpose

This Standard Operating Procedure (SOP) establishes the chemical extraction procedure for quantifying potentially bioavailable organic carbon present in aquifer sediments.

B.1.2 General Procedure

The potentially bioavailable organic carbon (PBOC) extraction method consist of a five step chemical extraction process. Three sequential 24-hour extractions using 0.1% pyrophosphate are followed with a 24-hour 0.5 N NaOH extraction and a final 24-hour 0.1% pyrophosphate extraction. The first sequential 0.1% pyrophosphate extractions (extractions 1-3) represent the loosely-extractable organic carbon associated with the sediment. And, the final two extractions (extractions 4-5), where a 0.5 N NaOH solution is followed by 0.1% pyrophosphate solution, represent the more strongly-associated organic carbon associated with the sediment.

B.1.3 Required Supplies and Equipment

This SOP requires all the following supplies and equipment for the BOC chemical extraction process.

- Aquifer sediment (dried at 70°C for 24-hour and sieved through 2-mm openings)
- 50 mL Polypropylene centrifuge tubes w/ centristar cap (www.fishersci.com)
- Analytical Balance
- 20 mL graduated cylinder
- 0.1% sodium pyrophosphate (pH 8.5, crystalline/certified ACS; www.fishersci.com)
- 0.5 N NaOH (pH 13, pellets/certified ACS; www.fishersci.com)
- Rotary Tumbler (Dayton 3M137B Motor or equivalent) to ensure proper mixing of exposed aquifer sediments and extracting solution
- Centrifuge (Model TJ-6R, TH.4 rotor and Refrigeration Unit or equivalent; www.beckman-coulter.com) required for solid separation

- Shimadzu Total Organic Carbon Analyzer (TOC- VCSN or equivalent; www.shimadzu.com) to measure extracted organic carbon

B.1.4 Procedure for PBOC Extraction Method

1. After sample collection, weigh 10 grams of aquifer sediment (dried at 70°C for 24-hour and sieved through 2-mm openings).
2. Place aquifer sample in polypropylene centrifuge tube.
3. For extraction 1, accurately measure 20 mL of 0.1% sodium pyrophosphate and combine with aquifer sediment in polypropylene centrifuge tube.
4. Place polypropylene centrifuge tube (which contains aquifer sediment and extracting solution) on rotary tumbler for a 24-hour cycle.
5. After a 24-hour extraction cycle on the rotary tumbler, centrifuge samples for 25 minutes at 2000 rpm for solid separation.
6. Decant supernatant, place in empty polypropylene centrifuge tube, and store at 4°C until analyzed for extracted bioavailable organic carbon.
7. For extraction 2-3, repeat steps 3-6.
8. For extraction 4, measure 20 mL of 0.5 N NaOH and combine with exposed aquifer sediments. Repeat steps 4-6.
9. For extraction 5, measure 20 mL of 0.1% sodium pyrophosphate and combine with exposed aquifer sediments. Repeat Steps 4-6.
10. Measure the extracted organic carbon in solution using a TOC Analyzer.

B.2 Total Organic Carbon (TOC)

The solid-phase organic carbon (TOC) content of sediment samples (total mass of organic carbon per mass sediment) was determined by elemental analysis using flash combustion and chromatographic separation (Costech Instruments). An ECS 4010 carbon gas chromatograph (GC) configuration with a 3 meter column was used for sample analysis. The gas flow rate within the GC column was 100 ml min⁻¹. Solid-phase organic carbon content was quantified using the thermal conductivity detector with a detection limit of 10 mg/kg carbon. For quality control, duplicate samples were analyzed for each sampling location. TOC data was reported as arithmetic mean for each location.

B.3 Hydrolyzable Amino Acid (HAA)

For hydrolyzable amino acids (HAA), aquifer sediment samples were placed in ampoules and hydrolyzed with 6 M HCl at 110°C for 22 hours. After hydrolysis, samples were neutralized with 1 M Na₂CO₃. HAA concentrations were determined using the EZ:faast Amino Acid Analysis Kit (Phenomenex, Inc. Torrance, CA). A HP 5890 gas-chromatograph (GC) equipped with a HP 5972 quadrupole mass detector was used for sample analysis. A Zebron GC column was provided with the EZ:faast Amino Acids Analysis kit. The GC column gas flow was 1 ml min⁻¹; and HAA were quantified using selected ion monitoring. The limit of quantification was 1 nmol mL⁻¹.

For quality assurance, all glassware was acid-rinsed (2 M HCL), rinsed three times with Milli-UV +water (Millipore) and combusted at 500°C for 3 hours. All plasticware was soaked in acid for a minimum of 12 hours, rinsed with Milli-UV+ water, and dried. Duplicate samples containing aquifer sediment were prepared for each sampling location. Concentrations of HAA were confirmed by internal and external standards.

APPENDIX C: DESCRIPTION OF SEQUENTIAL ELECTRON ACCEPTOR MODEL, 3D (SEAM3D)

SEAM3D is an advective-dispersive solute transport model that simulates the full range of natural attenuation processes (biodegradation, sorption, dilution and dispersion, volatilization, and diminishing source mass flux) in groundwater systems (Waddill and Widdowson, 1998; 2000). The SEAM3D Biodegradation Package simulates mass loss of electron donors (e.g., hydrocarbon compounds derived from light NAPL sources) that serve as growth substrates for heterotrophic bacteria in the subsurface, and the consumption of electron acceptors (EAs) associated with aerobic and anaerobic respiration. Mass loss terms due to biodegradation are functions of the specific process (e.g., sulfate reduction) and electron donor/acceptor concentrations. SEAM3D is innovative in that it allows for the evolution of redox conditions within a plume with time and space as solid-phase electron acceptors are depleted. SEAM3D also accounts for the contribution of aerobic biodegradation around the edges of a plume due to the mixing of dissolved oxygen. The SEAM3D Reductive Dechlorination Package ties the rate and extent of bioattenuation of chloroethenes (i.e., reductive dechlorination and aerobic and anaerobic direct oxidation) to the concentrations of electron acceptors (Widdowson 2004).

Another distinguishing feature of SEAM3D is the manner in which it explicitly simulates a NAPL source zone. The SEAM3D NAPL Package calculates the mass balance of each NAPL component using a field-scale mass transfer function that models mass flux at the grid-block size. SEAM3D solves the equation of mass balance for multiple species and categories of solutes including chlorinated volatile organic compounds (CVOCs) in the mobile aqueous phase

$$\theta R \frac{\partial C_i}{\partial t} = -\frac{\partial}{\partial x}(q_s C_i) + \frac{\partial}{\partial x}\left(\theta D \frac{\partial C_i}{\partial x}\right) + Q_s C_i^* \pm \sum R_{source/sink,i} \quad (C.1)$$

where C_i is aqueous phase concentration for CVOC, [M/L³]; x is distance, [L]; t is time, [T]; θ is aquifer porosity; q_s is Darcy's velocity, [L/T]; D is hydrodynamic dispersion coefficient, [L²/T]; Q_s is volumetric flow rate per unit aquifer volume representing fluid source/sink, [1/T]; and C_i^* is CVOC concentration associated with the point source/sink, [M/L³].

$\sum R_{source/sink,i}$ is the sum of all sources and sinks [M/L³/T]. CVOC removal mechanisms include biodegradation and physical removal mechanisms (i.e., volatilization and transpiration). Including CVOC mass loss due to reductive dechlorination and direct oxidation and CVOC mass source terms due to mass transfer NAPL dissolution and mass generated from biotransformation processes (e.g., reductive dechlorination), the source/sink terms is represented as

$$\sum R_{source/sink,lc} = \left(R_{source,i}^{DNAPL} + R_{source,i}^{bio}\right) - \left(R_{sink,lc}^{bio,EA} + R_{sink,lc}^{bio,ED}\right) \quad (C.2)$$

where $R_{source,i}^{DNAPL}$ is a source term for the dissolution of parent compounds from a DNAPL source [M L⁻³ T⁻¹]; $R_{source,i}^{bio}$ is a source term to account for the biogenic production of reductive

dechlorination daughter products [$M L^{-3} T^{-1}$]; $R_{sink,i}^{bio,EA}$ is a biodegradation sink term to account for the reduction of a chlorinated ethene [$M_{lc} L^{-3} T^{-1}$]; and $R_{sink,i}^{bio,ED}$ is a biodegradation sink term to account for the oxidation of a chlorinated ethene [$M_{lc} L^{-3} T^{-1}$].

The mass transfer rate between NAPL and groundwater is modeled in SEAM3D using a first order mass transfer function

$$R_{source,i}^{DNAPL} = K(C_i^{eq} - C_i) \quad (C.3)$$

where K is a time-dependent mass transfer coefficient, which is based on a revised form of the upscaled mass transfer function (Equation 1) as

$$K(t) = k^{NAPL} \left(\frac{V}{V_o} \right)^\beta \quad (C.4)$$

where V is the volume of NAPL present at time t per unit aquifer volume (i.e., within a given model cell in the numerical model), V_o is the NAPL volume per aquifer volume at time t_o , and k^{NAPL} is a field-scale mass transfer coefficient corresponding to V_o .

The NAPL volume is updated after each time-step assuming

$$\frac{dV}{dt} = \sum_{i=1}^N \frac{M_i^{NAPL}}{\rho_i} \quad (C.5)$$

where ρ_i is the mass density of pure species i and N is the number of soluble NAPL phase constituents.

Multiple NAPL functions may be applied to individual model cells to enable complex source “architectures” to be simulated. For example, mixtures of residual NAPL and NAPL pools or lenses may require specification of sources with values of the exponent β less than 1 (pools/lenses) and greater than 1 (residual). For the special case where $\beta = 0$, the mass transfer rate coefficient is independent of the NAPL mass present.

The equilibrium aqueous concentration of species i in contact with NAPL is computed based on Raoult’s Law as

$$C_i^{eq} = f_i C_i^{Sol} \quad (C.6)$$

where C_i^{eq} is the aqueous solubility of pure species i , and f_i is the mole fraction of species i in the NAPL. The latter is computed as

$$f_i = \frac{C_i^{NAPL} / \omega_i}{I^{NAPL} / \omega_i + \sum_{j=1}^N C_j^{NAPL} / \omega_j} \quad (C.7)$$

where C_i^{NAPL} is the NAPL phase mass of VOC species i (or j) per unit dry soil mass; I^{NAPL} is the NAPL phase concentration of “inert” (i.e., assumed insoluble) constituents; ω_I is the molecular weight of the “inert” species; and ω_i is the molecular weight of soluble constituent i (or j). Note that this model does not account for any cosolvency effects.

The sink term for the reductive dechlorination process is expressed as

$$R_{sink,i}^{bio,EA} = \frac{M_y}{\theta} v_i^{\max,EA} \left[\frac{\bar{C}_i}{\bar{K}_i^e + \bar{C}_i} \right] I_{i,li} \quad (C.8)$$

where M_y is the microbial biomass concentration of chlorinated ethene reducers [$M L^{-3}$]; $v_i^{\max,EA}$ is the maximum rate of reductive dechlorination for a chlorinated ethene i [$M M^{-1} T^{-1}$]; \bar{K}_i^e is the effective half saturation constant for a chlorinated ethene [$M L^{-3}$]; \bar{C}_i is the effective concentration of a chlorinated ethene [$M L^{-3}$]; and $I_{i,li}$ is an inhibition function defined by

$$I_{i,li} = \prod_{li=1}^3 \left[\frac{\kappa_{i,li}}{\kappa_{i,li} + \bar{E}_{li}} \right] I_{i,lj} \quad (C.9a)$$

where $I_{i,lj} = 1$ for $i = 1$ (source CVOC) (C.9b)

and $I_{i,lj} = \prod_{lj=1}^{i-1} \left[\frac{\kappa_{i,lj}}{\kappa_{i,lj} + \bar{C}_{lj}} \right]$ for $i = 2$ or 3 (C.9c)

where $\kappa_{i,li}$ is the EA inhibition coefficient [$M L^{-3}$] representing inhibition of the use of a chlorinated ethene by EA li ; $\kappa_{i,lj}$ is the EA inhibition coefficient [$M L^{-3}$] representing inhibition of the use of a chlorinated ethene by a higher molecular weight chlorinated ethene lj . It is assumed that the microbial population, M_y , only gain energy by respiring chlorinated ethenes and do not directly contribute to other TEAPs.

Production of a chlorinated daughter product and end products of reductive dechlorination (ethane and chloride) is expressed in terms of the rate of reduction of the parent compound

$$R_{source,i}^{bio} = \zeta_{i,i-1}^{dau} R_{sink,i-1}^{bio,EA} \quad (C.10)$$

where $\zeta_{i,i-1}^{dau}$ is the daughter product generation coefficient [$M M^{-1}$].

APPENDIX D: REMEDIATION ACTIVITIES AT EAST GATE YARD, FORT LEWIS, WA

Table D.1. EGDY site remediation history (USACE, 2008)

Date	Activity	Location
1995 - 2005	Pump-and-treat systems installed in Vashon Aquifer	One near EGDY second near highway I-5
2003 - 2005	Integrated pump test in Areas 1 and 3 in Nov 2003 and Sep 2005, respectively	EGDY
2003 - 2005	Source flux measurements in Areas 1 and 3 in Nov 2003 and Sep 2005, respectively	EGDY
2003 - 2006	TSR and monitoring in Areas 1, 2 and 3 in Dec 2003 - Aug 2004, Feb 2005 - Aug 2005, and Oct 2006 - Jan 2007, respectively	EGDY
2005-2006	Whey injection pilot tests	EGDY
2005 - 2007	Post-TSR monitoring in Areas 1,2 and 3 in May 2005, Sep. 2005, and Feb 2007, respectively	EGDY
2006 - 2008	Post-treatment soil coring in Areas 1,2 and 3 in Apr 2006, Apr 2006, and Mar 2008, respectively	EGDY
2009	Pump-and-treat system installed in Sea Level Aquifer	Near hospital

Note: TSR = thermal source removal

Table D.2. Summary of TSR operations at EGDY site (USACE, 2008)

Variable	Area 1	Area 2	Area 3
TSR treatment area (m ²)	2360	2080	1691
TSR max depth below ground surface (m)	10	16	9
TSR treatment volume (m ³)	23625	135953	15368
Energy on date	12/17/2003	02/14/2005	10/11/2006
Energy off date	08/04/2004	08/05/2005	01/26/2007
Duration (days)	231	172	107
Mass removal, TCE + DCE (kg)	2990	1340	1120

APPENDIX E: DESCRIPTION OF SAMPLING METHODS

Samples were collected from the subsurface units at each site that are most directly impacted by chlorinated solvents. At sites where multiple samples were obtained, where possible, samples were derived from the overlying unit that may provide a flux of organic carbon to the groundwater system.

Each sample was labeled and included an identification number. RPMs were advised to provide the sampling depth and approximate spatial coordinates of each sampling location. On-site personnel were advised to follow relevant sampling SOPs pertaining to health and safety and equipment decontamination.

Samples were typically obtained using direct-push equipment (e.g., Geoprobe®) or a drilling rig and conventional sampling equipment. Samples collected using a hand auger were obtained at a limited number of sites. Upon removal from the subsurface, sediment samples were transferred to glass containers with air tight lids. The addition of DI water was recommended to keep samples moist before jars were sealed. Sample jars were placed in a cooler (on ice to 4° C) and shipped via overnight carrier to Virginia Tech. Samples were then stored in a constant-temperature room (4°C) and subsequently analyzed for PBOC as described in Appendix C.

Site 45 at Marine Corps Recruit Depot (MCRD), Parris Island, SC was selected for intensive sampling primarily because of desirable site characteristics: well-characterized contaminant distribution, relatively simple hydrogeology, and ease of access to samples. Samples were collected in the surficial aquifer to the top of the uppermost confining unit (approximately to a depth of 16 ft below land surface). Site personnel and project PIs used a Geoprobe unit to collect 2-inch diameter sleeves of sediment. Sampling locations included areas outside the plume to evaluate the variability of background levels of PBOC and borings inside the plume.

APPENDIX F: SITE MONITORING DATA FOR PERFORMANCE OBJECTIVE 1

Table F.1. Summary of dissolved oxygen and hydrogen concentrations with corresponding standard deviations for selected sampling events.

Facility Name	Number of Sampling Events	Dissolved Oxygen (mg/L)	Standard Deviation	Number of Sampling Events	Hydrogen (nM)	Standard Deviation
NAS Pensacola, FL	4	0.03	0.09	3	0.95	1.64
NAES Lakehurst, NJ	4	1.98	1.86			
MCRD Parris Island, SC	4	0.07	0.03	1	2.07	0.91
Hill AFB, UT	5	3.79	1.55			
NAS Jacksonville, FL	1	0.86	0.92			
NTC Orlando, FL	1	0.50	0.22	1	5.67	1.76
NTC Orlando, FL	4	0.43	0.46			
NUWC Keyport, WA	2	0.36	0.33	2	2.03	1.81
NAS North Island, CA	3	0.33	0.28			
NSB Kings Bay, GA	2	0.00	0.00	2	0.98	0.36
Beale AFB, CA	3	6.42	0.83			

APPENDIX G: MODEL DESCRIPTION FOR SOURCE ZONE DEPLETION ANALYSIS (PERFORMANCE OBJECTIVE 2)

G.1 DNAPL Source Depletion Model

Field-scale DNAPL source dissolution and mass depletion over time is described by the model of Parker and Park (2004) and Park and Parker (2005). Considering the possibility of engineered manipulation in mass transfer kinetics, we describe the rate of contaminant mass dissolution in a source zone, J_i [$M T^{-1}$], versus time, t , by

$$J(t) = F_{mt} J_{cal} \left(\frac{M(t)}{M_{cal}} \right)^\beta \quad (G.1)$$

where $J_{cal} = J(t=t_{cal})$ and $M_{cal} = M(t=t_{cal})$ in which t_{cal} denotes a reference time selected for model calibration, M is the source contaminant mass remaining, β is a depletion exponent that reflects the DNAPL source “architecture,” and F_{mt} is a time-dependent dimensionless mass transfer enhancement factor.

Integration of the source mass balance equation employing Equation (G.1) as described by Park and Parker (2005) yields source mass remaining versus time after the release date t_o for $\beta \neq 1$

$$M(t) = \left[M_{ref}^{1-\beta} - F_{mt} B(1-\beta)(t-t_{ref}) \right]^{1/(1-\beta)} \quad (G.2)$$

where $B = J_{cal} / M_{cal}^\beta$. Considering remedial actions at dates $t_{rem 1}, t_{rem 2} \dots t_{rem n}$ when partial source mass removal and/or step changes in F_{mt} occur and stipulating that $t_o < t_{cal} < t_{rem 1}$, values of M_{ref} , t_{ref} and F_{mt} in Equation (G.2) are assumed to vary with time as follows

Time Period	F_{mt}	t_{ref}	M_{ref}
$t_o < t \leq t_{rem 1}$	$F_{mt 0} = 1$	$t_{ref 0} = t_{cal}$	$M_{ref 0} = M_{cal}$
$t_{rem 1} < t \leq t_{rem 2}$	$F_{mt 1}$	$t_{ref 1} = t_{rem 1}$	$M_{ref 1}$
$t_{rem n-1} < t \leq t_{rem n}$	$F_{mt n-1}$	$t_{ref n-1} = t_{rem n-1}$	$M_{ref n-1}$
$t > t_{rem n}$	$F_{mt n}$	$t_{ref n} = t_{rem n}$	$M_{ref n}$

in which $M_{ref n}$ for $n > 0$ is given by

$$M_{ref n} = M_{remo n} - \Delta M_{remo n} \quad (G.3)$$

$$M_{remo n} = \left[M_{rem n-1}^{1-\beta} - F_{mt n-1} B(1-\beta)(t_{rem n} - t_{rem n-1}) \right]^{1/(1-\beta)}$$

where $\Delta M_{rem\ n}$ is the mass removed from the source at time $t_{rem\ n}$ regarded as instantaneous. Sorenson (2006) reported that enhanced source zone biodecay caused dissolution rate coefficients to increase by factors of 2 to 6 in laboratory studies and 3 to 8 in field studies. Also, Parker and Park (2004) have shown that field-scale dissolution rate coefficients will vary inversely with changes in source zone Darcy flux (e.g., due to engineered or inadvertent permeability decreases due to amendment injection).

G.2 Groundwater Flow Field Mapping

For the purpose of DNAPL source function verification, we implemented Equation (G.1) in a semi-analytical transport model described by Parker et al. (2011) that considers multiple chlorinated volatile organic compound (CVOC) sources within an aquifer characterized by a Cartesian coordinate system in field mapping units (E,N) – e.g., northing and easting. Flow paths will generally be nonlinear. To apply a semi-analytical solution for contaminant transport to mildly nonlinear flow fields, we define a coordinate transformation for each DNAPL source (and later for ED injection galleries) to convert from field coordinates to linearized local coordinates (x,y) and back.

For each source j we define the origin of the local coordinate system to be at the center of the downgradient plane of the source – (E_0, N_0) in field coordinates. A streamline may be drawn through (E_0, N_0) guided by water level contours and dissolved plume data and selected coordinates along the streamline are used to fit a cubic polynomial of the form $N = N_0 + a(E-E_0) + b(E-E_0)^2 + c(E-E_0)^3$. The polynomial function is used to define the $(E,N) \rightarrow (x, y)$ mapping where x is the distance along the centerline and y is the transverse distance orthogonal to the centerline. Given a location in field coordinates (E^*, N^*) local coordinates can be found as follows (Figure G.1):

- 1) The orthogonal line that passes through (E^*, N^*) and intersects the streamline at $E = E_{cross}$ may be described by $N = A + BE$ where $A = N^* + BE_{cross}$ and $B = -(a + 2b + 3cX^2)^{-1}$
- 2) Solve recursively for E_{cross} using $E_{cross} = E^*$ initially then solve the cubic equation for E where the orthogonal line intersects the streamline.
- 3) Compute y as the distance from (E^*, N^*) to (E_{cross}, N_{cross})
- 4) Compute x as distance along streamline from (E_0, N_0) to (E_{cross}, N_{cross}) by integrating $[1 + N'(E)^2]^{1/2} dE$ from E_0 to E_{cross} where $N'(E) = dN/dE$. Calculate numerically using $dE = 10\text{ m}$.

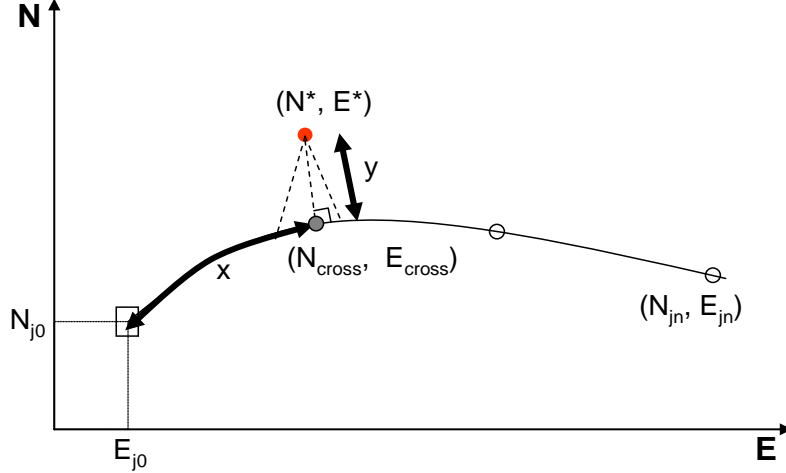


Figure G.1. Curvilinear streamline in (E,N) field coordinates and mapping to local (x,y) coordinates for source j.

G.3 Dissolved Plume Transport Model

Dissolved phase transport of contaminants emanating from DNAPL source zones in an unconfined aquifer is described by a 2-D vertically-averaged semi-analytical solution that employs the source zone function described above. The solution considers linear sorption and first-order decay. Spatially-variable decay within the aquifer can be described with up to three “zones” at different distances from the source that are characterized by different decay coefficients. Zone 1 represents the region $x < L_{12}$, Zone 2 is $L_{12} < x \leq L_{23}$, and Zone 3 is $x > L_{23}$. Leakage of contamination from the unconfined aquifer (unit A) to an underlying semi-confined aquifer (unit B) and dissolved transport in the lower aquifer due to the secondary source can be optionally considered. The solution for a single DNAPL source in the unconfined aquifer is

$$C_{Ai}(x, y, t) = \int_0^{t-t_o} \frac{J_{Ai}(t-t_o-\tau)}{4L_{zA}L_{yA}\phi_A(\pi R_A A_L v_A \tau)^{1/2}} \exp\left(-\frac{\lambda_{Ai}\tau}{R_A} - \frac{(R_A x - v_A \tau)^2}{4R_A A_L v_A \tau}\right) \times \left[\operatorname{erfc}\left(-\frac{y+L_{yA}/2}{2(A_T v_A \tau / R_A)^{1/2}}\right) - \operatorname{erfc}\left(-\frac{y-L_{yA}/2}{2(A_T v_A \tau / R_A)^{1/2}}\right) \right] d\tau \quad (\text{G.4})$$

where (x,y) are local coordinates indexed to the source, t is Julian date, t_o is the source release date, τ is a dummy integration variable, $R_A = 1 + \rho k_d / \phi$ is the retardation factor in which ρk_d is a dimensionless sorption coefficient, v_A is pore velocity, A_{LA} is longitudinal dispersivity, A_{TA} is transverse dispersivity, L_{zA} is aquifer thickness, L_{yA} is width of the source, ϕ_A is porosity, and λ_{Ai} is a first-order decay coefficient for Zone i . Integration of Equation (G.4) is performed numerically.

For Zone 1 $\lambda_{Ai} = \lambda_{A1}$ and computed from Equation (G.1) with “normal” calibrated values for J_{cal} and M_{cal} . For Zone 2 $\lambda_{Ai} = \lambda_{A2}$ and $J_{Ai}(t) = J_{A2}(t) = J$ computed from Equation (G.1) with values for J_{cal} and M_{cal} multiplied by a scaling factor S_2 defined as

$$S_2 = \frac{C_{A1}(x = L_{12}, y = 0, t; \lambda_{A1}, J_{A1})}{C_{A1}(x = L_{12}, y = 0, t; \lambda_{A2}, J_{A1})} \quad (G.5)$$

For Zone 3 $\lambda_{Ai} = \lambda_{A3}$ and $J_{Ai}(t) = J_{A3}(t) = J$ computed from Equation (G.1) with values for J_{cal} and M_{cal} multiplied by a scaling factor S_3 defined as

$$S_3 = \frac{C_{A1}(x = L_{23}, y = 0, t; \lambda_{A2}, J_{A2})}{C_{A1}(x = L_{23}, y = 0, t; \lambda_{A3}, J_{A1})} \quad (G.6)$$

If leakage from aquifer A to B is considered, Zone 2 can be treated as a leakage window and the decay coefficient is computed as $\lambda_{A2} = q_v / \phi_A L_{zA}$ where q_v is the vertical Darcy velocity in the leakage “window”.

The solution for aquifer B, which is characterized by a single uniform decay coefficient, is

$$C_B(x, y, t) = \int_0^{t-t_o} \frac{J_B(t-t_o-\tau)}{4L_{zB}L_{yB}\phi_B(\pi R_B A_{LB} v_B \tau)^{1/2}} \exp\left(-\frac{\lambda_B \tau}{R_B} - \frac{(R_B x - v_B \tau)^2}{4R_B A_{LB} v_B \tau}\right) \times \left[\operatorname{erfc}\left(-\frac{y + L_{yB}/2}{2(A_{TB} v_B \tau / R_B)^{1/2}}\right) - \operatorname{erfc}\left(-\frac{y - L_{yB}/2}{2(A_{TB} v_B \tau / R_B)^{1/2}}\right) \right] d\tau \quad (G.7)$$

where $J_B(t)$ is the mass leakage rate ($M T^{-1}$) from Aquifer A to Aquifer B computed as

$$J_B(t) = q_v \bar{C}_A A \quad (G.8)$$

where A is the area (L^2) of the “window” in plan view (or part of the window if divided into multiple “panes”), and \bar{C}_A is the average concentration in the window (or pane) computed in the A unit aquifer from **Error! Reference source not found.** at the x midpoint of the window or pane (i.e., compute C_A for several points on a transect through the window and average them). Store the computed J_B values at fixed delta t increments and employ the resulting look-up table to solve Equation (G.7).

Contaminant concentrations resulting from multiple sources in the A or B aquifers are computed by superposition of the individual source solutions after reverting back to field coordinates as

$$C(E, N, t) = \sum_{j=1}^{N_{source}} C_j(E, N, t) \quad (G.9)$$

Note that function calls on the RHS of Equation (G.9) require $(E, N) \rightarrow (x, y)$ mapping for each source j as illustrated in Figure G.2.

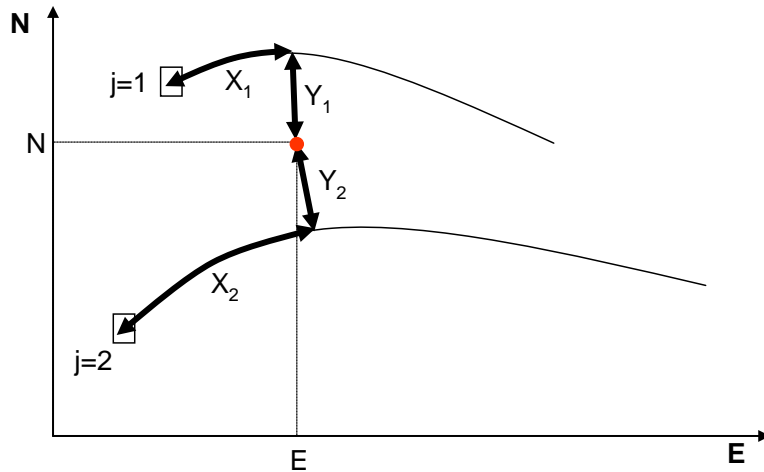


Figure G.2. Mapping of well location to linearized coordinates for two adjacent nonlinear streamlines in field coordinates for solution superposition.

G.4 East Gate Disposal Yard, Joint Base Lewis-McChord, WA

G.4.1 Model Calibration

Characterization of groundwater flow field. Groundwater flow at the EGDY site at Joint Base Lewis-McChord was characterized in USACE (2008). Streamlines commencing from each DNAPL source and from the “window” between the upper and lower aquifer units were digitized and fitted to third order polynomial equations of the form $y = ax+bx^2+cx^3$. The model computes travel distances from sources to the wells of interest along their streamlines. Coefficients of individual streamline equations are presented in Figure G.5. Since the locations of ED galleries 1 to 3 are immediately upgradient of Areas 1 to 3, their streamlines are similar to those of Areas 1 to 3. Polynomial coefficients can be estimated using Excel ‘SOLVER’ to solve the nonlinear least squares problem.

Origin	a	b	c
Area 1 (Source 1)	4.275E-01	5.615E-04	2.756E-08
Area 2 (Source 2)	2.605E-01	7.257E-04	6.437E-08
Area 3 (Source 3)	1.129E-01	1.244E-03	2.758E-07
Win 1	-9.570E-01	-8.070E-04	-1.510E-07
Win 2	-7.770E-01	-6.800E-04	-1.230E-07
Win 3	-1.171E+00	-9.984E-04	-1.780E-07

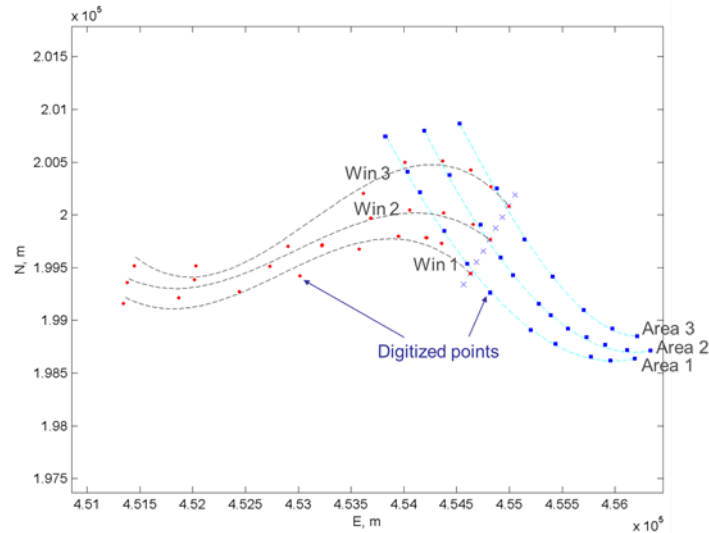


Figure G.5. Streamlines used to model groundwater flow at the EGDY Site.

Calibration using pre- and post-thermal data. Chlorinated solvent concentrations in groundwater reported by Truex et al. (2006) were utilized to construct time-series for each monitoring well. Chlorinated solvent species were converted to “TCE-equivalent” concentrations such that their H-demand for complete reduction is equal to that of TCE. The sum of H-equivalent concentrations of all chlorinated ethenes was taken as the total TCE-equivalent solvent concentration. Locations of monitoring wells with data used for model calibration are shown in Figure G.6.

Model calibration was performed for two different data sets:

- Pre-TSR calibration using TCE-equivalent dissolved concentrations from 26 monitoring wells distributed over the entire plume from 1995 through 2001 prior to TSR.
- Post-TSR calibration using dissolved concentration data for 26 monitoring wells distributed over the plume and 14 newer wells near source areas (Figure H-6 inset) from 1995 through 2009 plus estimated mass removal during TSR.

We assume that most of the contamination present in the SLA was transported from the Vashon aquifer through the “window” in the aquiclude. The Vashon aquifer is divided into three zones with different decay coefficients. Zone 1 extends from the DNAPL sources to the window; Zone 2 encompasses the window itself; and Zone 3 is the region downgradient of the window. The

model internally computes a first-order “decay” coefficient for the window zone as described in section H.1.3 to account for the advective flux to the SLA unit. The window zone is divided laterally into three sections to approximate the average TCE flux from the upper to lower aquifer. Fluxes are tabulated at discrete times in a lookup table and interpolated to define a smooth source function for the Vashon aquifer. The model uses 0.0001 d-1 as a prior estimate biodecay coefficients of for Zones 1 and 3. Prior estimates of other source and aquifer parameters were made based on information in various reports (Dinicola, 2005; Truex et al., 2006; USACE, 2008) summarized in Table H.3. The reference year (t_{cal}) for source mass and source flux was taken to be 2000.

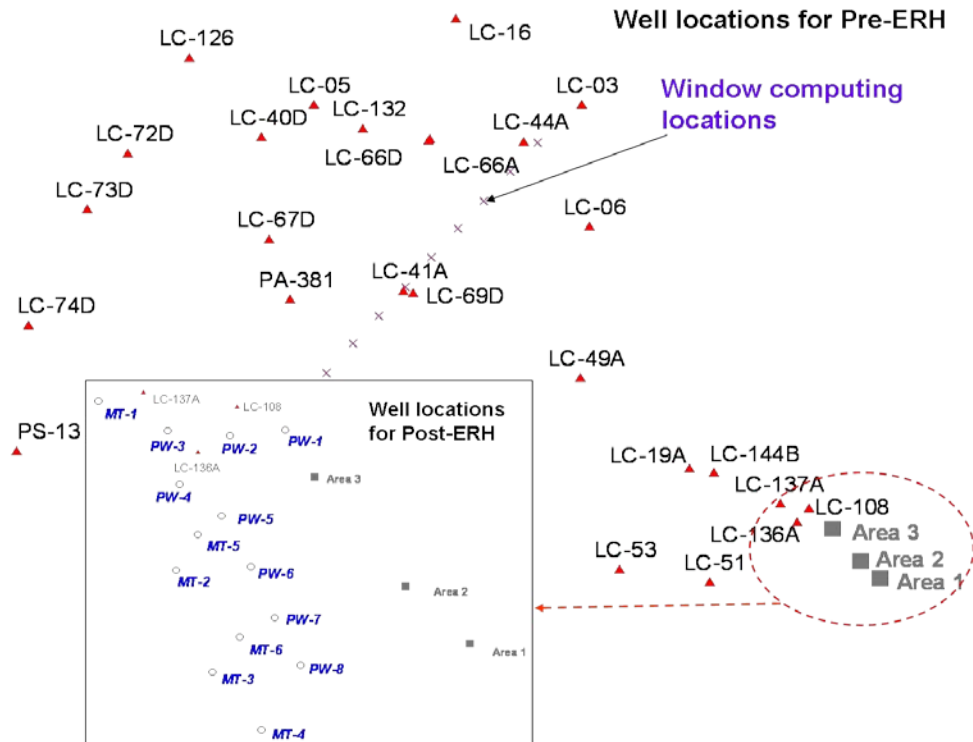


Figure G.6. Well locations used in calibration for the EGDY Site.

To model source zone mass dissolution and transport downstream, initial estimates of source and aquifer parameters were estimated from information in various reports (Dinicola, 2005; Truex et al., 2006; USACE, 2008) summarized in Table G.3. We calibrated model parameters to site data using 2000 as the reference year (t_{cal}) for source mass and source flux using both pre- and post-remediation data. Data include dissolved concentration data (total TCE-equivalents), source flux measurements, and DNAPL mass removed by TSR.

Table G.3. EGDY site characterization data.

Area	Parameters	Prior value ¹	STD ²	Reference
Area 1	Mass at 2000 (kg)	10330	0.63	USACE, 2008
	Flux at 2000 (kg/d)	0.75	1.00	USACE, 2008
	Release date	1970	3.00	USACE, 2008
	Width (m)	47	0.20	USACE, 2008
Area 2	Mass at 2000 (kg)	6495	0.56	USACE, 2008
	Flux at 2000 (kg/d)	0.32	1.00	USACE, 2008
	Release date	1970	3.00	USACE, 2008
	Width (m)	42	0.20	USACE, 2008
Area 3	Mass at 2000 (kg)	7987	0.60	USACE, 2008
	Flux at 2000 (kg/d)	0.42	1.00	USACE, 2008
	Release date	1970	3.00	USACE, 2008
	Width (m)	34	0.20	USACE, 2008
Vashon	q (m/d)	0.4	0.15	Truex et al., 2006; Dinicola, 2005
	porosity	0.29	-	Truex et al., 2006; Dinicola, 2005
	Retardation	1.21	0.15	Typical from literature
	Longitudinal dispersivity (m)	20	0.20	Estimated from correlation with plume length
	Transverse dispersivity (m)	2	0.20	Estimated from correlation with plume length
	Saturated depth (m)	30	0.20	Truex et al., 2006
	ED average (H-eq ppb)	48	0.15	Dinicola 2005
	EA average (H-eq ppb)	1977	0.15	Dinicola 2005
SLA	q (m/d)	1	0.15	Truex et al., 2006; Dinicola, 2005
	porosity	0.22	-	Truex et al., 2006; Dinicola, 2005
	Retardation	1.27	0.15	Typical from literature
	Longitudinal dispersivity (m)	20	0.20	Estimated from correlation with plume length
	Transverse dispersivity (m)	2	0.20	Estimated from correlation with plume length
	Saturated depth (m)	30	0.20	Truex et al., 2006
	natural ED average (H-eq ppb)	768	0.15	Dinicola, 2005
	natural EA average (H-eq ppb)	1977	0.15	Dinicola, 2005
Window	q _z (m/d)	0.05	0.50	Truex et al., 2006

¹ Prior estimates represent arithmetic mean for release date, geometric mean for other parameters.

² Standard deviations of prior estimates are dimensionless statistics for ln-transformed values for all parameters except release dates, which are in actual units.

We assume that most of the contamination present in the SLA was transported from the Vashon aquifer through the “window” in the aquiclude. The Vashon aquifer is divided into three zones with different decay coefficients. Zone 1 extends from the DNAPL sources to the window; Zone 2 encompasses the window itself; and Zone 3 is the region downgradient of the window. The model internally computes a first-order “decay” coefficient for the window zone as described in section xx.1.3 to account for the advective flux to the SLA unit. The window zone is divided laterally into three sections to approximate the average TCE flux from the upper to lower aquifer. Fluxes are tabulated at discrete times in a lookup table and interpolated to define a smooth source

function for the Vashon aquifer. The model uses 0.0001 d⁻¹ as prior estimate biodecay coefficients of for Zones 1 and 3.

Assuming Gaussian measurement errors and prior parameter distributions, we seek to minimize the negative log of the posterior measurement distribution, L , described by

$$L = \frac{1}{2}(\mathbf{y} - \mathbf{h}(\mathbf{s}))^T \mathbf{R}(\boldsymbol{\theta})^{-1} (\mathbf{y} - \mathbf{h}(\mathbf{s})) + \frac{1}{2}(\mathbf{s} - \mathbf{s}^*)^T \mathbf{Q}^{-1} (\mathbf{s} - \mathbf{s}^*) \quad (\text{G.10})$$

where \mathbf{y} is a vector of field measurements, \mathbf{s} is a vector of parameter values, \mathbf{s}^* is a vector of prior parameter estimates, $\mathbf{h}(\mathbf{s})$ is a vector of model predictions corresponding to the field measurements, \mathbf{R} is a matrix of measurement covariances corresponding to the vector of data types \mathbf{q} (e.g., measured contaminant concentration, source mass, source mass discharge rate, etc.), and \mathbf{Q} is the covariance matrix of prior parameter estimates. Cross-correlation terms are disregarded in \mathbf{R} and \mathbf{Q} .

Each model parameter and each data type may be log-transformed prior to application of Equation (G.10). For parameters or data types that are physically constrained to be non-negative and that are expected to exhibit a coefficient of uncertainty greater than ~20%, log-transformation is advisable. Also, calibration data types that exhibit ranges in the data set that extend over several orders-of-magnitude, log-transformation may be desirable if comparable relative error (as opposed to absolute error) is desired over the measurement range. Otherwise, the regression results will likely be controlled by absolute errors from a small number of large data values.

The magnitude of each data type's uncertainty (i.e., diagonal terms in \mathbf{R}) is generally not known *a priori*, but a posterior estimate can be made using the Restricted Maximum Likelihood (RML) algorithm (Kitanidis, 1987). Note that the final estimate of residual prediction uncertainty \mathbf{R} for each data type represents the portion of data variability that cannot be accounted for by the model, which may be due to sampling or measurement errors and/or to intrinsic limitations of the model to represent all processes in the field. For simplicity, we will refer to this uncertainty as the "residual" error. A gradient-based nonlinear optimization algorithm is used to find the solution that minimizes Equation (G.10).

A linearized approximation of the parameter posterior covariance matrix is computed from the final results as

$$\text{cov}(\mathbf{s}) \approx (\mathbf{H}^T \mathbf{R}(\boldsymbol{\theta})^{-1} \mathbf{H} + \mathbf{Q}^{-1})^{-1} \quad (\text{G.11})$$

where $H_{ij} = \partial h_i / \partial s_j$ is a sensitivity matrix. Incorporating prior estimates of parameters and their uncertainty into the regression objective function greatly reduces non-uniqueness problems in the inverse solution and allows many more parameters to be calibrated than would be possible with unconstrained optimization. This not only allows refinement of parameters with relatively low uncertainty that may otherwise be assumed at their prior estimates, but allows interactions among more parameters, through the covariance matrix, to be taken into consideration in the error analysis. In addition to variable constraints on parameters associated with the stipulation of prior

parameter uncertainty, absolute upper and lower constraints may also be placed on any parameters.

Final estimates of calibrated parameters are tabulated in Table G.4. Posterior uncertainty (S_{InC}) in dissolved concentration was estimated as 0.79 for the pre-ERH calibration and 0.77 for the post-ERH calibration indicating the additional data collected during and after ERH reduces prediction uncertainty slightly. Comparisons of observed and predicted concentrations for pre- and post-ERH calibration are shown in Figure G.7. The most notable change in the post-ERH calibration is a decrease in source masses and fluxes in 2000 by about half on average, with greater variations for individual sources, conditioned by measured mass removal and post-ERH flux data.

Table G.4. Calibration summary for the EGDY site.

	Pre-TSR	Post-TSR	Post-TSR Data
SInC	0.7891	0.7667	Additional GW concentration data
Correlation	0.7858	0.7796	
Mcal_1 (kg)	16580	3831	2990 kg removed by Aug 2004
Mcal_2 (kg)	9851	5339	1340 kg removed by Aug 2005
Mcal_3 (kg)	3403	5133	1120 kg removed by Jan 2007
Mcal_sum	29834	14302	5450 kg total
Jcal_1 (kg/d)	0.81	0.43	
Jcal_2 (kg/d)	0.34	0.06	
Jcal_3 (kg/d)	0.72	0.50	
Jcal_sum	1.87	0.99	
beta_1	0.9238	0.9823	
beta_2	1.0010	1.0300	
beta_3	1.1500	1.0900	
A _{TSR_1} (m ²)	2748	2736	
A _{TSR_2} (m ²)	2754	2822	
A _{TSR_3} (m ²)	2579	6774	

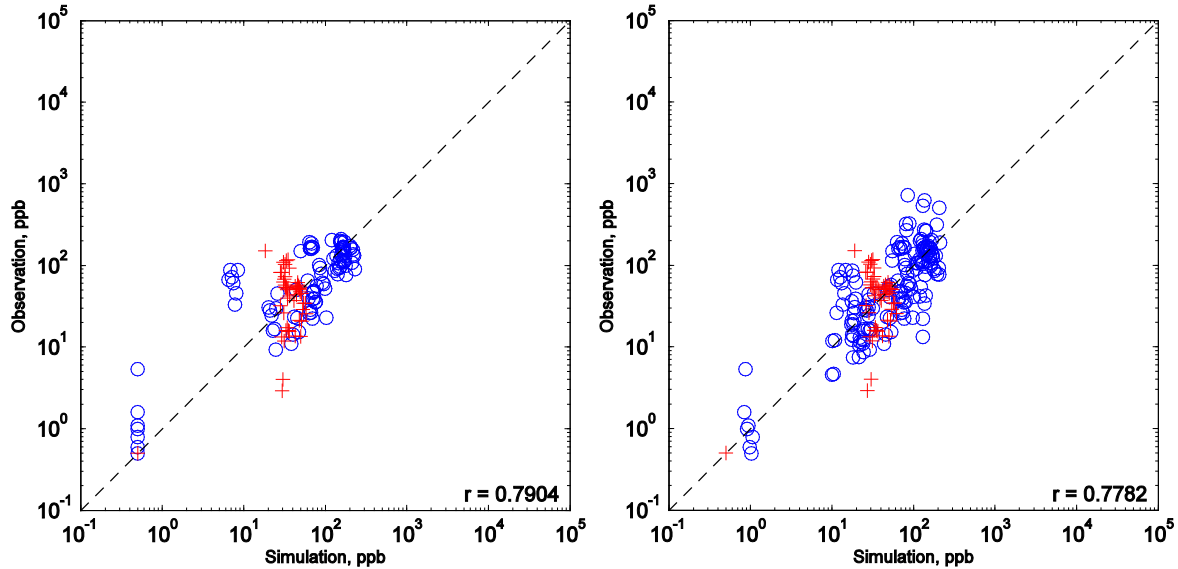


Figure G.7. Observed vs. simulated concentrations for pre-ERH (left) and post-ERH calibration (right) at the EGDY site. Blue (o) = Vashon aquifer; Red (+) = SLA aquifer.

G.4.2 Model Verification

Uncertainty in simulated remediation performance characterized using a Monte Carlo (MC) modeling approach. Liu et al. (2010) have shown that linearized uncertainty methods compare well with more rigorous and much more computationally intensive Markov Chain Monte Carlo methods when data is not inordinately noisy and reasonable prior information is available to condition parameter estimates. Thus, we utilize linearized uncertainty propagation methods to generate conditional parameter realizations.

Monte Carlo simulations are performed by generating N_{mc} equiprobable realizations of calibrated model parameters based on parameter best estimates and covariances determined from calibration. Performance simulations are run for each of the parameter sets. For simulations of model output used for calibration (e.g., dissolved contaminant concentration), "noise" representing measurement error and intrinsic model error is applied to each simulated output value based on the distribution of residual error determined during model calibration. Since our focus here is on verification of the source depletion function, we simulate source mass discharge totaled across all three sources over time from 2000 to 2100. As source discharge measurements were not used for calibration, no residual error is applied to Monte Carlo simulations of discharge rates. Source mass reduction by thermal treatment is treated as a deterministic input variable in the simulations set to the field-measured mass removal for each source.

Multiple measurements of source mass discharge were performed for the three DNAPL source zones before and after TSR treatment, but were not utilized during calibration. Measurements were performed using downhole passive flux units and different pump test methods (USACE, 2008). Total source discharge was determined for each method by summing over sources and maximum, minimum and median total measured discharge was determined.

Results of Monte Carlo simulations of total source discharge versus time with 95 and 99 percent confidence bands are shown in Figure G.8a for the calibration using pre-TSR data and in Figure G.8b using the post-TSR data set. Max, min and median estimates of discharge rates from field measurements prior to and after TSR are also depicted.

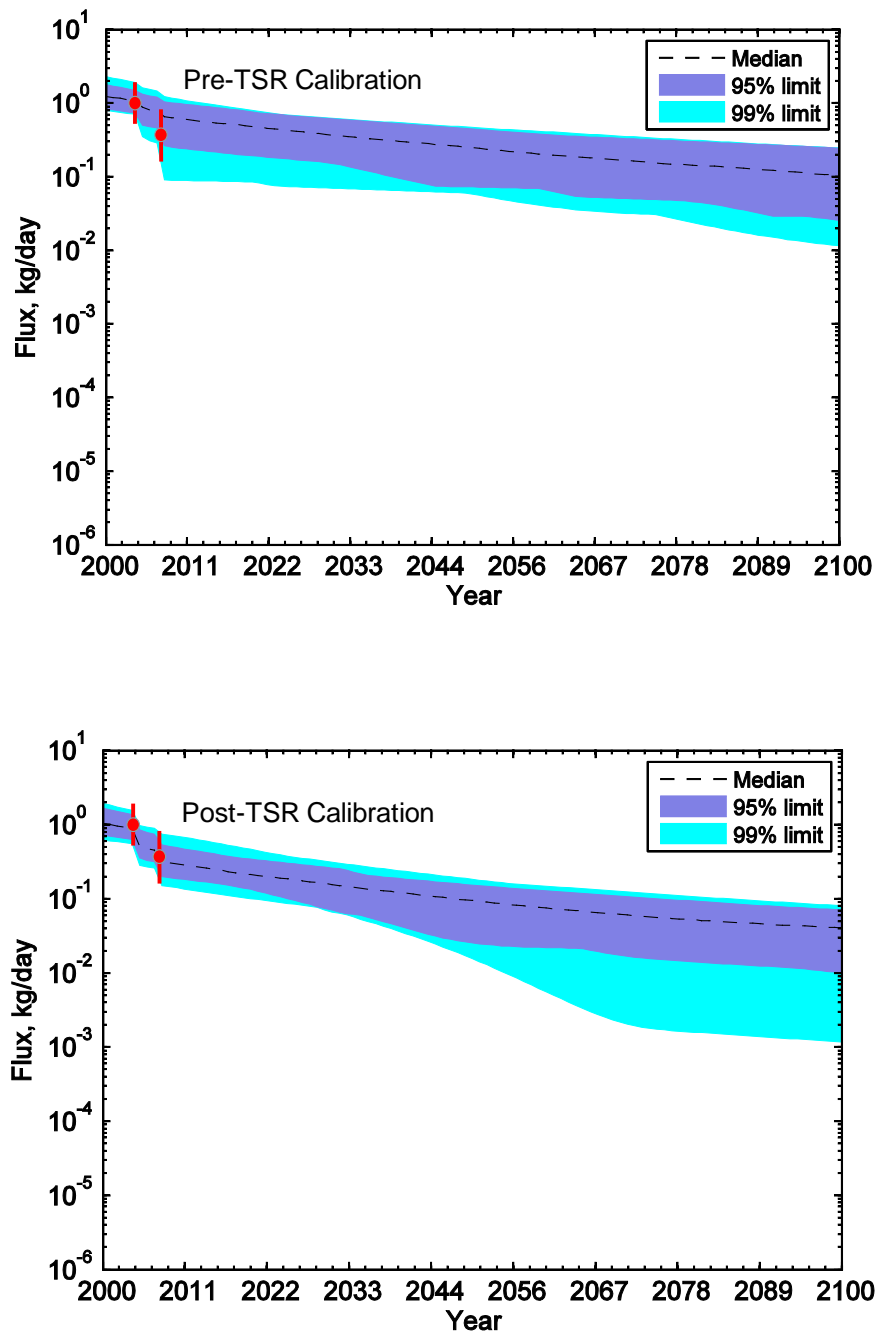


Figure G.8. Simulated total source mass discharge rate for EGDY from 2000 to 2100 based on pre-TSR (top) and post-TSR calibration (bottom). Dashed lines represent predicted best estimates and shades areas are their confidence limits. Red lines denote the range of field-measured discharge before and after TSR and red circles represent median values.

Stepwise reductions in source discharge due to source mass reductions by TSR between 2004 and 2007 are evident in the graphs. A slight narrowing of 95% confidence bands for the post-TSR calibration is evident, reflecting an improvement in model precision associated with the additional calibration data. Also notable is a somewhat more rapid decline in source discharge rate with time for the post-TSR calibration, which reflects substantially lower source mass estimates for the post-TSR calibration. Nevertheless, the confidence band for the pre-TSR calibration largely overlaps that for the pre-TSR calibration.

The second point, which is most important for our present objective, is that model-simulated mass discharge agrees well with simulated values. Specifically, median measured values lie within 95% prediction confidence bands for both pre- and post-TSR calibration simulations, which meets the criteria set for determining model validity. Although confidence limits are narrower for the post-TSR calibration, median measured values actually lie closer to the center of the 95% confidence band, emphasizing the earlier observation that more and better data available for calibration may be expected to improve model accuracy as well as model precision.

It is also interesting to note that measurement uncertainty for source discharge is significantly greater than the uncertainty in model simulations of discharge. This is not unreasonable considering that the calibration approach integrates much more data over the entire plume over a longer time-frame. This may not be the case on sites with few wells and shorter data time-series. Although it would be interesting and useful to compare model predictions of source discharge with field data in the future for longer term verification, the present analysis provides a sound basis for utilizing the proposed DNAPL source depletion model for long term sustainability assessment.

Predicted concentration versus time at a downgradient compliance well following actual TSR with no additional active remediation indicates a 50% probability of dropping below 5 $\mu\text{g/L}$ after 2180 using the pre-TSR calibration (Fig. G.9). The date drops to 2145 for the post-TSR calibration and the upper confidence band is much narrower, emphasizing the strong influence of data available for calibration on source depletion uncertainty.

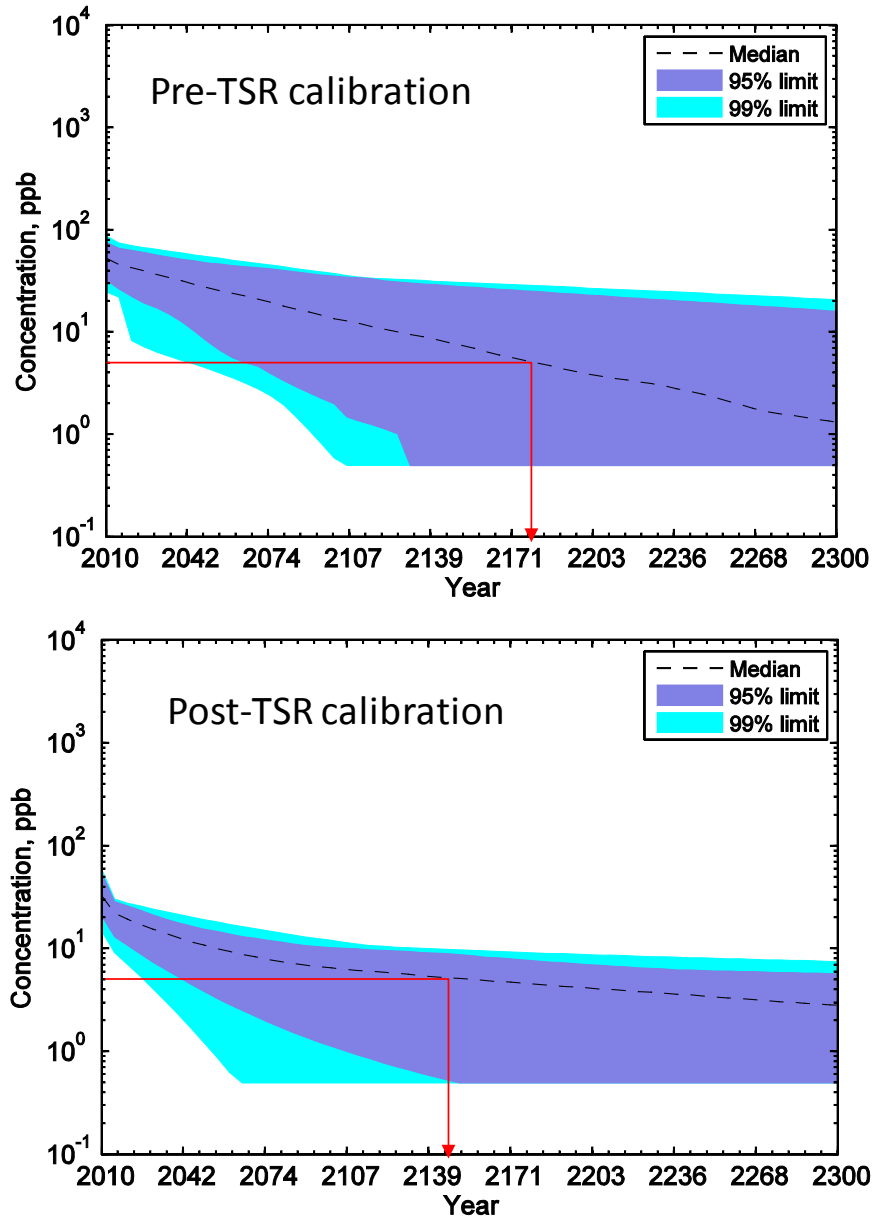


Figure G.9. Simulated solvent concentration versus time for EGDY site based on pre-TSR calibration (top) and post-TSR calibration (bottom). Dashed lines are median estimates and shaded areas are confidence limits. Red arrows indicate 50% probability time to reach 5 mg/L. Note that computed concentrations are truncated below 0.5 mg/L.

G.5 Areas I&J, NAES Lakehurst, NJ

G.5.1 Model Calibration

Characterization of groundwater flow field. Five NAPL sources were identified in previous investigations. Groundwater flow at Areas I and J was characterized using a contour map of observed water levels in November 1998 (Dames and Moore 1999). Since equipotential lines does not show a significant curvilinear flow pattern within the model domain, streamlines from five sources (N1, N2, N3 for the north plume and S1, S2 for the south plume) were described as straight lines, i.e., $y=ax$. Values of the coefficient 'a' for the five sources were -0.32, -0.18, -0.27, -1.73 and -0.7, which correspond to 17.7, 10.2, 15.1, 60.0, and 35.0 degrees clockwise from due east, respectively.

Calibration using dissolved CVOC concentration data. Parameter calibration was performed using a total of 165 CVOC concentration measurements from monitoring wells from 1996 through 2003. The sum of CVOC concentrations were stoichiometrically-weighted to obtain TCE-equivalent concentrations for model calibration. Model calibration yielded a posterior estimate of ln-concentration uncertainty (SlnC) of 0.97 and a correlation coefficient of 0.72 between observed and simulated concentrations (Figure G.10). Prior values for parameters were initially estimated from Dames and Moore (1999). Table G.5 and Figure G.10 summarize the calibration results.

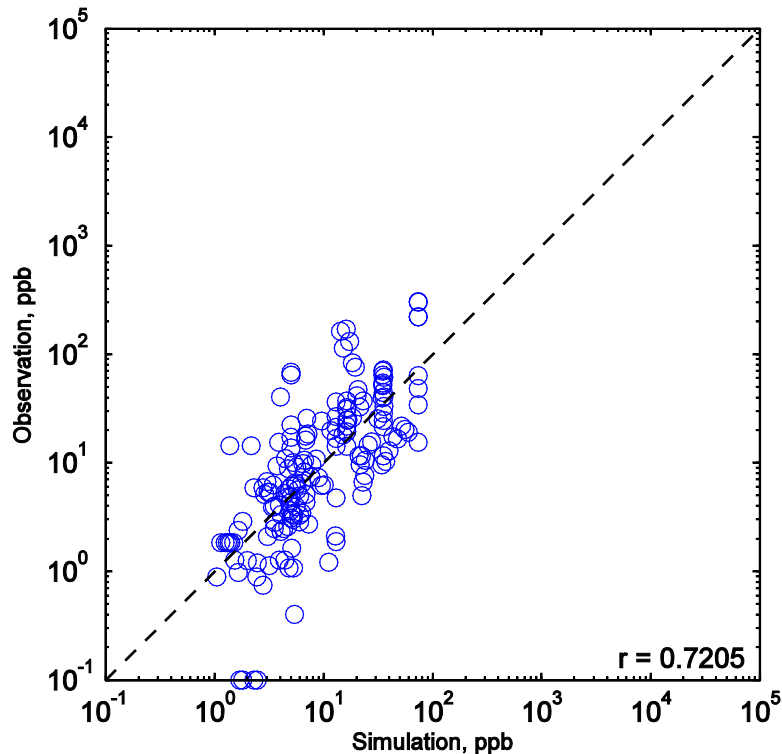


Figure G.10. Observed vs. simulated CVOC concentrations for Areas I&J.

Table G.5. Site characterization and calibration summary for Areas I & J.

Source	Parameter	Prior ¹	STD ²	Calibration	Remark
N1	Flux at 1990 (kg/d)	6.00E-03	2	9.06E-03	Width 50 m
	Release date	1958	-	1958	
	Mass at 1990 (kg)	1000.0	2	1944.8	
	Beta	1.10	1	0.92	
	Zone 1 decay coef ³	1.30E-03	0.5	1.30E-03	Up to 500 m from N1
	Zone 2 decay coef ³	9.00E-05	0.5	8.99E-05	Beyond 500 m
N2	Source discharge ⁴ (kg/d)	5.50E-03	2	6.44E-03	Width 25 m
	Release date	1958	-	1958	
	Source mass ⁴ (kg)	145.0	2	281.9	
	Beta	0.85	1	0.48	
	Zone 1 decay coef ³	1.30E-03	0.5	1.30E-03	Up to 600 m from N2
	Zone 2 decay coef ³	9.00E-05	0.5	8.99E-05	Beyond 600 m
N3	Source discharge ⁴ (kg/d)	1.50E-04	2	1.58E-04	Width 25 m
	Release date	1958	-	1958	
	Source mass, 1990 ⁴ (kg)	1.5	2	1.5	
	Beta	8.50E-01	1	8.65E-01	
	Zone 1 decay coef ³	9.00E-05	0.5	8.99E-05	Entire
	Zone 2 decay coef ³	9.00E-05	0.5	8.99E-05	Entire
S1	Source discharge ⁴ (kg/d)	1.00E-03	2	2.73E-04	Width 25 m
	Release date	1958	-	1958	
	Source mass, 1990 ⁴ (kg)	2.5	2	0.3	
	Beta	0.85	1	0.93	
	Zone 1 decay coef ³	3.80E-03	0.5	3.80E-03	Up to 300 m from S1
	Zone 2 decay coef ³	9.00E-05	0.5	8.99E-05	Beyond 300 m
S2	Source discharge ⁴ (kg/d)	3.00E-03	2	1.62E-03	Width 50 m
	Release date	1958	-	1958	
	Source mass, 1990 ⁴ (kg)	10.0	2	2.1	
	Beta	0.85	1	0.30	
	Zone 1 decay coef ³	1.90E-03	0.5	1.90E-03	Up to 200 m from S2
	Zone 2 decay coef ³	9.00E-05	0.5	8.99E-05	Beyond 200 m
Aquifer	Darcy velocity (m/d)	0.06	0.25	0.04	
	Porosity	0.30	-	0.30	
	Retardation	1.20	0.25	1.22	
	Longitudinal dispersivity (m)	40.00	0.5	91.24	
	Transverse dispersivity (m)	4.00	0.5	20.00	Upper limit
	Saturated depth (m)	20	0.25	21.18	

¹ Prior estimates represent arithmetic mean for release date, geometric mean for other parameters.

² Standard deviations are ln-transformed except for beta, which are in actual units.

³ Biodecay 1 for N1 and N2 and Biodecay 2 for all sources were calibrated synchronously.

⁴ Calibration date for source discharge and source mass was 1990 for all sources, however, mass removal was not considered due to lack of data. Values may be closer to post-recovery conditions.

G.5.2 Model Verification

Total source mass discharge summed over all five sources was simulated from 2000 to 2100 (Figure G.11). Source mass reduction by contaminated sediment removal performed in 1993 was not considered due to lack of information, resulting small source mass calibrated at S1 and S2 for the calibration year 1990. The simulated source mass discharge curve shows very persistent mass dissolution with the upper 95% limit barely decreasing from 0.023 to 0.018 kg/d over the 100-year simulation period, while the lower 95% limit drops only slightly more from 0.007 to 0.0008 kg/d over the same period.

Since no measurements of source mass discharge are available, model verification criteria cannot be directly evaluated for this site. Furthermore, since noise in concentration data (Figure G.10) is substantially greater than the uncertainty in predicted source discharge, it may take many years of monitoring before predictions can be verified or simulation performance substantially improved by recalibration.

Nevertheless, from a practical standpoint, the model indicates a very high probability that MNA will not be successful within a reasonable time frame without partial source mass reduction. Following source reduction measures, data on mass removed and dissolved concentration decreases in monitoring wells near source zones should enable model refinement by recalibration to better assess the prospects for successful MNA.

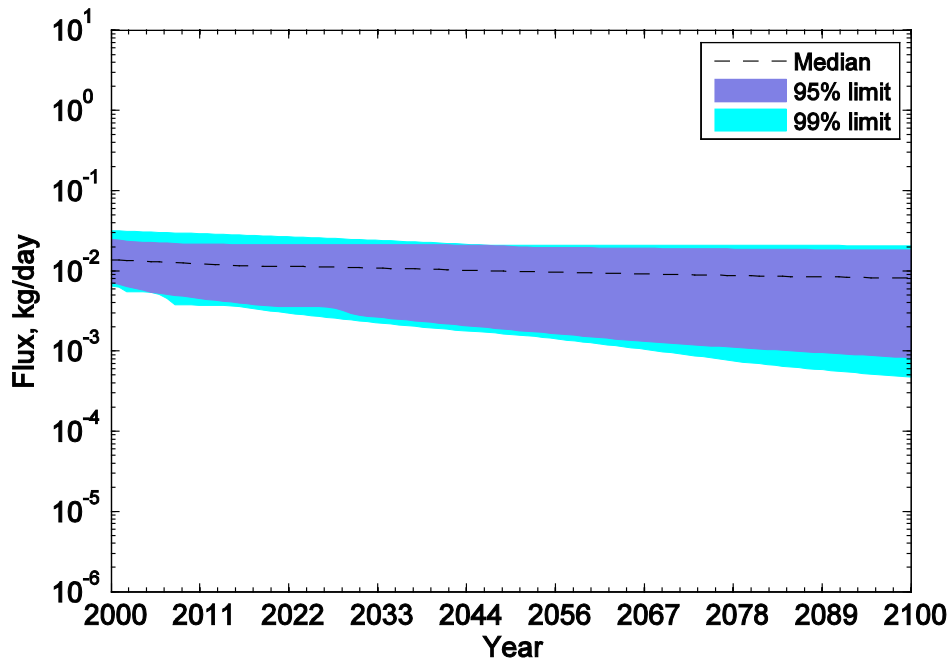


Figure G.11. Source mass discharge simulated in Area I & J for 2000-2100.

G.6 Site 45, MCRD Parris Island, SC

G.6.1 Model Calibration

Characterization of groundwater flow field. Here, we model the south plume only assuming its source is located near two manholes that connect sanitary sewers at the southeastern corner of the new dry-cleaning facility. Groundwater flow at the Parris Island site was characterized using a contour map of June 2008 water levels and CVOC data from monitoring wells in 2006-2008 (Vroblesky et al. (2009)). The model domain extends covers the source to the southeastern boundary of the south plume. Since equipotential lines does not show a significant curvilinear flow pattern within the model domain, streamlines are assumed to be straight lines, i.e., $y=ax$. The prior value of coefficient 'a' was estimated -1.00 (45 degrees south of due east) and this flow direction was fitted as a calibration parameter.

Calibration using dissolved CVOC concentration data. Parameter calibration was performed using a total of 74 CVOC concentration values measured from 2005 through 2008 in monitoring wells. Depth averages of total CVOC concentrations were stoichiometrically weighted to obtain PCE-equivalent concentrations for model calibration. The range of observed PCE-equivalent concentrations is around four orders of magnitude (1 ppb to 73 ppm).

A prior value of $\ln C$ uncertainty (SlnC) of 2.78 was estimated as the natural log standard deviation of the calibration data. Calibration yielded a posterior SlnC of 2.00 showing reduced prediction uncertainty. Calibration performance is reasonable with a correlation coefficient of 0.78 between the observed and simulated concentrations (Figure G.12). Prior values for parameters were initially estimated from Vroblesky et al. (2009). Table G.6 summarizes site characterization data and calibration results

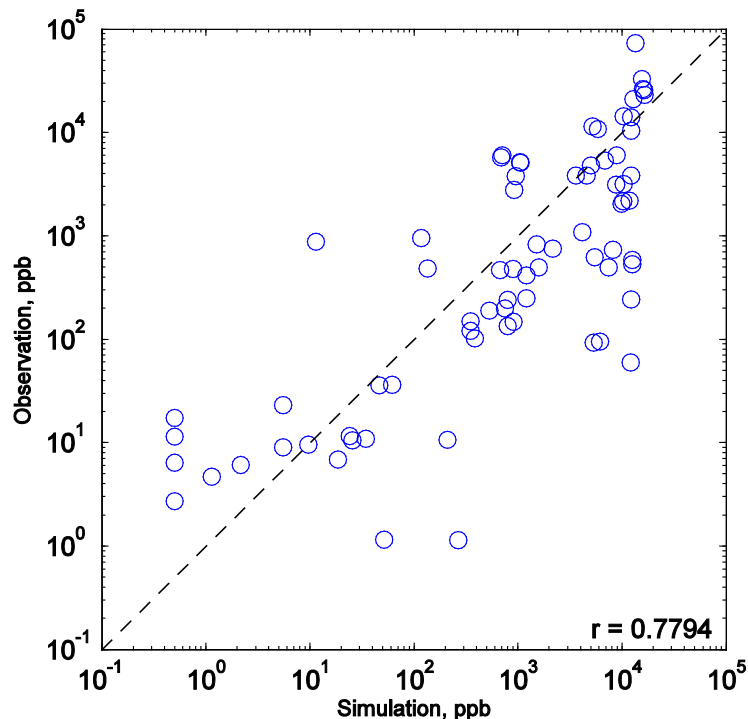


Figure G.12. Observed vs. simulated concentrations for Parris Island.

Table G.6. Site characterization and calibration summary for Parris Island.

Source	Parameter	Prior ¹	STD ²	Calibration	Remark
N1	Flux at 1990 (kg/d)	1.20E-03	2	1.17E-03	
	Release date	1975.00	10	1972.90	
	Mass at 1990 (kg)	5.0	2	19.4	
	Beta	1.20	1	1.26	
	Width (m)	7.00	2	4.17	
Aquifer	Flow direction (deg)	-45.00	6	-40.28	+ to counter clockwise
	Darcy velocity (m/d)	0.00	0.5	0.00	
	Porosity	0.35	0.03	0.35	
	Retardation	1.43	0.5	0.15	
	Longitudinal dispersivity (m)	20.00	0.5	1.12	
	Transverse dispersivity (m)	0.50	0.5	0.24	
	Saturated depth (m)	3.5	0.25	3.22	
	natural ED average (H-eq ppb)	2992	0.25		
	natural EA average (H-eq ppb)	2880	0.25		

¹ Prior estimates represent arithmetic mean for release date, geometric mean for other parameters.

² Standard deviations of prior estimates are dimensionless statistics for ln-transformed values for all parameters except release date, beta, and porosity, which are in actual units.

G.6.2 Model Verification

The calibrated model was used to simulate total source mass discharge and its confidence limits from 2000 through 2100 (Figure G.13). Since no direct measurements of source mass discharge are available for this site, model verification criteria could not be evaluated. In any case, given the broad simulation confidence bands, statistical verification would not be very meaningful anyway. The results indicate a 5% probability that the source may be essentially clean by around 2025, while a 50% probability exists that source discharge will take more than 100 years to decrease more than an order of magnitude. Provided there are no serious consequences of continuing to monitor the plume without further active remediation, periodic model recalibration should reduce prediction uncertainty and enable more accurate assessment of performance and of the advisability of further actions.

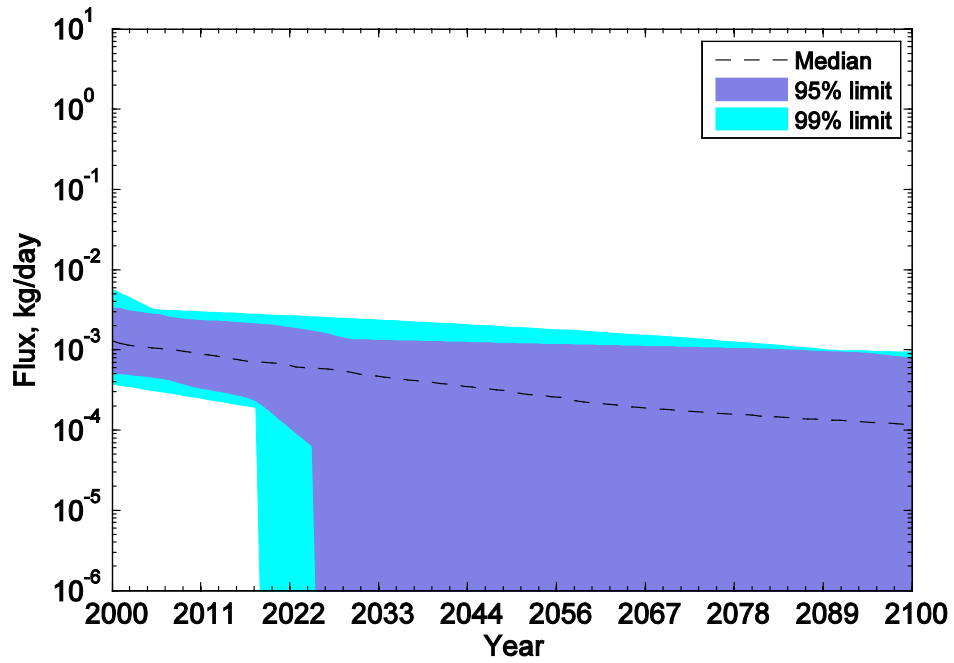


Figure G.13. Source mass discharge simulated in Parris Island for 2000-2100.

APPENDIX H: MODEL DESCRIPTION FOR SUSTAINABILITY ASSESSMENT (PERFORMANCE OBJECTIVE 3)

H.1 Modeling Objective and Approach

A site model was developed for simulating groundwater flow and solute transport at Site 45, Marine Corps Recruit Depot, SC. The hydrogeology and distribution of CVOC contamination at Site 45 are described in considerable detail in Section 4 of this report. The model was calibrated to redox conditions based on observed site conditions. The carbon distribution was based on the results of a field investigation described in Section 5. Thus, the objective of the model was to evaluate long-term sustainability of redox conditions over the estimated remediation timeframe (Appendix G). Using the range of carbon measured at Site 45, uncertainty of the sustainability assessment was also evaluated.

H.2 Model Domain and Grid Discretization

The active domain of the flow model (Figure H.1) covers approximately 49,280 square meters (~0.05 km²). The finite difference grid was rotated 37.5 degrees (counter-clockwise relative to a west-to-east x-axis) to coincide with the principal direction of flow (generally northwest to southeast) observed in the surficial aquifer at the Site. The active domain contains 110 rows running in a northwest-southeast direction and 112 columns oriented in a southwest-northeast direction (a total of 12,320 cells). Cell nodes are spaced equally at a distance of 2 meters along the lateral axes. Vertically, the model includes a single, 3.5 meter-thick layer representing only the permeable fraction of the surficial aquifer.

Groundwater flow was simulated using MODFLOW-2000 (Harbaugh et al., 2000). Due to the absence of detailed long-term transient data, simulations were performed assuming steady-state flow. Contaminant transport was simulated using SEAM3D (Waddill and Widdowson, 2000). The primary objective of the STS assessment was matching the observed DO concentrations in the aquifer where CVOC contamination was present. The best available data set (Voroblesky et al., 2009) was utilized to provide the most spatial coverage at the Site.

H.3 Boundary Conditions

No-flow boundary conditions were applied at the southwest and northeast extremes of the model domain. General head (Cauchy-type) boundary conditions were applied to the up-gradient (i.e., northwest) and down-gradient (i.e., southeast) extremes of the model domain using the MODFLOW GHB package (Figure H.2). Both boundary condition types reflect consistency with the observed hydraulic gradient in the vicinity of the dissolved contaminant plumes (Voroblesky et al., 2009). Head specifications at the up-gradient and down-gradient general head boundaries were 1.42 and 0.57 meters respectively. These head assignments were based on extrapolated local head measurements within the primary area of concern. Conductance parameters for the GHB boundaries were determined during model calibration which is discussed below.

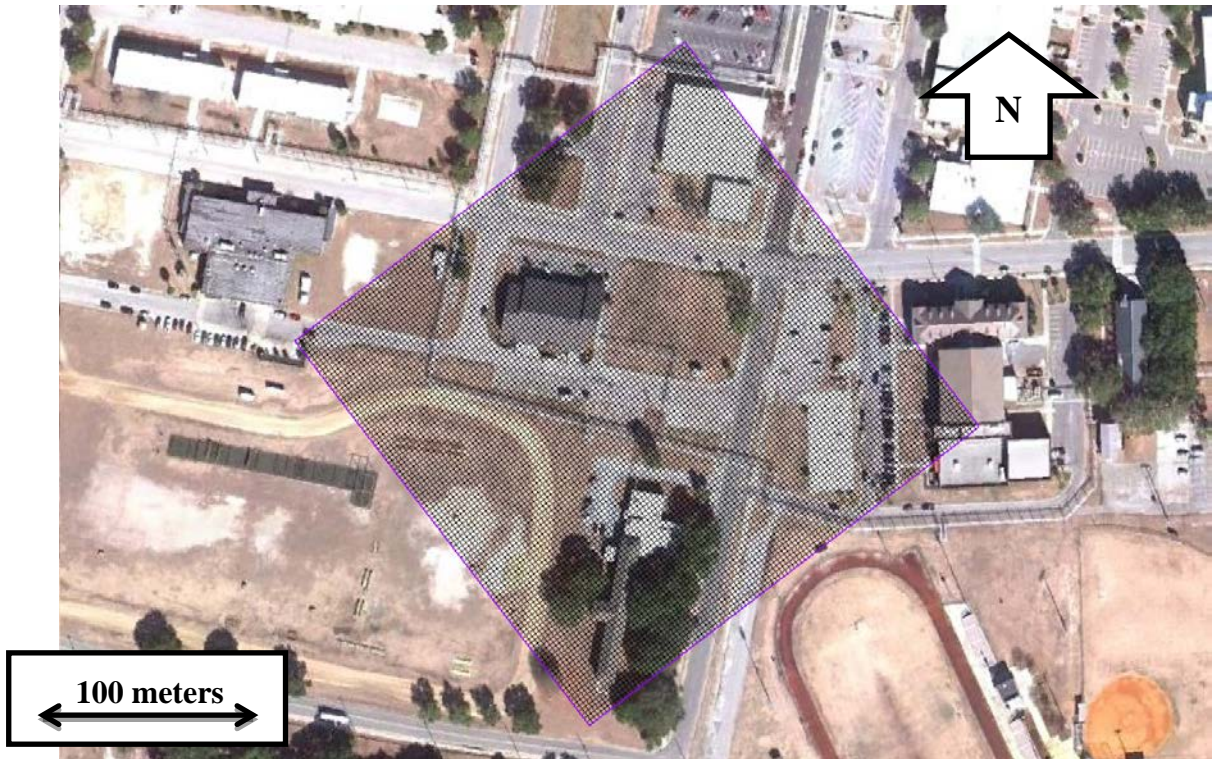


Figure H.1. Description of active model domain and finite difference grid.

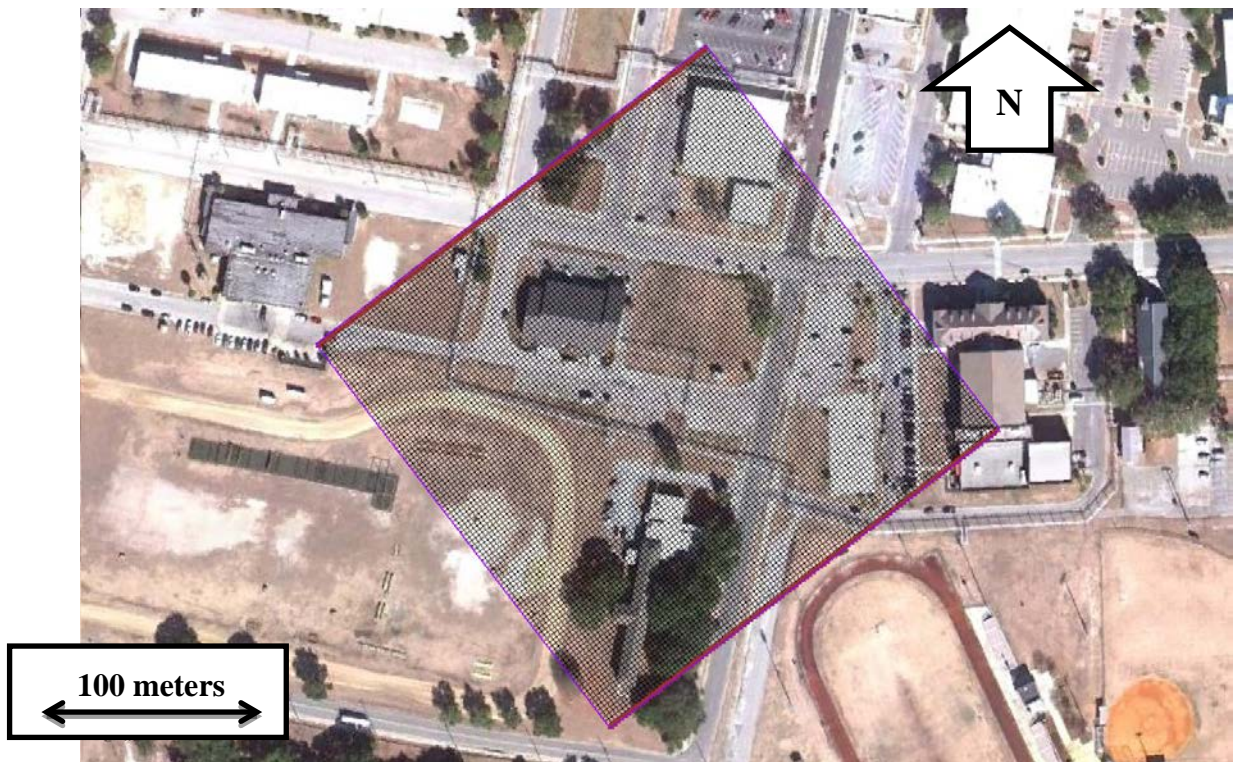


Figure H.2. Depiction of boundary conditions applied to flow model (plan view). Maroon highlights indicate locations of general head boundaries.

A no-flow boundary was also assigned at the base of the model. This boundary condition represents the contact between the relatively permeable surficial unit and an underlying clay confining unit which has been previously identified as generally extensive and intact (Voroblesky et al., 2009).

The primary source of groundwater recharge at the Site is infiltration of precipitation, particularly in areas where impervious or low-permeability surficial cover is not present (Voroblesky et al., 2009). The influence of precipitation recharge is represented in the model using the MODFLOW RCH package. The model domain was separated into zones of permeable and impermeable land cover using aerial imagery, and recharge rates for both zones were initially estimated using scaled average annual precipitation for the region (Figure H.3). The recharge rates were refined using parameter estimation according to the process described below.



Figure H.3. Depiction of precipitation recharge zones. Light shading indicates impermeable or low-permeability land cover as identified from aerial imagery.

Buried municipal sewer lines located in the vicinity of the contaminant plumes have been previously verified, in some locations, as lacking complete integrity (Voroblesky et al., 2009). Thus, in some locations, these leaky sewer lines represent potential sinks for groundwater as leakage into the conduit and transfer would result in general loss from the saturated system. These sinks for groundwater were simulated in the model using the MODFLOW DRN package. Locations of known leakage were explicitly represented in the model by specifying the drain elevation according to the observed hydraulic heads in the vicinity of the sewer conduits. Four (4) drain sections (Figure H.4) were allowed to vary using section-specific conductance parameters which were ultimately determined using parameter estimation (described below).

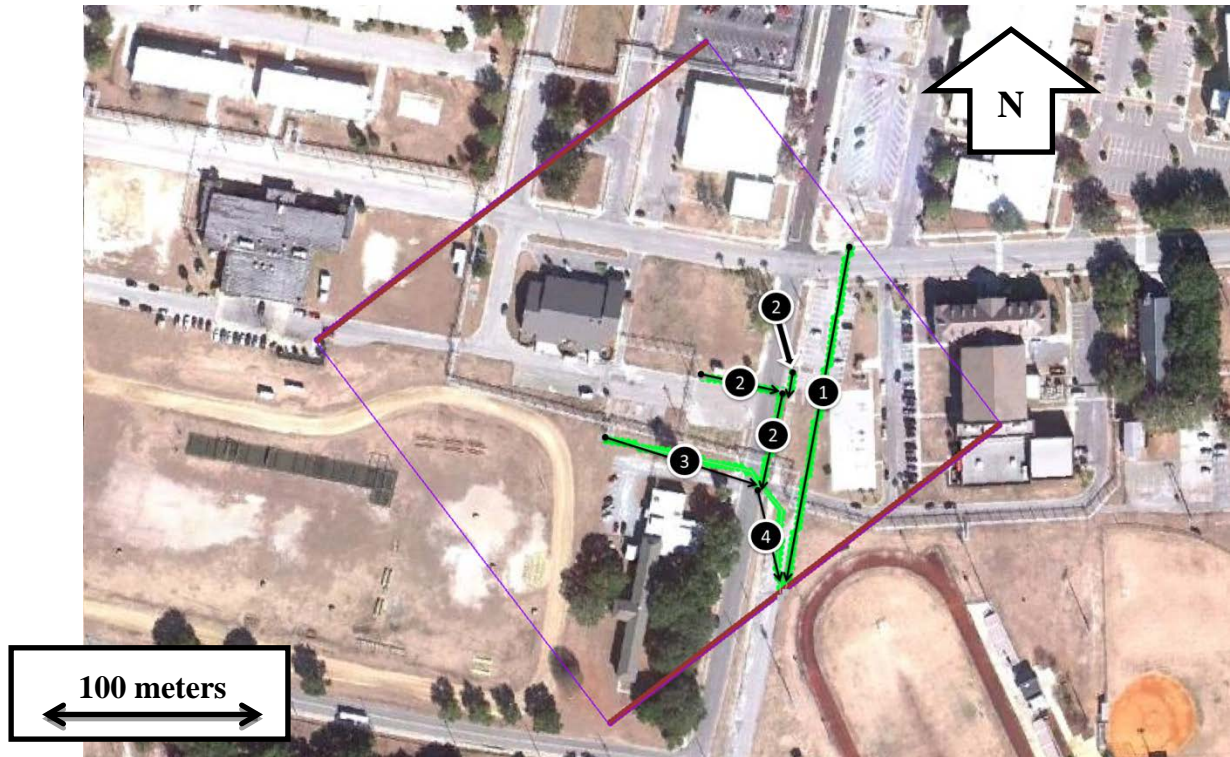


Figure H.4. Groundwater sink cells (drain cells) generalized into numeric zones. Cells highlighted in green indicate locations with active drain cells.

H.3 Material Properties

The single layer model represents the permeable fraction of the surficial aquifer at the Site. Previous investigations have identified the more permeable materials present in the shallow zone as varying from sands to silty sands; however, detailed information regarding spatial differences in composition was not available. Therefore, the simulated material in the subsurface was assumed to be homogeneous and isotropic. The hydraulic conductivity of this material was initially estimated as the reported mean for the site (Voroblesky et al., 2009), but this value was ultimately refined using parameter estimation (described below).

H.3 Calibration to Observed Conditions

Model calibration was initially performed using a manual (i.e., trial-and-error) technique based on initial estimates of the variable parameters. Ultimately, calibration was refined using automated parameter estimation facilitated by PEST (Doherty, 2005). Hydraulic head measurements in the surficial aquifer provided the basis for developing an objective function which was minimized by PEST by varying the aforementioned conductance, recharge and hydraulic conductivity parameters individually. Parameter estimates were constrained within a range defined as reasonable for each specific group (e.g., hydraulic conductivity based on minimum and maximum reported for site (Voroblesky et al., 2009)). Log transformations were

initially applied to each parameter to provide flexibility, but final calibration was performed without transformation. The simulated water table elevations produced by the PEST-facilitated calibration process are shown in Figure H.5.

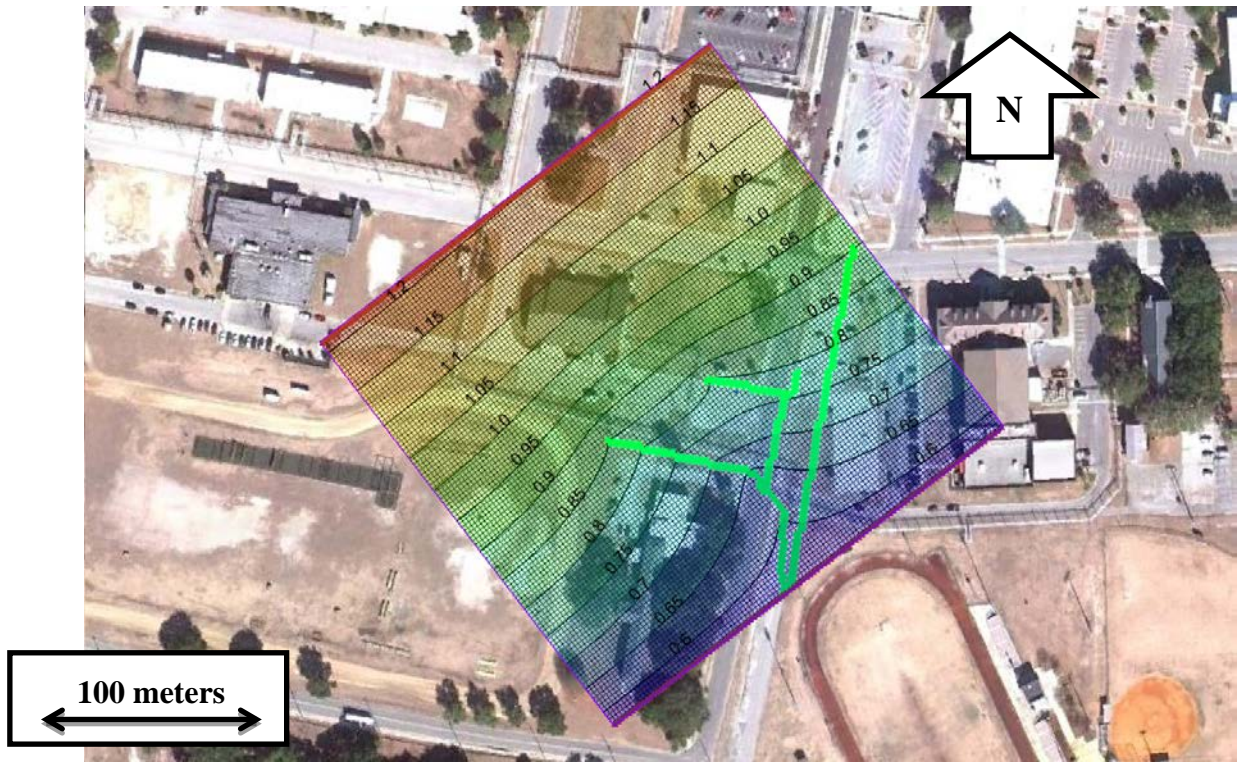


Figure H.5. Depiction of simulated water table elevation in surficial aquifer. Head contours represent groundwater elevation in meters above sea level.

Groundwater level data used to calibrate the flow model were recorded June 27, 2008 at 24 unique locations (Figure H.6). While two well screens are present in the surficial aquifer at the Site, the shallow screens (SU wells) displayed greater local variability in observed head which may be attributed to preferential recharge/discharge zones which have not been previously identified. These data were recognized as more difficult to simulate given the uncertainty associated with attempting to quantify these local influences; therefore, the data recovered from the deeper screens (SL wells) were chosen as being the most appropriate targets for model calibration. An additional factor contributing to this choice is the observation that, in general, the most permeable fraction of the surficial unit resides below 10 feet below ground surface (bgs), which is a depth that coincides more directly with the SL screens.

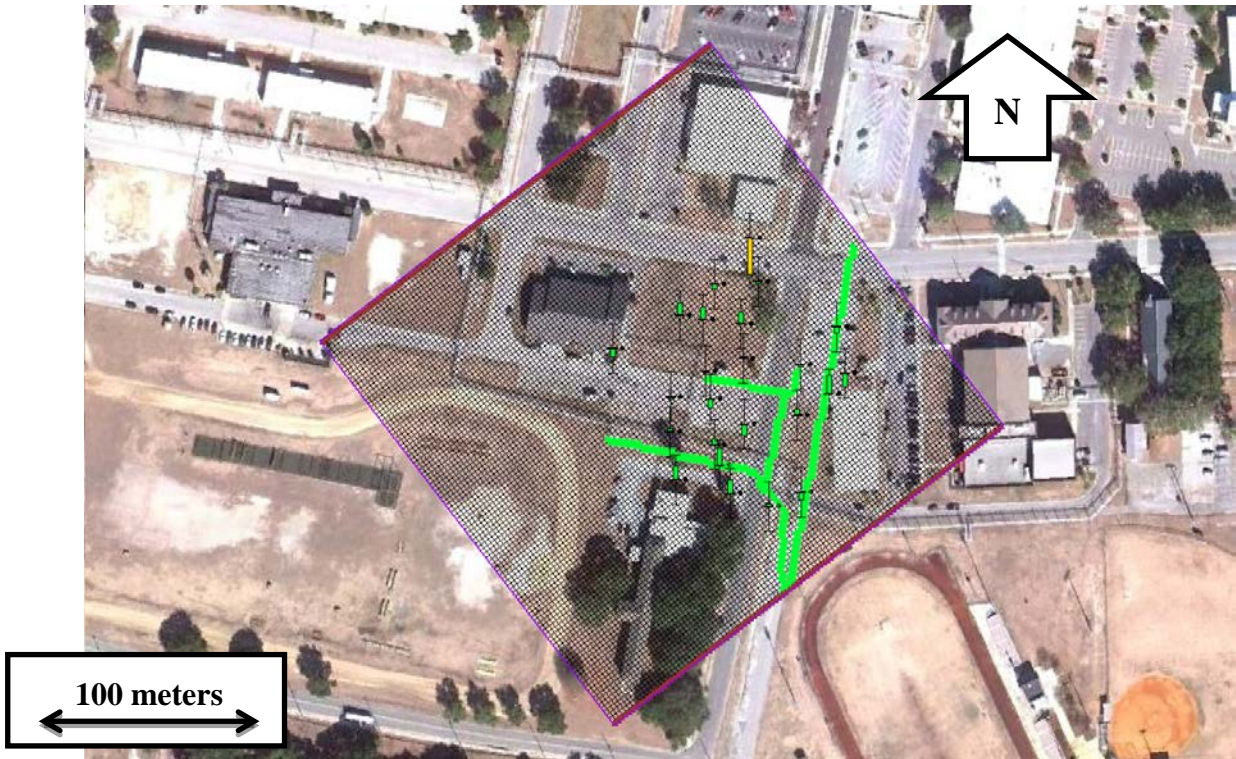


Figure H.6. Locations of water level targets. Green bars indicate simulated result within 0.05 meters of observed groundwater elevation. Yellow bar indicates location where residual (observed head – simulated head) is equal to 0.072 meters.

The PEST-facilitated calibration process produced model-predicted heads which compare very favorably with the observed condition (Figure H.7). The maximum and minimum head residuals (observed head – simulated head) for the calibration target dataset were 0.072 meters and -0.037 meters, as compared to the total head difference within the model domain of slightly more than 0.5 meters. The calibrated model produced an average head residual of 0.001 meters and an average absolute head residual of 0.019 meters. In summary, the calibrated model is an excellent reproduction of the observed condition when compared to observed groundwater levels in the shallow aquifer.

Model-predicted groundwater velocities were also compared to previously reported conditions for the purpose of independently evaluating the predicted rate of flow in the model (Voroblesky et al., 2009). The Darcy groundwater velocity in the calibrated model roughly matches the average value observed at the Site using passive flux measurements (calculated 0.0076 meters per day versus observed 0.0082 meters per day). However, it is important to note that the PEST-predicted hydraulic conductivity for the homogeneous and isotropic media slightly exceeded the reported maximum for the site (6.40 meters per day versus 4.57 meters per day). This hydraulic conductivity value not only provided the best match to the observed heads, but it also resulted in the closest agreement with the observed Darcy velocity in the primary area of concern.

Vrobley et al. (2009) reported DO levels ranging from 0.7 mg/L to below detection (< 0.025 mg/L). These DO concentrations in groundwater were obtained from monitoring wells with 5-ft well screens in the lower depth of the shallow aquifer. DO concentrations were reported as >1

mg/L at one well (MW20-SL) on two out of six sampling events but levels were typically closer to 0.2 mg/L at this location. It was interesting to note that DO levels at the source well (MW25-SL) were never below detection for the three sampling events reported at this location. Results show that order-of-magnitude differences in the PBOC levels in the model did not impact calibration of the SEAM3D model to the DO data (Figure H.7). The results demonstrate that the modeling objective was achieved using the pre-determined error criterion (± 0.25 mg/l) for DO concentrations applied to the STS assessment.

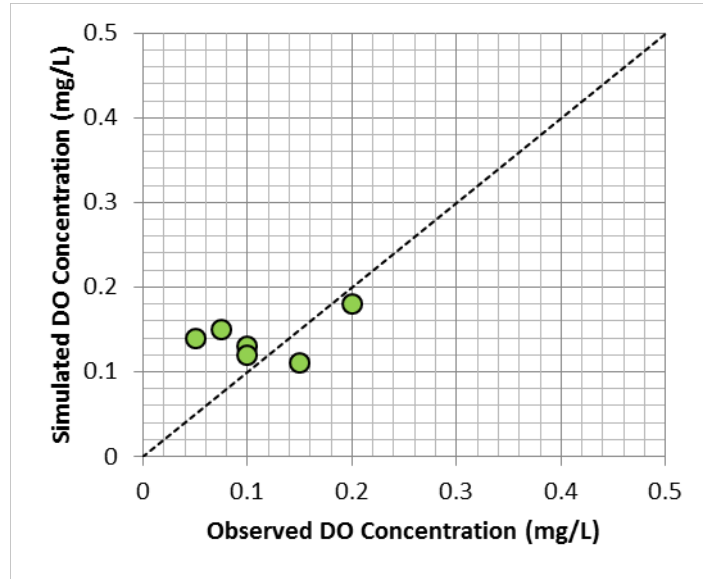


Figure H.7 Comparison between observed and simulated dissolved oxygen (DO) concentrations in the surficial aquifer at Site 45.

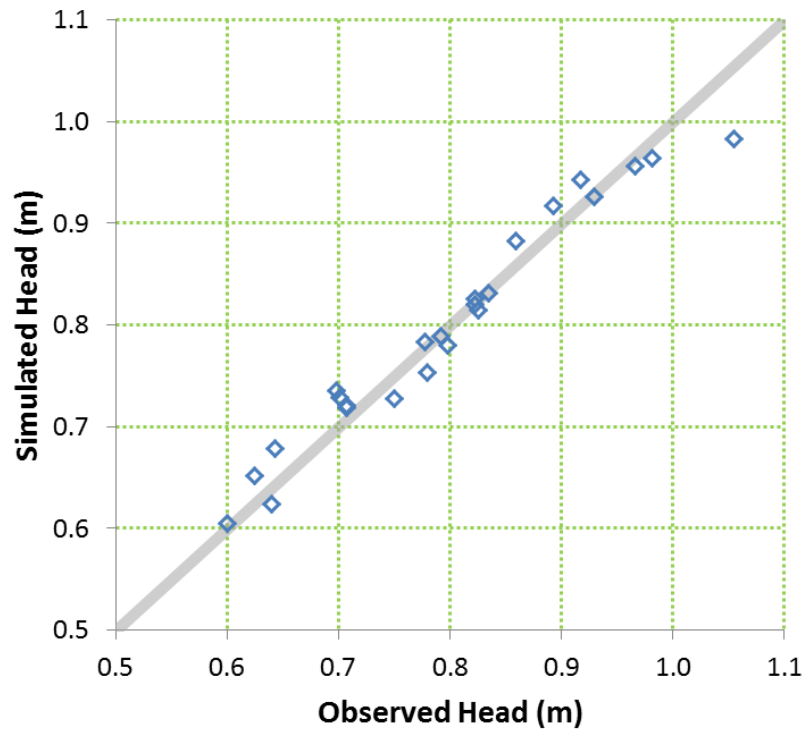


Figure H.7. Comparison between observed and simulated groundwater elevations in surficial aquifer. Observed data represent groundwater elevation measurements taken from SU-screened wells on June 27, 2008.